Momordica foetida facilitates glucose uptake independent of AMPK2α and PI3K to attenuate hyperglycemia-induced oxidative stress via a JNK-STAT3 mediated pathway in HepG2 cells

By

Tshamano Fulufhelo Netshitangani

BSc (Biochemistry and Genetics) (UKZN), BSc.B Hons (Biochemistry) (University of Venda)

Student number: 214559795

Submitted in fulfilment of the requirements for the degree of

Master of Medical Science

Discipline of Medical Biochemistry

School of Laboratory Medicine and Medical Sciences,

College of Health Sciences

University of KwaZulu-Natal,

Durban

2022

Supervisor: Dr R.B. Khan

DECLARATION

I, **Netshitangani Tshamano Fulufhelo**, Student Number: **214559795** declare that

i. The research reported in this dissertation, except where otherwise indicated, is my original work.

ii. This dissertation has not been submitted for any degree or examination at any other university

iii. This dissertation does not contain other person's data, pictures, graphs or other information, unless specifically acknowledged as being sourced from other persons.

iv. This dissertation does not contain other person's writing, unless specifically acknowledged as being sourced from other researchers. Where other written sources have been quoted then:

   a. Their words have been re-written, but the general information attributed to them has been referenced.

   b. Where their exact words have been used, their writing has been placed inside quotation marks, and referenced.

v. Where I have reproduced a publication of which I am an author, co-author or editor, I have indicated in detail which part of the publication was actually written by myself alone and have fully referenced such publications.

vi. This dissertation does not contain text, graphics or tables copied and pasted from the internet, unless specifically acknowledged, and the source being in the dissertation and in the reference sections.

Signed: [redacted] **Date:** 13 June 2022

Miss TF Netshitangani

Signed: [redacted]

Dr RB Khan

ACKNOWLEDGEMENTS

I thank the Almighty God for this opportunity and for providing me with strength throughout the year.

I would like to express my gratitude to my family for being my biggest supporters and cheerleaders. I am honoured and will forever be grateful.

I would like to sincerely thank Dr RB Khan for granting me this opportunity and for her guidance.

I would also like to thank Mr S Mposula, Mr S Mcoyi, Ms N Muvhulawa and Mrs A Sinyani for their patience, guidance, and perseverance throughout this journey.

Gratitude to NRF for funding my project.

TABLE OF CONTENTS

LIST OF FIGURES

CHAPTER 2

LIST OF TABLES

LIST OF ABBREVIATIONS

µM	Micromolar
mM	Millimolar
MTT	Methylthiazol tetrazolium
ºC	Degrees Celsius
µL	Microliter
nm	Nanometer
$\Delta\Psi m$	Mitochondrial membrane potential
β-cell	Beta cells
•OH	Hydroxyl radical
$^1O_2$	Singlet oxygen
8-oxoGuo	oxidized 8-oxo-7,8-dihydro-2′-deoxyguanosine
ADA	American Diabetes Association
AMPK	Adenosine monophosphate-activated protein kinase
AMPK2α	AMP-activated protein kinase 2 alpha
AOPP	Advanced oxidation protein products
aPKC	Atypical protein kinases C λ and ζ isoforms
ATP	Adenosine triphosphate
BCA	Bicinchoninic acid
cDNA	Complementary DNA
CAT	Catalase
DAG	Diacylglycerol
DM	Diabetes mellitus
DNA	Deoxyribonucleic acid
ERK	Extracellular-signal-regulated kinase
G6P	Glucose 6-phosphate
G6Pase	Glucose-6-phosphatase
GK	Glucokinase
GLUT	Glucose transporter
GLUT2	Glucose transporter 2
GLUT4	Glucose transporter 4
GLUT5	Glucose transporter 5

GLUT8	Glucose transporter 8
GLUT9	Glucose transporter 9
GP	Glycogen phosphorylase
GPx1	Glutathione peroxidase 1
GR	Glutathione reductase
GS	Glycogen synthase
GSH	Reduced glutathione
GSK3	Glycogen synthase kinase 3
GSSG	Glutathione disulfide
H_2O_2	Hydrogen peroxide
HEPG2	Human hepatocellular carcinoma cell line
HIV/AIDS	Human immunodeficiency virus, acquired immunodeficiency syndrome
HOCl	Hypochlorous acid
IDF	International Diabetes Federation
IR	Insulin receptor
IRS	Insulin receptor substrate
JNK/SAPK	Jun N-terminal kinase stress-activated kinases/ tress-activated protein kinase
LDH	Lactose Dehydrogenase
mg	Milligram
ml	Milliliter
M. foetida	*Momordica foetida* Schumach. et Thonn
MAPK	Mitogen-activated protein kinase
MDA	Malondialdehyde
mRNA	Messenger RNA
NADPH	Nicotinamide adenine dinucleotide phosphate
NF-kB	Nuclear factor-kB
$NO^{\bullet}$	Nitric oxide
NO_2	Nitrogen dioxide
NRF2	Nuclear factor erythroid 2 [NF-E2]-related factor 2
$O_2^{\bullet -}$	Superoxide
O_3	Ozone
OGG1	8-Oxoguanine glycosylase

ONOO•	Peroxynitrite
ONOO	Peroxynitrite radical
ONOOH	Peroxynitrous acid
OXPHOS	Oxidative phosphorylation
PP1	Protein phosphatase-1
p38-MAPK	p38 mitogen-activated protein kinases
PDK1	Phosphoinositide-dependent protein kinase 1
PH-domain	Pleckstrin homology domain
PIP3	Phosphatidylinositol triphosphate
PI3K	Phosphatidylinositol 3-kinase
PKB/AKT	Protein kinase B
PKC	Protein kinase C
p-p38	Phospho-p38
p-Erk	Phospho-extracellular-signal-regulated kinase
p-STAT	Phospho- signal transducer and activator of transcription 3
qPCR	Quantitative polymerase chain reaction
RBD	Relative band density
RNA	Ribonucleic acid
RLU	Relative light units
RNS	Reactive nitrogen species
ROO.	Peroxyl radical
ROOH	Organic hydroperoxide
ROS	Reactive oxygen species
PI3K	Phosphoinositide 3-kinase
SDS-PAGE	Sodium dodecyl-sulfate polyacrylamide gel electrophoresis
SOD2	Manganese superoxide dismutase
STAT3	Signal transducer and activator of transcription 3
T2DM	Type 2 Diabetes Mellitus
T1DM	Type 1 Diabetes Mellitus
TGF-β1	Transforming growth factor- β1
V	Voltage

ABSTRACT

Introduction: The exponential rise in the global prevalence and incidence of type 2 diabetes is concerning. Hyperglycemia is a hallmark of type 2 diabetes that induces oxidative stress, leading to impairment of vital liver metabolic pathways. Metformin is the first-line treatment for type 2 diabetes mellitus. However, *Momordica foetida* has been used in folk medicine for the treatment and management of diabetes mellitus in various parts of the world including South Africa.

Aim: In the present study, the cytoprotective effects of *M. foetida* on liver impaired glucose metabolism and oxidative stress damage were investigated on high glucose induced HepG2 cells, with Metformin as a positive drug control.

Methods: The *M. foetida* leaves were used to prepare an aqueous lyophilized extract. The HepG2 cells were serum starved for 1 hour, then exposed to hyperglycemic conditions (30mM D-glucose) for 24 hours. Cells were treated with various concentrations (125 - 1000 µg/ml) of the lyophilized *M. foetida* aqueous extract for 24 hours, and the 3-(4,5-dimethylthiazol-2-yl)-2-5-diphenyltetrazolium bromide (MTT) assay evaluated the effects of high glucose and *M. foetida* on the metabolic activity of HepG2 cells. Antioxidants and pro-oxidants were assessed and quantified using luminometry, thiobarbituric acid reactive substances (TBARS) and nitric oxide synthase (NOS) assays. Western blot and quantitative real-time (qPCR) were used to observe the effects high glucose and *M. foetida* on signaling pathways and antioxidant response.

Results: Glucose uptake in hyperglycemic conditions was mediated by increased gene expression of adenosine monophosphate-activated protein kinase alpha 2 *(AMPK*α2) (p<0.05) and *phosphatidylinositol 3-kinase (PI3K)* (p<0.05), but *glucose transporter 2 (GLUT2), glucokinase (GK) and glycogen synthase (GS)* were downregulated (p<0.05). Interestingly, an opposing response was noted for Metformin and *M. foetida* treatments, where *AMPKα2* (p<0.05) and *PI3K* (p<0.05) were downregulated, whereas *GLUT2, GK* and *GS* were upregulated (p<0.05) compared to the hyperglycemic control. When compared to the hyperglycemic conditions control, *M. foetida* treatments and Metformin showed an increase in glucose uptake. Hyperglycemic conditions induced toxicity indicated by increased extracellular lactate dehydrogenase (LDH) and decreased adenosine triphosphate (ATP), but Metformin and *M. foetida* decreased LDH activity back to

normoglycemic levels, indicating reduced cytotoxicity. Increased mitochondrial membrane potential ($\Delta\Psi m$) in hyperglycemic conditions was accompanied by increased lipid peroxidation ($p<0.05$) and reactive nitrogen species (RNS) ($p<0.05$). The $\Delta\Psi m$ was increased further by *M. foetida*, with minimal effect on reactive oxygen species (ROS) production but effectively increasing RNS ($p<0.05$). Oxidative damage was reduced in the hyperglycemic control but was increased by Metformin and *M. foetida* treatments prompting the activation of *p53* in these cells ($p<0.05$). Effective oxidative stress response was mounted by *NRF2* ($p<0.05$) and antioxidants SOD2 ($p<0.05$) and GSH, but GPx1 and *CAT* ($p<0.05$) were decreased. Interestingly, Metformin and *M. foetida* induced *CAT* ($p<0.05$) and GPx1 ($p<0.05$) in the antioxidant response, consequently decreasing GSH. Metformin decreased *NRF2* ($p<0.05$) and SOD2, while *M. foetida* increased *NRF2* significantly and had no effect on SOD2 relative to the hyperglycemic control. Hyperglycemic conditions downregulated the oxidative stress response by MAPK (p-p38, pJNK and pERK1/2) ($p<0.05$). However, Metformin upregulated pJNK ($p<0.05$) and pERK1/2 ($p<0.05$), but p-p38 ($p<0.05$) was downregulated. Interestingly, *M. foetida* upregulated pJNK ($p<0.05$), downregulated pERK1/2 ($p<0.05$) and had no effect on p-p38. Hyperglycemic conditions also increased pSTAT3, which was downregulated by Metformin and *M. foetida* treatments ($p<0.05$).

Conclusion: Taken together, the results demonstrated that *M. foetida* enhanced the metabolic activity and reduced cell cytotoxicity in HepG2 cells. Furthermore, *M. foetida* facilitated glucose uptake independent of AMPK2α and PI3K. The main source of oxidative stress was increased RNS, which was alleviated by an effective MAPK/JNK and antioxidant response involving *CAT*.

Key words: T2DM, high glucose, oxidative stress, liver glucose metabolism, *M. foetida,* antioxidants

CHAPTER 1: INTRODUCTION

1.1 Background

Diabetes mellitus (DM) is a class of metabolic disease characterized by chronic hyperglycemia with disorders of protein, carbohydrate and fat metabolism triggered by defective insulin action, insulin secretion or both (Amini *et al*., 2020, Alberti and Zimmet, 1998a). It has been classified into type1, type 2 and gestational diabetes, amongst others (AmericanDiabetesAssociation, 2017). Type 2 diabetes mellitus (T2DM) is characterized by resistance to insulin action and relative insufficient insulin resulting in hyperglycemia, and accounts for about 90% of all types of diabetes around the globe (Galicia-Garcia *et al*., 2020, Yaribeygi *et al*., 2020b, Williams *et al*., 2020). The incidence of T2DM is increasing at an alarming rate in developed and developing countries because of urbanization, physical inactivity, unhealthy diet and obesity (Galicia-Garcia *et al*., 2020, Chatterjee *et al*., 2017b). According to the International Diabetes Federation (IDF), 536.6 million people worldwide were living with diabetes in 2021, with that number anticipated to increase to 643 million by 2030 and 783.2 million by 2045 (Ogurtsova *et al*., 2022, Sun *et al*., 2022). Furthermore, 24 million people in Africa have diabetes in 2021 (Sun *et al*., 2022). This number is anticipated to increase to 33 million by 2030 and 55 million by 2045 (Sun *et al*., 2022). South Africa had the highest number of adults living with diabetes in Africa in 2019 (Kok *et al*., 2021, Williams *et al*., 2020). Furthermore, with 4.2 million adults (20-79 years), South Africa had the highest incidence once again in 2021 (Sun *et al*., 2022). Thus, diabetes is a serious disease that requires intervention.

Maintaining normal plasma glucose and glucose homeostasis is dependent on the liver, which is a significant insulin target organ (Wang *et al*., 2020). Insulin stimulates glycogen synthesis and lipogenesis in the liver, while suppressing glucose synthesis and fatty acid oxidation (Batista *et al*., 2021). Thus, impairment in insulin production or activity leads to tissue inability to take up glucose, resulting in hyperglycemia, a hallmark of T2DM (Rochette et al., 2014b). The binding of insulin to the insulin receptor initiates the mitogen-activated protein kinase (MAPK) cascade and the phosphatidylinositol 3-kinase (PI3K)/protein kinase B (AKT) cascade, which further activate downstream transcriptional factors (Yung and Giacca, 2020). Moreover, the PI3K/AKT cascade regulates cellular responses such as lipid synthesis, protein synthesis, glycogen synthesis and glucose uptake, whereas the MAPK

cascade regulates cell growth and proliferation (Lennicke and Cochemé, 2021, Olivares-Reyes *et al*., 2009a).

Complications of T2DM include failure of various organs, long-term damage and dysfunction (Lee *et al*., 2021, Alberti and Zimmet, 1998b). The adverse effects associated with diabetic complications are primarily induced by inflammation and hyperglycemia-induced oxidative stress (Aslam *et al*., 2019, Dewanjee *et al*., 2009). Oxidative stress prevails when pro-oxidants including reactive oxygen species (ROS) and reactive nitrogen species (RNS) are in excess of antioxidants (Yaribeygi *et al*., 2020b, Tangvarasittichai, 2015b). Oxidative damage in T2DM pathogenesis occurs as a result of impaired cellular defense mechanisms and/or the formation of ROS (Dewanjee *et al*., 2009). Mitochondria are a major source of oxidative stress caused by high levels of glucose, oxygen and ROS produced as a by-product of metabolism (Alkahtani *et al*., 2021).

The superoxide anion ($O_2^{\bullet-}$) is a ROS that is largely formed by NADPH oxidase (NOXs) in the mitochondrial electron transport chain (complex I, II and III) (Sies and Jones, 2020). In the mitochondria, superoxide dismutase (SOD) reduces $O_2^{\bullet-}$ to hydrogen peroxide (H_2O_2) (Lennicke *et al*., 2015). In the Fenton reaction, iron (II) interacts with H_2O_2 to yield hydroxyl radicals ($^{\bullet}OH$), which causes oxidative damage to deoxyribonucleic acid (DNA), lipids and proteins (Zhao, 2019). Of note, H_2O_2 dual properties depend on its localization and concentration (Unuofin and Lebelo, 2020). At low doses, it serves as a secondary messenger, stimulating signal transduction pathway kinases such as mitogen-activated protein kinase (MAPK), extracellular signal-regulated kinase (ERK), p38-MAPK, phosphoinositide 3-kinase (PI3K), protein kinase B (AKT), and signal transducer and activator of transcription 3 (STAT3) (Unuofin and Lebelo, 2020). In contrast, at high concentrations, it acts as an anti-apoptotic agent altering mitochondrial membrane integrity (Unuofin and Lebelo, 2020).

Antioxidant properties include lowering ROS production and increasing cellular antioxidant systems. Therefore, a reduction in antioxidants is one of the significant causes of T2DM pathogenesis (Dewanjee *et al*., 2009). The nuclear factor erythroid 2-related factor 2 (NRF2), a key regulator of antioxidant defense mechanism, promotes the synthesis of

antioxidant enzymes in response to elevated levels of H_2O_2 (Dare et al., 2021, Lennicke et al., 2015). Moreover, NRF2 is activated in response to signal transduction pathways preventing oxidative stress (Sies and Jones, 2020, Lennicke *et al*., 2015). Reduced glutathione (GSH), an intracellular antioxidant, and antioxidant enzymes such as catalase (CAT), superoxide dismutase (SOD), glutathione peroxidase (GPx) detoxify ROS and RNS effectively (Dare et al., 2021, Unuofin and Lebelo, 2020). After SOD2 dismutates $O_2^{\bullet-}$ to H_2O_2, CAT detoxifies it to oxygen and water (Zhu *et al*., 2021, Gounden *et al*., 2015). In addition, GPx reduces hydroperoxides to alcohol and H_2O_2 to water, using GSH as a cofactor (Zhu *et al*., 2021, Gounden *et al*., 2015). Because nitric oxide (NO) is vital in glucose metabolism, low NO levels play a significant role in the pathogenesis of T2DM (Bahadoran *et al*., 2020). Peroxynitrite ($ONOO^-$), an oxidant involved in RNS generation is produced when NO reacts with $O_2^{\bullet-}$ (Unuofin and Lebelo, 2020, Yuan *et al*., 2019). Excess NO and $ONOO^-$ production have also been associated with oxidative stress, enzyme dysfunction, DNA damage and inflammation (Sokolovska *et al*., 2020). Hyperglycemia-induced oxidative stress has been implicated in T2DM microvascular complications such as retinopathy, neuropathy and nephropathy (Asmat *et al*., 2016, Fowler, 2008).

T2DM is treated using insulin therapy and oral hypoglycemic agents (Inzucchi *et al*., 2015). The latter include and are not limited to metformin, sulfonylureas, glinide and α-glucosidase inhibitors (Prasad *et al*., 2020, Wilke *et al*., 2019, Meenakshi *et al*., 2010). To regulate glycemic levels, these oral hypoglycemic agents are being used in polytherapy or monotherapy (Kim *et al*., 2019, Wilke *et al*., 2019, Meenakshi *et al*., 2010). Lactic acidosis, hypoglycemia, renal failure and weight gain have all been documented as side effects of T2DM medicines (Blahova *et al*., 2021). For monotherapy, metformin is still the first-line medicine for T2DM treatment (Cock *et al*., 2021, Inzucchi *et al*., 2015). Conversely, metformin has a range of side effects including prolonged gastrointestinal and poor glycemic regulation (Yang *et al*., 2019). Biguanides and sulfonylureas have been shown in studies to have no effect on the progression of diabetes complications (Pareek *et al*., 2009b). The reactions of patients to these medications vary (Hussain *et al*., 2020). Thus, micro- and macro-vascular injury, secondary complications and immunological variations could all play a role in these variations (Hussain *et al*., 2020). Since ancient times, therapeutic foods have been effectively used to prevent diabetes and its related complications due to their availability, safety and effectiveness (Prasad *et al*., 2020, Dewanjee *et al*., 2009). The medicinal plant antioxidants are well documented and can be used as therapeutic agents

that can scavenge free radicals, thereby preventing diabetes and controlling normal blood glucose (Unuofin and Lebelo, 2020, Nazarian-Samani *et al*., 2018, Rajendiran *et al*., 2018, Sen *et al*., 2010).

Momordica foetida Schumach. et Thonn is an indigenous African medicinal plant that is also known as Bitter cucumber and Nngu in Tshivenda belongs to the Cucurbitaceae family, genus *Momordica* (Oloyede and Aluko, 2012, Maanda and Bhat, 2010). It is a herbaceous perennial climber that is distributed in Africa (Mulholland *et al*., 1997a). *Momordica foetida* is widely distributed in South Africa's sub-tropical regions, including the Vhembe district in Limpopo province (Magwede *et al*., 2019). Commercially, it is cultivated for its nutritional value, and it is often used in folk medicine (Maanda and Bhat, 2010). The leaves of *M. foetida* are harvested and eaten when prepared as a cooked vegetable in Gabon, Sudan, Uganda, Tanzania, South Africa, Malawi and other African countries (Maanda and Bhat, 2010). The leaves can be stewed with other vegetables or used as a meat sauce with peanuts and honey (Maanda and Bhat, 2010).

The roots and leaves are traditionally used for the treatment of headache, stomachache, earache, coughing, intestinal problems, boils and smallpox (Muronga *et al*., 2020, Mulholland *et al*., 1997a). *Momordica foetida* is utilized for the treatment of various ailments such as diabetes, malaria symptoms, hypertension and fever (Baharvand-Ahmadi *et al*., 2016b, Pareek *et al*., 2009b, Abo *et al*., 2008a). Crude extracts have been shown to have anti-diabetic, antiviral, antilipogenic, antiplasmodial, antimicrobial, antimalarial, anthelmintic bioactivity, antioxidant and chemopreventative properties in pharmacological studies (Baharvand-Ahmadi *et al*., 2016b, Semenya *et al*., 2012b, Abo *et al*., 2008a, Narendhirakannan *et al*., 2005b, Mulholland *et al*., 1997b). Because of its high content in phenolic and flavonoid compounds, *M. foetida* aqueous extract has antioxidant activity (Semenya *et al*., 2012b). It is used to treat stomachache because of its hypoglycemic properties which decrease the amount of glucose in the bloodstream while also stimulating appetite and assisting in the process of digestion (Muronga *et al*., 2020).

This study was undertaken to evaluate the cytoprotective effect of *M. foetida* on hyperglycemia-induced oxidative stress in HepG2 cells.

1.2 Problem statement / Rationale

Diabetes mellitus (DM) is a non-communicable metabolic disease with high incidence and mortality rates (Yaribeygi *et al*., 2020b). The incidence and prevalence of type 2 diabetes (T2DM) have increased globally over the years (Motala *et al*., 2022, Sun *et al*., 2022, Williams *et al*., 2020). In 2021, 24 million individuals were estimated to have DM in Africa, with South Africa accounting for 4.2 million (Sun *et al*., 2022). T2DM affects all vital organs, including the kidney, cardiovascular system and liver (Abdollahi *et al*., 2021, Alam *et al*., 2014). Insulin resistance in the liver causes hyperglycemia and consequently disrupts glucose metabolism in T2DM (Demir *et al*., 2021, Mu *et al*., 2019, Mohamed *et al*., 2016). Abnormal inflammatory response and enhanced oxidative stress stimulate pro-apoptotic gene transcription and damage hepatocytes, which contributes to diabetic liver damage (Mohamed *et al*., 2016). Moreover, uncontrolled hyperglycemia causes kidney failure due to functional changes in the nephron and hemodynamic dysregulation (Singh *et al*., 2022, Badal and Danesh, 2014). The current drugs used to treat T2DM in the sub-Saharan Africa public health care sector includes insulin, metformin and glibenclamide (Prasad *et al*., 2020, Kim *et al*., 2019, Wilke *et al*., 2019, Inzucchi *et al*., 2015, Meenakshi *et al*., 2010). Although antidiabetic treatments are frequently beneficial, current treatments have adverse side effects and are ineffective in reducing clinical complications (Cock *et al*., 2021, Bahmani *et al*., 2014, Meenakshi *et al*., 2010, Venkatesh *et al*., 2010). For many years, folk medicine has used a variety of medicinal plants in the treatment and management of T2DM (Bourebaba *et al*., 2021, Kumar *et al*., 2021, Karigidi *et al*., 2020, Bahmani *et al*., 2014, Pareek *et al*., 2009b). In addition to accessibility and affordability, medicinal plants contain secondary metabolites that are responsible for therapeutic effects. It is therefore imperative that more studies are conducted on medicinal plants for the treatment and management of T2DM. Addition to the herbal medicine database is imperative so that they can be made available to the public, potentially leading to the development of effective and affordable plant-based drugs with fewer side effects.

1.3 Significance / Implications

Majority of people in developing and underdeveloped countries cannot afford basic care. Diabetes mellitus is a global epidemic, and the treatments are expensive. Medicinal plants are a viable solution in such countries, especially in rural areas as they are easily accessible at no cost. *Momordica foetida* is used to treat T2DM in the Limpopo province of South Africa. Furthermore, the leaves of *M. foetida* have been found to be a potential source of antioxidants. However, its effects against hyperglycemia-induced oxidative stress and

associated damage that promotes diabetic complications are not known. Understanding the hypoglycemic, antioxidant and anti-inflammatory effects of *M. foetida* will help and add more insights to the practice of traditional medicine. The findings could serve as a foundation for future ethnopharmacology studies on the benefits of *M. foetida* in T2DM management. In addition, the cultivation of *M. foetida* will be beneficial to society and the economic growth of South Africa.

1.4 Research questions

- Does hyperglycemia induce oxidative stress in HepG2 cells?
- Does *M. foetida* inhibit hyperglycemia in HepG2 cells, and by what mechanism?
- Does *M. foetida* inhibit the hyperglycemia-induced oxidative stress in HepG2 cells?

1.5 Hypothesis

Momordica foetida ameliorates hyperglycemia-induced oxidative damage in HepG2 cells.

1.6 Aim

To investigate the effect of hyperglycemia on the induction of oxidative stress in HepG2 cells, as well as the ability of *M. foetida* to ameliorate the effect of hyperglycemia-induced oxidative stress.

1.7 Objectives

To evaluate the effects of *M. foetida* on glucose homeostasis in HepG2 cells under hyperglycemic conditions by determining the

- effect on glucose homeostasis by
    - assessing glucose uptake in treated cells
    - observing the effect on signaling pathways using western blotting (pERK/ERK, p-p38/p38, pSTAT3/STAT3, pJNK/JNK) and qPCR (*PI3K, AKT, AMPKα_2, GLUT2, glucokinase, glycogen synthase*)
- induction of oxidative stress by
    - measuring pro-oxidant production using the TBARS, as well nitrate and nitrite levels with the NOS assay
    - quantifying antioxidant expression using luminometry (GSH) and western blotting (SOD2, catalase and GPx) and qPCR (*NRF2*)

CHAPTER 2: LITERATURE REVIEW

2.1. The liver control of glucose homeostasis

2.1.1 Structural organisation of the liver

In an average adult, the liver makes up 2% of body weight and is slightly heavier in men than in women (Mahadevan, 2020). It is located in the upper abdominal cavity's epigastrium, where it functions as the largest multifunctional abdominal organ (Chaudhari *et al*., 2017). The falciform ligament divides the liver externally into a smaller left lobe and a larger right lobe (Sibulesky, 2013). The right lobe of the liver contains the caudate and quadrate lobes (Chaudhari *et al*., 2017). There are three primary networks in the liver (Figure 2.1A): one outlet (hepatic vein), hepatocytes (metabolic epithelial cells) and two inlets (portal vein and hepatic artery) (Lorente *et al*., 2020). The inlets transport deoxygenated blood and oxygenated blood to the liver respectively (Lorente *et al*., 2020). The liver's smallest functional units, the lobules (Figure 2.1B), are formed by hepatocyte cords and sinusoids (Lorente *et al*., 2020). The filtration and metabolic functions are performed by cells in the porous lobule system (Lorente *et al*., 2020). The sinusoids (Figure 2.1B, C), which are evenly distributed throughout the liver, make up the hepatic microcirculation (Lorente *et al*., 2020). In the sinusoids (Figure 2.1B, C), deoxygenated and oxygenated blood mix and are subsequently carried to the hepatic vein (Lorente *et al*., 2020). The role of sinusoid cells includes defense, filtration, fat storage and phagocytosis (Scott *et al*., 2004, Sasse *et al*., 1992). Hepatocytes are the primary cellular unit of the liver, accounting for 60% of its volume (Dutta *et al*., 2021, Touboul *et al*., 2012). Hepatocytes are responsible for metabolizing drugs, blood purification, intermediate metabolic activities, synthesis of coagulation factors and bile synthesis, storage and secretion (Dutta *et al*., 2021, Schulze *et al*., 2019, Tabibian, 2014, Washabau and Day, 2012).

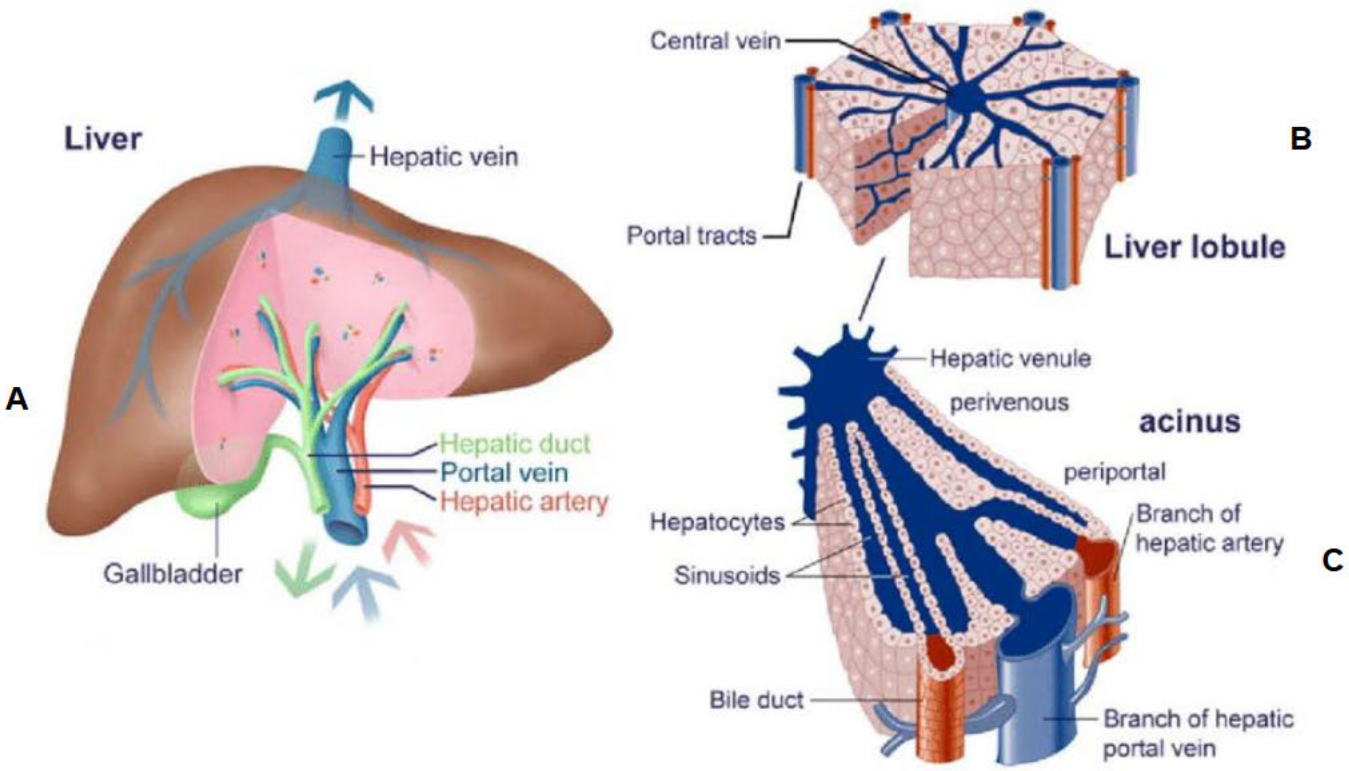

Figure 2.1: A) Gross structure of the liver showing the blood supply to the liver. At the microscopic level, the smallest functional unit of the liver is the lobule **(B)**, which is comprised of multiple acini **(C)** with rows of hepatocytes separated by sinusoids (Adapted from (Cunningham, 2003)).

2.1.2 Functions of the liver

Xenobiotic metabolism, detoxification of drugs, glucose and lipid metabolism are the main metabolic functions of the liver (Chiang, 2014). The liver receives nutrients, hormones, medicines and metabolites from the small intestine via the enterohepatic circulation; similarly, bile acids are transported from the liver to the small intestine (Chiang, 2014). The liver is the sole organ that converts cholesterol to bile acids; modifications in bile acid homeostasis are associated with inflammation and pathogenesis of metabolic diseases like non-alcoholic fatty liver disease, as well as defects in hepatic metabolic homeostasis (Chiang and Ferrell, 2018). The liver is also primarily responsible for stabilizing blood glucose levels in the body through its significant role in the storage and production of glucose (Aslam *et al.*, 2019, Roder *et al.*, 2016). The liver stores glucose as glycogen, thus glycogenesis is an important metabolic pathway in the fed state (Roder *et al.*, 2016). Glycolysis, glycogenesis, glycogenolysis and gluconeogenesis are some of the pathways that the liver utilizes to regulate and stabilize blood glucose levels (Alamri, 2018). Within 2-6 hours following meal consumption, glycogenesis takes place (Postic *et al.*, 2004). Conversely, glycogenolysis (glycogen degradation) and gluconeogenesis (synthesis of

glucose from non-carbohydrate sources) takes place during fasting (Figure 2.2A), thus the liver plays a significant role in supplying glucose during fasting (López-Soldado *et al.*, 2020, Rines *et al.*, 2016, Elujoba *et al.*, 2005).

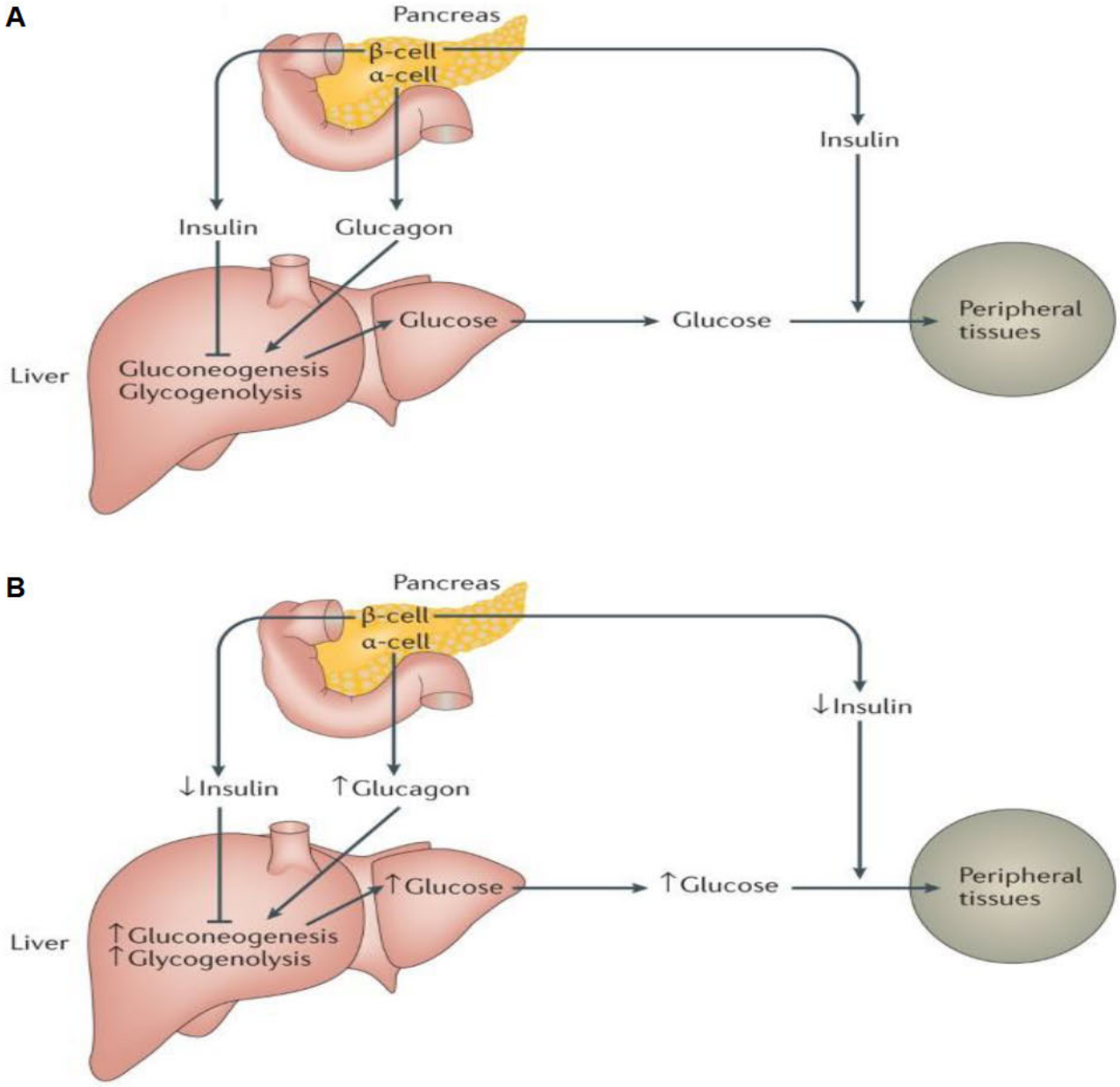

Figure 2.2: Glucose metabolism in the non-diabetic **(A)** and diabetic **(B)** liver. Insulin activity by pancreatic β-cell is reduced in diabetics, however, glucagon action by pancreatic α-cell is increased. Thus, gluconeogenesis, glycogenolysis and glucose release into the bloodstream is promoted by this, while glucose absorption into peripheral tissues is diminished (Adapted from (Rines *et al.*, 2016)).

2.1.3 Glucose transporters

To maintain normal blood glucose levels, glucose transporters (GLUTs) regulate tissue-specific glucose uptake and metabolism in adipose tissue, liver and skeletal muscle (Chadt and Al-Hasani, 2020). The GLUTs are transmembrane proteins that facilitate glucose

diffusion across the plasma membrane (Cholkar *et al*., 2013). In humans, there are 14 GLUTs, with 5 isoforms present in the liver; GLUT1, GLUT2, GLUT5, GLUT8 and GLUT9 (Chadt and Al-Hasani, 2020). GLUT2 is primarily abundant in pancreatic beta cells (β-cells), as well as the liver and kidney (Navale and Paranjape, 2016). In β-pancreatic cells, GLUT2 facilitates glucose entry that results in insulin secretion (Al-Ishaq *et al*., 2019). In contrast, GLUT2 is involved in the absorption and reabsorption of glucose in the tubule cells of the kidney (Navale and Paranjape, 2016). Moreover, GLUT2 promotes glucose uptake in the liver during feeding (prandial state) (Kinsella *et al*., 2021). Following the prandial state, the postprandial state occurs, in which GLUT2 is upregulated to inhibit hyperglycemia and to release stored glucose into the bloodstream during fasting (Kinsella *et al*., 2021). Glucose transporters are therefore vital for the liver to regulate blood glucose (Zhang *et al*., 2019). Hyperglycemia develops in diabetics due to impaired glycogen synthesis, degradation of glycogen and gluconeogenesis, which consequently raises the production of hepatic glucose (Figure 2.2B) (Li *et al*., 2020). In addition, liver disorders such as cirrhosis and liver fibrosis can develop as a result of impaired metabolic activities in the liver (Alamri, 2018).

2.1.4 Regulation of glycogen synthesis in the liver

The regulation of blood glucose homeostasis is facilitated by liver glycogen (Li and Hu, 2020). The liver stores glycogen in the fed state so that a supply of glucose is available during fasting (Li and Hu, 2020). For glycogenesis to occur, glycogen synthase (GS) must be activated and glycogen phosphorylase (GP), which functions in glycogenolysis, must be inhibited (Figure 2.3) (Han *et al*., 2016). During fasting, active and dephosphorylated glycogen synthase kinase 3 (GSK3) phosphorylates GS thereby inactivating it (Figure 2.3). Inhibition of GSK3 is also facilitated by adenosine monophosphate-activated protein kinase (AMPK) and insulin phosphorylation (Han *et al*., 2016, Kasangana *et al*., 2019). In addition, AMPK may increase hepatic insulin sensitivity by activating the PI3K-AKT signaling pathway (Yan *et al*., 2018). Conversely, phosphatases such as protein phosphatase-1 (PP1), catalyze the dephosphorylation of GS, which leads to activation of GS (Figure 2.4) (Li and Hu, 2020). PP1, which can deactivate GP while activating GS, is principally responsible for the reciprocal control of GS and GP (Figure 2.4) (Chen *et al*., 2015). Furthermore, higher glucose 6-phosphate (G6P) concentrations due to hepatic glucokinase (GK) activity allosterically promotes GS, hence increasing glycogen synthesis (Chen *et al*., 2015). The excess glucose also inhibits the enzyme GP, which regulates glycogen degradation (Zhang *et al*., 2019).

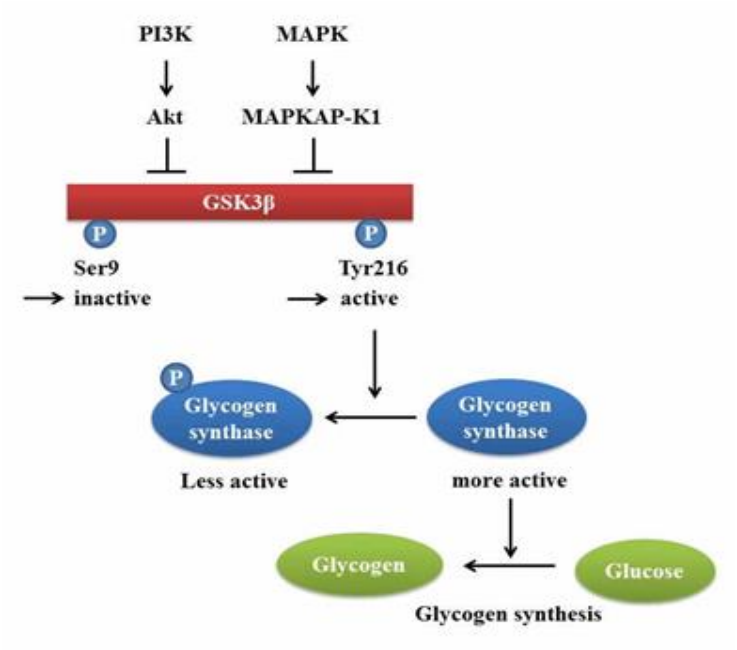

Figure 2.3: Phosphorylation and activation of GSK3β. AKT and MAPKAP-K1 phosphorylate Ser9 of GSK3β, resulting in inhibition of activity. The inhibition of GSK3β decreases the phosphorylation of glycogen synthase, leading to an increase in the active form, since phosphorylated glycogen synthase is less active. As a result, glycogen synthesis is promoted (Adapted from (Han *et al*., 2016, Chen *et al*., 2015)).

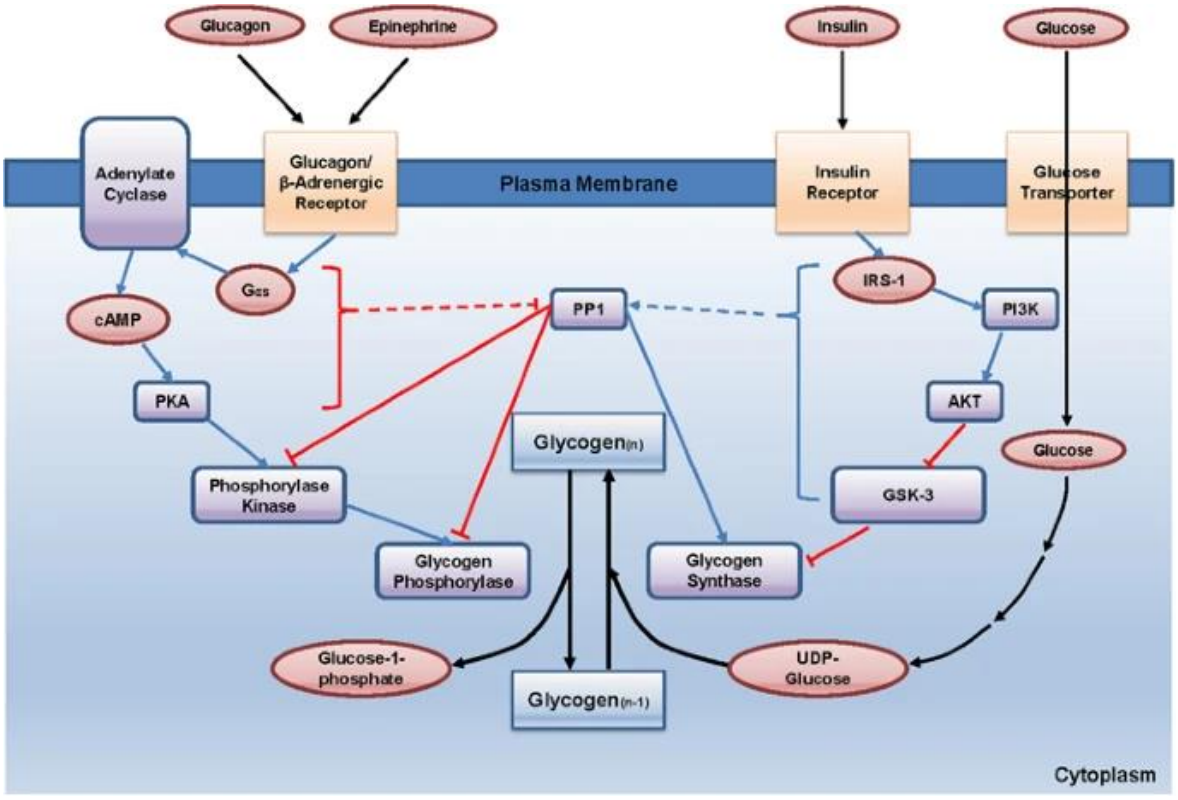

Figure 2.4: Regulation of glycogen synthesis in the liver. Glucagon and epinephrine stimulate the cAMP signaling pathway, which activates PKA, which further phosphorylates phosphorylase kinase and glycogen phosphorylase, inhibiting glycogen synthesis. In the presence of high glucose, insulin binding to the insulin receptor simultaneously stimulates the PP1 pathway and PI3K/AKT pathway, which decreases GSK3 activity, which in turn phosphorylates glycogen synthase, promoting glycogen synthesis (Adapted from (Han *et al*., 2016)).

Hepatic GK is a glucose-phosphorylating enzyme that catalyzes the conversion of glucose into G6P in the liver, and is a vital step in the pentose phosphate, glycogen synthesis and glycolysis pathways (Han *et al*., 2016, Vella *et al*., 2019). In hepatocytes, it functions as a gatekeeper for glucose metabolism (Li *et al*., 2019). In the presence of low glucose concentrations, the GK regulatory protein (GKRP) regulates hepatic GK by binding the enzyme thus inactivating it (Vella *et al*., 2019, Agius, 2016). In contrast, in the presence of fructose and high glucose concentrations, GKRP dissociates from GK consequently activating GK (Agius, 2016). Hepatic GK has emerged as a potential gene therapy-based method for controlling diabetic hyperglycemia due to its allosteric activation that enhances blood glucose absorption and glucose tolerance in the liver (Vella *et al*., 2019, Han *et al*., 2016). Allosteric activators of GK include fructose 2,6-bisphosphatase and 6-phosphofructo-2-kinase (Agius, 2016). Hepatocellular glucose-6-phosphatase (G6Pase) facilitates the conversion of G6P from glycogenolysis and gluconeogenesis to glucose, which may then be released into the bloodstream (Van Schaftingen and Gerin, 2002, Nozaki *et al*., 2020). The G6Pase activity is inhibited by an increase in GS activity (Kasangana *et al*., 2019). Phosphorylation of AMPK regulates glucose homeostasis in the liver by activating GS activity while inhibiting G6Pase (Kasangana *et al*., 2019). The inhibition of oxidative stress and ROS generation is also dependent on AMPK activity; research has shown that activation of AMPK inhibits ROS generation and oxidative stress in endothelial cells via increased expression of antioxidant enzymes in the mitochondria (Wang and Zou, 2018, Yan *et al*., 2018).

In type 2 diabetes mellitus (T2DM), all these physiological pathways are disrupted, resulting in hyperglycemia in the postprandial phase, as well as the fasting phase (Li *et al*., 2019). Since dysfunction of hepatic AMPK plays a role in the initiation and progression of T2DM, it is anticipated that activation of AMPK may aid in the treatment of T2DM (Yan *et al*., 2018).

2.2 Diabetes mellitus

2.2.1 Incidence of diabetes mellitus

Diabetes mellitus (DM) is a non-communicable metabolic disease with high incidence and mortality rates (Yaribeygi *et al*., 2020b). It is the 5th leading cause of mortality across the globe and has been regarded as a silent outbreak (Pheiffer *et al*., 2021, Baharvand-Ahmadi *et al*., 2016a). The incidence of DM is increasing at an alarming rate in developing countries

due to obesity, inactive lifestyle and energy-rich diets (Williams *et al*., 2020, Pareek *et al*., 2009b, Abo *et al*., 2008b). Other risk factors of DM include environmental factors, smoking, genetic predisposition, hypertension and dyslipidemia (Semenya *et al*., 2012a).

In 2019, 463 million people globally were estimated to be living with DM (Chami and Khaled, 2022, Aschner *et al*., 2021, Teo *et al*., 2021, Williams *et al*., 2020). According to the International Diabetes Federation Diabetes (IDF), in 2021, about 536.6 million people worldwide suffer from DM (Ogurtsova *et al*., 2022, Sun *et al*., 2022). This number is expected to rise to 643 million by 2030 and 783.2 million by 2045 (Ogurtsova *et al*., 2022, Sun *et al*., 2022). In 2021 about 24 million people were estimated to have DM in Africa (Sun *et al*., 2022). It is predicted that the number will rise to 33 million in 2030 and 55 million in 2045 (Sun *et al*., 2022). In addition, the number of men living with DM was a bit higher than in women, 17.7 million more with the prevalence of 10.8% (men) and 10.2% (women) (Sun *et al*., 2022). South Africa was reported to have the highest incidence of DM in the African region in 2019 (Kok *et al*., 2021, Williams *et al*., 2020). South Africa had 4.2 million people living with DM in 2021 (Figure 2.5B), with the prevalence of 10.8% (20-79 years) (Atlas, 2021, Sun *et al*., 2022). Of note, in 2021 6.7 million adults (20-70 years) were estimated to have died from DM and its complications (Sun *et al*., 2022). Diabetes was also responsible for 416 000 mortalities in Africa (Atlas, 2021). Furthermore, women's mortality rates were higher than men's (Atlas, 2021, Sun *et al*., 2022).

The sociodemographic prevalence of DM in South Africa was last published in 2016 (Lee *et al*., 2021, Pheiffer *et al*., 2021). Lee *et al*. (2021) reported that the prevalence of DM was significantly higher in females than in males and increased with age. Furthermore, black Africans are the most commonly diagnosed ethnic group, followed by coloured and white ethnicities (Lee *et al*., 2021). The rising prevalence of DM is due to urbanization and being overweight or obese (Lee *et al*., 2021). There is still difficulty in the management of DM in both adults and children globally and effective treatment is yet to be developed (Narendhirakannan *et al*., 2005a).

A

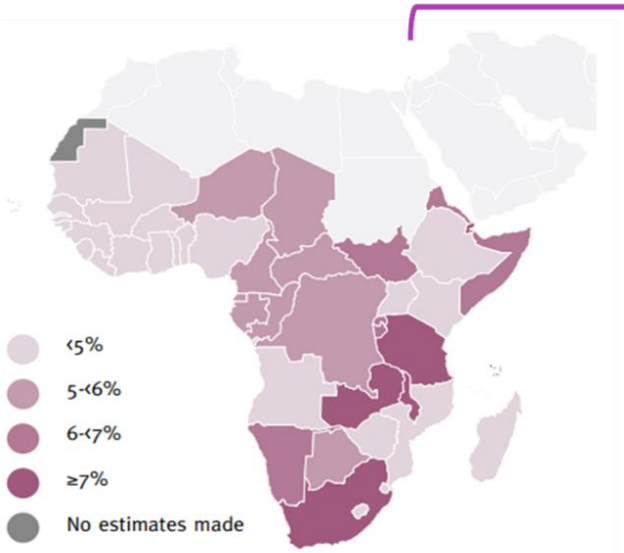

Top 5 countries for age-adjusted prevalence of people with diabetes (20–79 years)	2011	2021
United Republic of Tanzania	2.8%	12.3%
Zambia	4.8%	11.9%
Comoros	8.6%	11.7%
South Africa	7.1%	10.8%
Seychelles	12.4%	8.5%

B

Top 5 countries for number of people with diabetes (20–79 years)	2011	2021
South Africa	1.9m	4.2m
Nigeria	3.1m	3.6m
United Republic of Tanzania	472,900	2.9m
Ethiopia	1.4m	1.9m
Democratic Republic of the Congo	730,700	1.9m

Figure 2.5: (A) Prevalence of diabetes mellitus in Africa region. In 2021, diabetes mellitus was estimated to have affected 24 million adults (20-79 years), accounting for 4.5% prevalence. The prevalence is projected to increase to 4.8% and 5.2% in 2030 and 2045 respectively. United Republic of Tanzania, Zambia, Comoros, South Africa, and Seychelles had the highest prevalence between 8.5% and 12.3%. No estimation has been made in Western Sahara. **(B)** Five countries with the highest diabetes incidence in IDF African region. South Africa had the highest incidence, followed by Nigeria. Ethiopia and Democratic Republic of Congo had the lowest incidence of diabetes (Adapted from (Sun *et al*., 2022)).

2.2.2 Pathogenesis of diabetes mellitus

DM is characterized by elevated blood glucose levels (hyperglycemia) resulting from insufficient insulin production, insulin resistance, or both (Amini *et al*., 2020, Alberti and Zimmet, 1998a). Insulin, a hormone produced by pancreatic beta cells of the islets of Langerhans, regulates glucose, lipid and protein metabolism (Magkos *et al*., 2010, Joshi *et al*., 2007). It increases glucose uptake in muscle and inhibits adipose tissue lipolysis, as well as muscle and whole-body proteolysis (Magkos *et al*., 2010). Moreover, insulin inhibits the production of hepatic glucose and triglyceride oxidation (Batista *et al*., 2021, Magkos *et al*., 2010). Insulin regulates the amount of glucose in the blood by allowing glucose to enter fat and muscle cells via GLUT4 transporters (Asmat *et al*., 2016). Glucose is then converted to energy, which is stored in the cells (Rochette et al., 2014b). GLUT2 expression is reduced in most organs, including the liver, in T2DM patients (Zhang *et al*., 2019). Glycogen synthase (GCS) activity is inhibited in T2DM patients, which impairs the ability of hepatocytes to store glycogen (Zhang *et al*., 2019).

2.2.2.1 Insulin signaling

Insulin binding to the extracellular α-subunit of its cognate receptor initiates the insulin signaling cascade (Figure 2.6), thereby resulting in the autophosphorylation of various tyrosine residues in the beta-subunit (Batista *et al*., 2021, Rains and Jain, 2011). In succession, the activated insulin receptor (IR) phosphorylates insulin receptor substrate proteins (IRS proteins) which leads to the activation of Ras–mitogen-activated protein kinase (MAPK) and PI3K–AKT signaling pathways (Lennicke and Cochemé, 2021, Taniguchi *et al*., 2006). IRS1/2 activation is inhibited by reduced tyrosine phosphorylation and elevated serine phosphorylation, impeding further activation of the PI3K/AKT pathway (Yung and Giacca, 2020). At the plasma membrane, tyrosine-phosphorylated IRS1/2 recruits the heterodimeric p85/p110 PI3K, which generates the lipid second messenger phosphatidylinositol triphosphate (PIP3) thus inducing a serine/threonine phosphorylation cascade of pleckstrin homology domain (PH-domain) containing proteins (Saltiel, 2021). The serine/threonine-AKT, phosphoinositide-dependent protein kinase 1 (PDK1) and atypical protein kinases C λ and ζ isoforms (aPKC) are recruited to the plasma membrane by PIP3 via the PH domain (Saltiel, 2021, Fröjdö *et al*., 2009). AKT and aPKCs are activated when PDK1 phosphorylates a threonine residue in the catalytic domain's activation loop (Fröjdö *et al*., 2009). When these kinases are activated many insulin responses occur (Figure 2.6), including lipogenesis through up-regulation of the synthesis of the fatty acid

synthase gene, glycogen synthesis through phosphorylation of GSK3 and GLUT4 translocation to the plasma membrane (Rains and Jain, 2011).

The insulin-stimulated translocation of the GLUT4 at the plasma membrane is regulated by AKT, leading to elevated glucose uptake (Mancusi *et al*., 2020). When IRS1/2 is activated, it recruits Grb2, which binds to SOS and initiates the extracellular signal-regulated kinase (Erk1/2) MAPK pathway (Figure 2.5) (White and Kahn, 2021, Rains and Jain, 2011). The p38 mitogen-activated protein kinases (p38-MAPK) and Jun N-terminal kinase (JNK) stress-activated kinases have been reported to be phosphorylated in response to insulin, even though their activation is primarily dependent on inflammatory cytokines and stress signals (Yung and Giacca, 2020). Defects in the insulin signaling pathway have been linked to insulin resistance (Naicker *et al*., 2016). Hyperglycemia causes insulin resistance by promoting the formation of reactive oxygen species (ROS), which impede insulin-induced tyrosine autophosphorylation of IR (Mancusi *et al*., 2020).

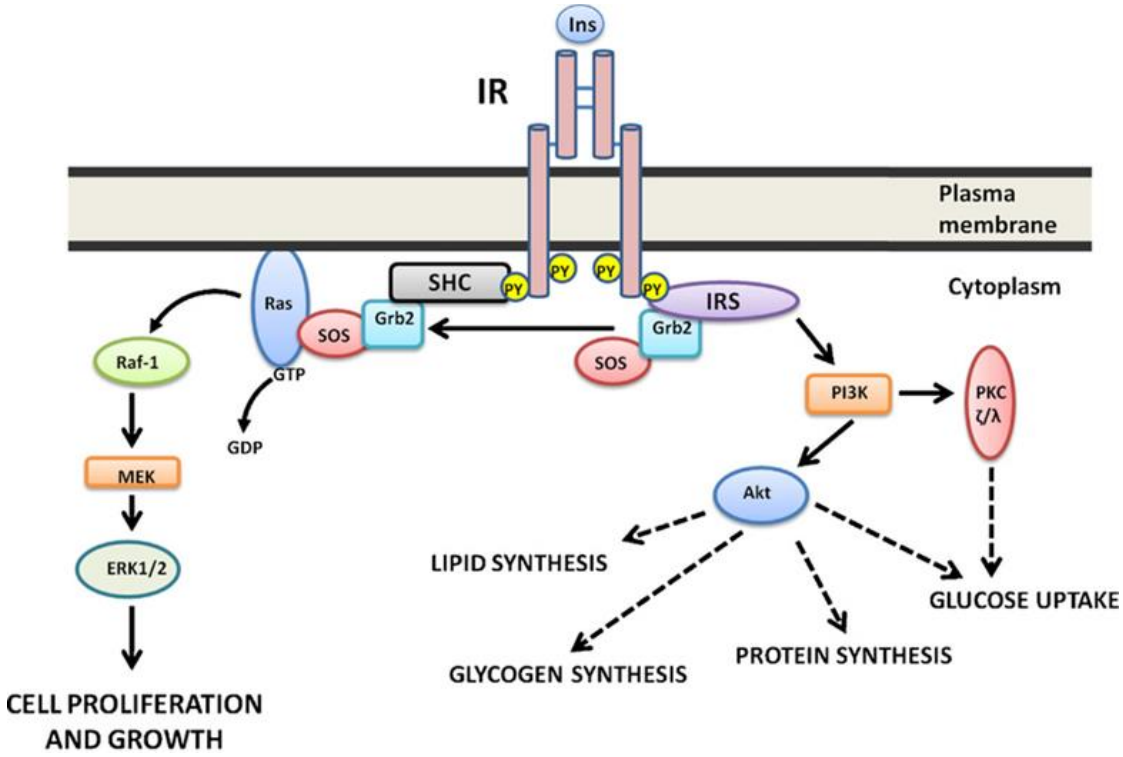

Figure 2.6: Insulin signaling pathway. Insulin binding to the alpha subunit of the insulin receptor causes a conformational change in the insulin receptor (IR). As a result, the tyrosine residue on the B subunit is auto-phosphorylated. The phosphorylated tyrosine also phosphorylates IRS-1 and Src homology and Collagen (SHC). Growth factor receptor-bound protein 2 (Grb2) binds to both SHC and IRS-1 docking sites. Grb2 acts as an adaptor protein for Son of Sevenless (SOS). RAS binding to SOS activates the MAPK pathway, which controls the growth and proliferation of cells. When PI3K binds to the IRS subunit, the PI3K pathway is activated and regulates metabolic functions such as lipid synthesis, glycogen synthesis, protein synthesis, and glucose uptake. PI3K also activates protein kinase c (PKC) which induces glucose uptake (Adapted from (Olivares-Reyes *et al*., 2009b)).

Insulin action is not required by the liver during the fasting period (Asmat *et al*., 2016). Defects in insulin production or action result in tissue's inability to take up glucose leading to hyperglycemia, a hallmark of DM (Rochette et al., 2014b). Insulin plays an important role in lipid, carbohydrate and protein metabolism as an anabolic hormone (Rosenbloom *et al*., 2009). Therefore, insulin defects affect the metabolism of carbohydrates, lipids, glucose, glycoproteins and protein (Aslam *et al*., 2019, Kharroubi and Darwish, 2015, Alberti and Zimmet, 1998a).

2.2.2.2 Symptoms of diabetes mellitus

Early symptoms of DM include weight loss, blurred vision, polydipsia and polyuria (Cock *et al*., 2021, Mukhtar *et al*., 2020). The majority of people with diabetes are asymptomatic and may have hyperglycemia for a prolonged period, which might cause some complications before diagnosis (AmericanDiabetesAssociation, 2019). Non-ketotic hyperosmolar and ketoacidosis might occur in cases where DM is uncontrolled leading to stupor, coma and possibly death (Umpierrez, 2020, Dhatariya, 2019, Alberti and Zimmet, 1998a). Hyperglycemia is the prime cause of microvascular (retinopathy, neuropathy and nephropathy) and macrovascular (stroke, peripheral arterial disease and coronary artery disease) complications (Fowler, 2008). Thus, diabetic patients are at high risk of developing cerebrovascular, cardiovascular, and peripheral vascular diseases (Williams *et al*., 2020). Neuropathy and nerve damage may lead to foot ulcers which can result in amputations, while nephropathy may lead to renal failure and retinopathy may lead to blindness (Cock *et al*., 2021).

Patients are also at risk of erectile dysfunction and autonomic neuropathy (Hussain *et al*., 2020). Moreover, sexual dysfunction affects diabetic men at a slightly higher rate than diabetic women and the occurrence increases with age (Wooton and Melchior, 2018). Sexual dysfunction is a common but often overlooked complication of diabetic autonomic dysfunction, which affects the nerve supply to the genitals, which controls arousal (Holloway, 2019, Wooton and Melchior, 2018). Research has shown that oxidative stress is associated with the pathogenesis of DM and its complications (Tang *et al*., 2017). A decrease in antioxidant levels occurs due to an increase in reactive oxygen species (ROS) induced by hyperglycemia (Tang *et al*., 2017). Interestingly, high dietary antioxidant consumption has

been proposed as a promising and cost-effective strategy for erectile function (Akomolafe *et al*., 2018, Mykoniatis *et al*., 2018).

2.2.3 Classification of diabetes mellitus

The American Diabetes Association (ADA) classified DM into 4 categories: type 1, type 2, gestational and other types of diabetes mellitus (AmericanDiabetesAssociation, 2017). Classification of diabetes is challenging especially at an early stage as some patients are asymptomatic (Atkinson *et al*., 2014). Gestational diabetes mellitus (GDM) is characterized as any level of glucose intolerance with first affirmation during pregnancy (AmericanDiabetesAssociation, 2004). Most women with GDM appear to have marked chronic insulin resistance that is instigated by pregnancy (Buchanan and Xiang, 2005). Increased risk of type 1 diabetes after GDM has been linked to markers of islet cell-coordinated autoimmunity while the risk of type 2 diabetes is enhanced by factors like obesity that elevate insulin resistance (AmericanDiabetesAssociation, 2004). Other types of DM are triggered by various factors such as drug or chemical-induced diabetes; utilization of glucocorticoid in post-organ transplant or HIV/AIDS treatment, exocrine pancreas diseases like cystic fibrosis, monogenic diabetes syndromes like maturity-onset diabetes of the young and neonatal diabetes (AmericanDiabetesAssociation, 2017).

According to the IDF, more than 1.2 million children and adolescence worldwide were living with type I DM in 2021, with Europe and South Asia having the highest prevalence and Africa having the lowest incidence (Sun *et al*., 2022). Type I DM (T1DM) is characterized by autoimmune destruction of pancreatic β-cells resulting in absolute insulin loss (Atkinson *et al*., 2014). Environmental factors such as viral infection and an unsuitable diet for infants may also contribute to the fluctuating incidence of T1DM throughout the years (Williams *et al*., 2020, Atkinson *et al*., 2014). Currently, T1DM cannot be prevented (Atkinson *et al*., 2014). People living with T1DM require a daily injection of insulin for survival, thus maintaining the normal blood glucose level (Williams *et al*., 2020).

2.2.4 **Type 2 diabetes mellitus**

Type 2 diabetes mellitus (T2DM) is characterized by hyperglycemia caused by resistance to insulin action and relatively insufficient insulin (Galicia-Garcia *et al*., 2020, Yaribeygi *et al*., 2020b). Reduction of glucose uptake by adipose and muscle tissue and an increase in glucose production in the liver occurs because of insulin resistance (Bahmani *et al*., 2014).

T2DM represents about 90% of all types of diabetes around the globe (Motala *et al*., 2022, Kumar *et al*., 2021, Williams *et al*., 2020). The prevalence of type 2 diabetes is high and rising worldwide, with Asians, Canadians, and Afro-Americans among the populations having the highest frequency (Williams *et al*., 2020, Sun *et al*., 2022). India is considered the epicenter of the T2DM epidemic (Banerjee *et al*., 2019, Pareek *et al*., 2009b, Narendhirakannan *et al*., 2005b). Interestingly, Africa recorded the lowest number of diabetic patients and has the lowest prevalence (Motala *et al*., 2022). According to Motala *et al*., 2022 T2DM is more prevalent in Africans who live in cities than in those who live in rural regions due to factors like unhealthy diet and sedentary lifestyles.

T2DM is commonly diagnosed in obese and overweight adults, but can equally occur in children and adolescents (Dabelea *et al*., 2014). Although it is known that the incidence and prevalence of T2DM in adults have steadily increased, new epidemiological data suggest that the emerging incidence and prevalence of T2DM in children and adolescents is concerning (Sun *et al*., 2022). Even though the majority of obese people do not develop hyperglycemia, a minority of obese people do as they cannot compensate for insulin resistance to maintain normal blood glucose levels due to apoptosis of β-cells, which can lead to the development of T2DM (Rochette et al., 2014a). Furthermore, most obese people do not develop T2DM because hyperinsulinemia can occur, which increases β-cell mass (Rochette et al., 2014a). Thus, they secrete enough insulin to compensate for the level of insulin resistance and regulate glycemia (Al-Goblan *et al*., 2014). There is a direct connection between T2DM and risk factors like sedentary lifestyle, age, obesity, family history, overweight and ethnicity yet the causes are not fully known (Alberti and Zimmet, 1998a, Mukhtar *et al*., 2020, Williams *et al*., 2020). β-cell dysfunction and insulin resistance are induced by both environmental factors and genetic makeup (Unuofin and Lebelo, 2020). Medications such as atypical antipsychotics, thiazide diuretics and glucocorticoids have been reported to increase the risk of T2DM (AmericanDiabetesAssociation, 2017).

The gradual increase of T2DM over the years is associated with physical inactivity, unhealthy diet and obesity (Chatterjee *et al*., 2017). Genetic factors also affect the epidemiology of T2DM; however, it is not the main determinant (Chatterjee *et al*., 2017). Lifestyle intervention to regulate impaired glucose, as well as treatment with metformin and thiazolidinediones, is extensive evidence proposed to impede the progression of T2DM (Kim *et al*., 2019, Chatterjee *et al*., 2017). Unlike type 1 diabetes, type 2 diabetes patients do not

require exogenous insulin for survival (Rosenbloom *et al*., 2009). In nations where customary tests without symptoms are not conducted, the diagnosis of T2DM is usually delayed due to moderate symptoms at the onset (Kharroubi and Darwish, 2015). Untreated hyperglycemia during this period aggravates the occurrence of long-term complications (Kharroubi and Darwish, 2015).

2.2.5 Treatment of type 2 diabetes mellitus

Oral hypoglycemic agents and insulin therapy are primarily prescribed for the treatment of T2DM (Prasad *et al*., 2020, Inzucchi *et al*., 2015). Current oral hypoglycemic agents include metformin, sulfonylureas, glinide and α-glucosidase inhibitors which are used either in polytherapy or monotherapy to regulate glycemic levels (Kim *et al*., 2019, Wilke *et al*., 2019, Meenakshi *et al*., 2010). Metformin is usually the first drug recommended for T2DM (Kim *et al*., 2019, Inzucchi *et al*., 2015). It is the only biguanide drug derived from a plant (Inzucchi *et al*., 2015). Metformin activates AMPK thereby increasing glucose uptake in peripheral tissue, preventing postprandial marked hyperglycemia and reducing the production of hepatic glucose (Inzucchi *et al*., 2015, Cock *et al*., 2021). It is cost-effective; however, it causes vitamin deficiency, abdominal cramping, diarrhoea and dehydration (Inzucchi *et al*., 2015). Sulfonylureas inhibit ATP-sensitive potassium plasma membrane channels of pancreatic β-cells, thereby increasing insulin secretion (Inzucchi *et al*., 2015). Disadvantages of sulfonylureas are weight gain, hypoglycemia and short durability (Inzucchi *et al*., 2015). Biguanides and sulfonylureas have been shown in studies to have no effect on the progression of diabetes complications (Pareek *et al*., 2009b). Thus, current treatments cause adverse side effects and have not been effective in minimizing or preventing clinical complications (Bahmani *et al*., 2014, Meenakshi *et al*., 2010, Venkatesh *et al*., 2010). Moreover, these treatments are often beneficial just during the outset of disease and lose efficiency as the condition progresses (Cock *et al*., 2021). Rural residents have chosen alternatives from traditional healers who use plant-based preparations to treat diabetes since they cannot afford these expensive treatments with adverse effects (Oyedemi *et al*., 2009). In order to develop plant-based therapies for the treatment and maintenance of T2DM, this has intensified the search for medicinal plants with anti-diabetic properties (Cock *et al*., 2021, Pareek *et al*., 2009).

2.3 Medicinal plants

Medicinal plants have been utilized globally as remedies in the treatment and management of a diverse range of ailments (Abo *et al*., 2008b). These medicinal plants are used traditionally without information on the medical properties and constituents they possess (Sagbo *et al*., 2018, Dewanjee *et al*., 2009). In traditional folk medicine, they have been effectively utilized for centuries to produce novel drugs with little or no adverse side effects (Yang *et al*., 2019, Tang *et al*., 2017, Dewanjee *et al*., 2009). In addition, medicinal plants are also cost-effective, readily available and effective (Tang *et al*., 2017, Dewanjee *et al*., 2009, Bahmani *et al*., 2014). The majority of indigenous people in South Africa rely on traditional healers and herbalists for the treatment of infections and diseases such as DM (Oyedemi *et al*., 2009).

Medicinal plants with anti-diabetic properties are used in ethnomedicine and ayurvedic medicine systems (Bourebaba *et al*., 2021, Karigidi *et al*., 2020, Pareek *et al*., 2009a). The efficiency of medicinal plants in managing blood glucose levels and reducing long-term complications in T2DM is well documented (Salleh *et al*., 2021, Karigidi *et al*., 2020, Salehi *et al*., 2019, Bahmani *et al*., 2014, Pareek *et al*., 2009a). Research studies have shown a significant increase in the utilization of medicinal plants; therefore, the cultivation of medicinal plants would be beneficial to society and economic growth (Bourebaba *et al*., 2021, Cock *et al*., 2021). Medicinal plants possess antioxidants such as flavonoids, ascorbic acid (vitamin C), carotenoids, tocopherol (vitamin E), phenolics and tannins (Karigidi *et al*., 2020, Unuofin and Lebelo, 2020, Germoush *et al*., 2019, McCune and Johns, 2002). Polyphenols have been shown to have significant antioxidant properties, either by stimulating the endogenous antioxidant defense response or scavenging free radicals (Kumar *et al*., 2021, McCune and Johns, 2002).

2.3.1 Anti-diabetic medicinal plants

The drumstick tree (*Moringa oleifera*) is widely distributed in subtropical and tropical regions of Africa and Asia (Tang *et al*., 2017). Cambodian *M. oleifera* leaf extracts were reported to decrease hyperglycemia and possess antioxidant properties (Tang *et al*., 2017). Sterculiaceae (*Helicteres isora*), distributed in the Andaman Islands and India, was reported to reduce blood glucose levels and regenerate the liver, as well as the pancreatic islets of diabetic rats, while extracts of wild leek (*Allium ampeloprasum*) from northern Europe and central Asia exhibit anti-oxidant, hypoglycemic and hypolipidemic properties (Rahimi-

Madiseh *et al*., 2017, Venkatesh *et al*., 2010). Black and green tea possess tannins that lower blood glucose levels, but green tea has been reported to contain more antioxidants than black tea (McCune and Johns, 2002). An *in vivo* study of whole plant extracts of Tridax daisy (*Tridax procumbens*) that is widely distributed in India were found to possess anti-hyperglycemic properties and no traits of toxicity were observed (Pareek *et al*., 2009a). *T. procumbens* was observed to be more effective in reducing blood sugar than Glibenclamide, an anti-diabetic medicine prescribed for T2DM (Pareek *et al*., 2009a). A study conducted in the Eastern Cape of South Africa demonstrated that plant extracts of *Strychnos henningsii* and *Leonotis leonorus* were effective in reducing diabetes symptoms such as polyuria and glycosuria with no adverse side effects (Oyedemi *et al*., 2009).

2.3.2 Momordica foetida Schumach. et Thonn

Momordica foetida Schumach. et Thonn, also known as Bitter cucumber and Nngu in Tshivenda, is an indigenous African medicinal plant that belongs to the Cucurbitaceae family, genus *Momordica* (Oloyede and Aluko, 2012, Maanda and Bhat, 2010). It is widely distributed in sub-tropical regions of Africa (Odeleye and Oyedeji, 2008). In South Africa, *M. foetida* is widely distributed in the Vhembe district, Limpopo province (Figure 2.7) (Magwede *et al*., 2019). *M. foetida* is a monoecious perennial vine with green leaves, which have a glabrous surface (Figure 2.8A, B). The leaves (Figure 2.8A, B) are simple, alternate, with no stipules, a widely ovate-cordate to the triangular-cordate blade, and a deeply cordate base (Komakech, 2017). The flowers (Figure 2.8B) have an orange or reddish coloured center and cream white petals (Acquaviva *et al*., 2013, Hyde, 2002). The Ovid of the fruit (Figure 2.8C) is 7.5x5cm with prickles (Hyde, 2002). When the fruit is ripe (Figure 2.8D), it has a bright orange color with black seeds covered by a consumable red pulp (Fern, 2014, Froelich *et al*., 2007).

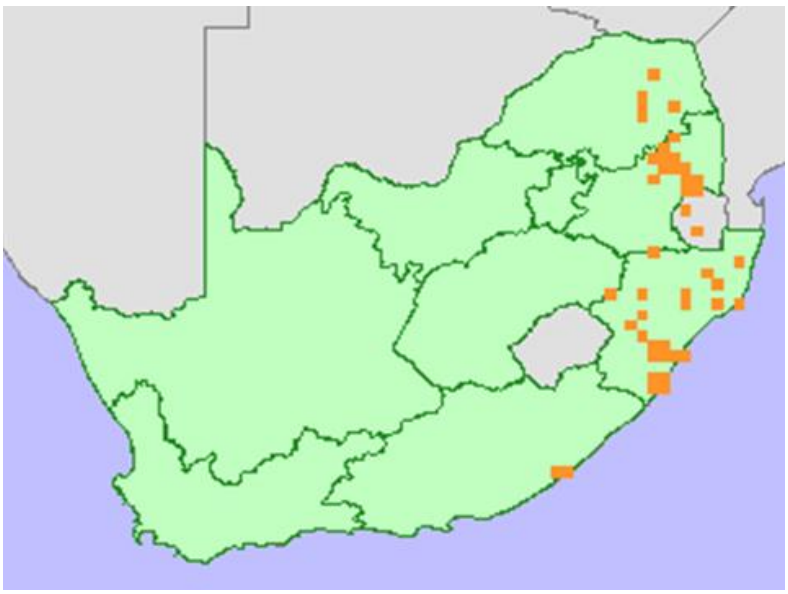

Figure 2.7: Distribution of *Momordica foetida* in South Africa. *M. foetida* is widely distributed in three provinces: KwaZulu-Natal, Limpopo and Mpumalanga, with minimal distribution in the Eastern Cape (Adapted from (Foden, 2005)).

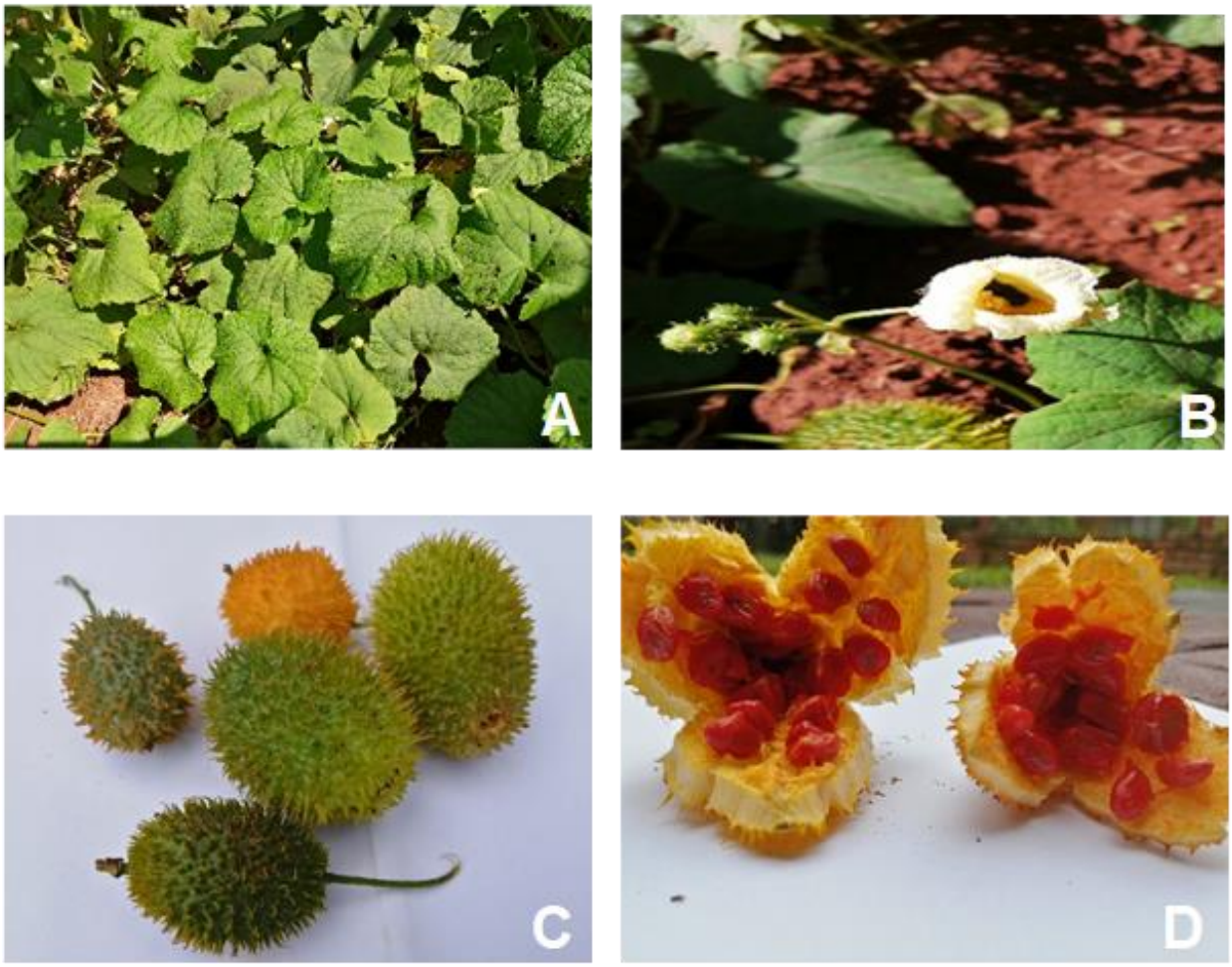

Figure 2.8: *Momordica foetida* morphology appearance. **(A)** matured leaves, **(B)** monoecious flower with white petals and orange center, **(C)** green unripe fruits and orange ripe fruit, and **(D)** ripe fruits with red pulp covering the black seeds (Prepared by author).

2.3.2.1 Phytochemical content of M. foetida

Phytochemical studies demonstrated that *M. foetida* possesses secondary metabolites such as polyphenols, saponins, flavonoids, tannins, alkaloids, steroids and triterpenoids (Soh *et al*., 2020, Odeleye and Oyedeji, 2008). The whole plant was used to extract glycosides and alkaloids, while the leaves were used to extract polyphenolic and curcubitane triterpenoids (Adenike, 2020, Mulholland *et al*., 1997b). A number of bioactive chemicals are found in the *M. foetida* plant, including sitosterylglucoside, 5, 25-stigmastadien3-ylglucoside, and 1-hydroxyfriedel-6-en-3-one (Molehin and Adefegha, 2014, Froelich *et al*., 2007). A recent study demonstrated that Momordiside compounds, 3β-hydroxy-7-oxo-23(R)-cucurbita-5,24-diene-23-O-β-D glucopyranoside and 3β-hydroxy-7β-methoxy-23(R)-cucurbita-5,24-diene-23-O-β-D-glucopyranoside exhibited antioxidant activity (Soh *et al*., 2020).

2.3.2.2 Traditional uses of M. foetida

The bitter leaves of *M. foetida* are added to green leafy vegetables such as kale and stew as spice by the Venda tribe (Magwede *et al*., 2019, Maanda and Bhat, 2010). In Tanzania, Uganda, Gabon, Kenya, Sudan and Ghana the ripe fruit pulp is consumed (Oloyede and Aluko, 2012). *M. foetida* is also consumed by cattle and is appropriate for weight gain in rabbits (Oloyede and Aluko, 2012). In Venda, leaf extracts are used in medicine for the treatment of various ailments (Magwede *et al*., 2019, Maanda and Bhat, 2010). Plant extracts of *M. foetida* may be used for the treatment of boils (Odeleye and Oyedeji, 2008). Leaf extracts are traditionally used in Ethiopia, Uganda and Somalia for the treatment of malaria (Asnake *et al*., 2016, Acquaviva *et al*., 2013). Leaf or root extracts are used by the Zulu tribe in South Africa in the treatment of stomachache, hypertension, and boils (Ndhlala *et al*., 2011, Mulholland *et al*., 1997a). Leaf and root extracts are traditionally used in Cameroon and Uganda for abortion and to facilitate difficult labor (Fern, 2014, Noumi and Djeumen, 2007, Mulholland *et al*., 1997a). The fruit pulp is used in Tanzania as a repellent for moths, ants and weevils (Mulholland *et al*., 1997a). Regulation of blood sugar and blood pressure is achieved by using a decoction of leaves that is administered orally (Mokganya and Tshisikhawe, 2019). The plant has been used traditionally to treat DM (Omokhua-Uyi and Van Staden, 2020b, Zobolo and Mkabela, 2006). Its use has also been reported as a treatment of liver disease and tiredness (Asnake *et al*., 2016). The leaves are crushed and rubbed on areas of the body bitten by the Naja nigricollis cobra just few minutes after the attack to prevent inflammation (Fern, 2014).

2.3.2.3 In vitro and in vivo molecular effects of M. foetida

A pharmacological study revealed that *M. foetida* is an effective antimuscarinic and antinicotinic agent (Odeleye and Oyedeji, 2008). The *M. foetida* plant extracts also inhibit oxidative stress in muscle cells (Maanda and Bhat, 2010). The ability of the aqueous extract of *M. foetida* to inhibit plasma lipid peroxidation *in vitro* and adipogenesis of human mesenchymal stem cells can be directly associated with the aqueous extract's high phenolic content and radical scavenging ability (Omokhua-Uyi and Van Staden, 2020a). In 2008, van de Venter *et al*. published an *in vitro* study that demonstrated an increase in glucose consumption in mouse myoblast muscle cells (C2C12) treated with *M. foetida* whole plant extract (van de Venter et al., 2008). In addition, a recent *in vivo* study demonstrated that various sections of *M. foetida* including the leaves showed hypoglycaemic effects in fasting and alloxan-treated diabetes model rats, while foetidin, an isolated compound from the leaves, only showed hypoglycaemic effects in fasted rats (Omokhua-Uyi and Van Staden, 2020a). The lack of synergistic compounds, which may be present in the whole plant or fruits used in folkloric medicinal preparations, was ascribed to the inadequate action in diabetic rats (Omokhua-Uyi and Van Staden, 2020a). *In vivo* and *in vitro* studies demonstrated that *M. foetida* exhibited anti-malarial properties, conforming to its traditional use by healers and herbalists (Waako *et al*., 2005). Antibacterial, anti-plasmodial, anti-lipogenic and antioxidant properties are documented for *M. foetida* (Odeleye and Oyedeji, 2008, Asnake *et al*., 2016, Waako *et al*., 2005, Soh *et al*., 2020, Acquaviva *et al*., 2013). The anti-inflammatory activity of *M. foetida* is yet to be studied.

2.4 Oxidative stress

Oxidative stress prevails when pro-oxidants in the body are in excess of antioxidants (Yaribeygi *et al*., 2020b, Tangvarasittichai, 2015b). Free radicals are reactive molecules with an unpaired electron that are categorized into reactive oxygen species (ROS) and reactive nitrogen species (RNS) (Sen *et al*., 2010, Devasagayam *et al*., 2004). Free radicals are produced by exogenous substances such as cigarette smoke, pesticides, alcohol, pollution, UV light and ionization radiation (Sen *et al*., 2010). Intracellularly, oxidative phosphorylation is the primary source of free radicals. In addition, RNS and ROS are also produced by macrophages and neutrophils in response due to the increased expression of NADPH oxidase (NOX), NOS, and xanthine oxidase (Leuti *et al*., 2019, Sen *et al*., 2010). Uncoupled endothelial nitric oxide synthase (NOS), xanthine oxidase and NADPH oxidases play a role in the production of ROS (Weseler and Bast, 2010).

Nitric oxide ($NO^{\bullet}$), peroxynitrous acid (ONOOH), nitrogen dioxide (NO_2), and peroxynitrite ($ONOO^{\bullet}$) are examples of RNS, while superoxide ($O_2^{\bullet}$), hydroxyl radical ($^{\bullet}OH$), hydrogen peroxide (H_2O_2), peroxyl radical ($ROO^{\bullet}$), singlet oxygen ($^1O_2$), organic hydroperoxide (ROOH), and ozone (O_3) are examples of ROS (Figure 2.9) (Hussain *et al*., 2020, Unuofin and Lebelo, 2020, Rahimi-Madiseh *et al*., 2017, Devasagayam *et al*., 2004). Free radicals play an important role in apoptosis, homeostasis and cell signaling pathways such as extracellular-signal-regulated kinase (ERK) and mitogen-activated protein kinase (MAPK) (Weseler and Bast, 2010, Cho and Wolkenhauer, 2003). ROS and RNS also act as secondary messengers and are involved in aging and the development of various diseases such as cardiovascular diseases, cancer and diabetic complications (Oloyede and Aluko, 2012, Weseler and Bast, 2010). Metal-binding proteins (ceruloplasmin, lactoferrin, ferritin, and albumin), non-enzymatic oxidants, enzymatic oxidants, phytonutrients and phytochemicals form part of the antioxidant defense system (Sen *et al*., 2010).

Non-enzymatic oxidants include flavonoids, reduced glutathione (GSH), ascorbic acid, α-tocopherol, α-lipoic acid and carotenoids, while glutathione reductase (GR), superoxide dismutase (SOD), glutathione peroxidase (GPx) and catalase (CAT) is part of the enzymatic antioxidants (Figure 2.9) (Ibrahim *et al*., 2021, Cordero-Herrera *et al*., 2015, Morón and Castilla-Cortázar, 2012, Moussa, 2008). Enzymatic antioxidants, which detoxify free radicals, are the first line of defense against these radicals (Kumar *et al*., 2021, Lennicke *et al*., 2015). Antioxidants are important because they neutralize excessively produced ROS, protecting cells from injury and preventing interference with homeostasis (Tang *et al*., 2017, Rahimi-Madiseh *et al*., 2017). Cell damage due to oxidative stress impacts cell function and structure (Asmat *et al*., 2016). Macromolecules such as DNA, lipids and proteins are prone to oxidative damage that leads to permanent modification (Sen *et al*., 2010, Tangvarasittichai, 2015a).

DNA oxidation induces DNA single- and double-strand breaks at oxidized bases (purines and pyrimidines) and abasic sites (apurinic/apyrimidinic site) (Thompson and Cortez, 2020). Due to its low oxidation capacity, guanine is the most vulnerable DNA base (Deavall *et al*., 2012). It is therefore not surprising that the most well-known DNA damage caused by oxidative stress is the formation of 8-hydroxyguanosine (8-OH-G) (Birben *et al*., 2012). The first cellular damage caused by free radical reactions is lipid peroxidation, which is a typical marker of diabetes. ROS can disrupt the lipid bilayer structure in the membrane and

cause lipid peroxidation (Birben *et al*., 2012). These may, in turn, increase the permeability of tissue and inactivate membrane-bound enzymes and receptors (Birben *et al*., 2012). Unsaturated aldehydes and malondialdehyde (MDA) are lipid peroxidation products that may form protein cross-links that inactivate several cellular proteins (Birben *et al*., 2012). MDA is a key biomarker of oxidative stress and lipid peroxidation caused by free radicals (Tiwari *et al*., 2013, Klisić *et al*., 2018). When ROS react with specific amino acids, they produce non-functional, denatured and modified proteins, which can exacerbate oxidative stress (Asmat *et al*., 2016, Tiwari *et al*., 2013). Protein oxidation has several side-chain targets including tyrosine, cysteine, and methionine (Tiwari *et al*., 2013, Birben *et al*., 2012). Protein carbonyls and advanced oxidation protein products (AOPP) are protein oxidation products that are significant biomarkers of oxidative stress (Tiwari *et al*., 2013). Chlorinated oxidants, such as hypochlorous acid (HOCl) and chloramines, react with plasma proteins to generate AOPP during oxidative stress (Gryszczyńska *et al*., 2017). Hence these modified molecules are used as oxidative stress biomarkers in *vivo* and *in vitro* studies (Tangvarasittichai, 2015a).

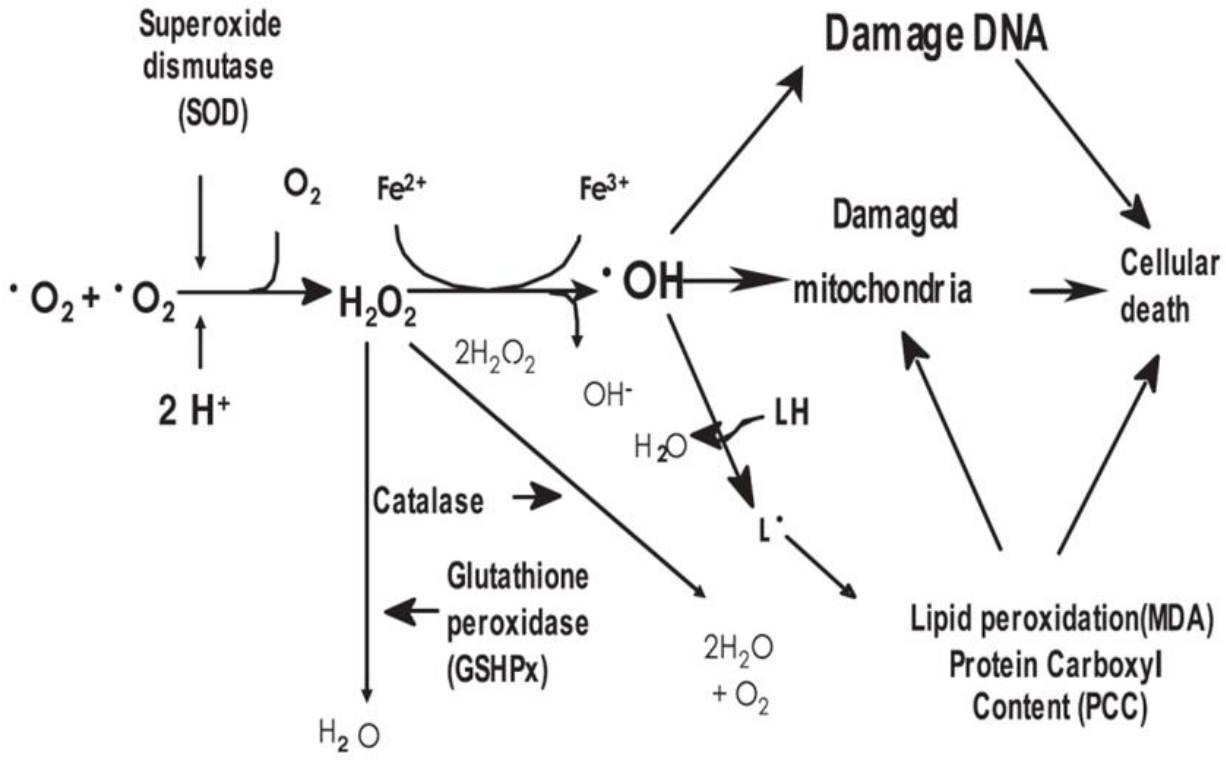

Figure 2.9: Role of antioxidant enzymes in oxidative stress mechanism. Catalase, glutathione peroxidase, and cytochrome C all neutralize H_2O_2. H_2O_2 is neutralized by catalase to $2H_2O$ and O_2, whereas glutathione peroxidase to H_2O. The reaction of H_2O_2 and ferric ions (Fe^{2+}), produces a highly reactive $^{\cdot}OH$ radical is the primary cause of oxidative damage in the cell which leads to cellular death (Adapted from (Morón and Castilla-Cortázar, 2012)).

Intracellular antioxidants GSH, SOD and CAT are also oxidative stress biomarkers (Tangvarasittichai, 2015a). SOD is the main defense enzyme responsible for the direct

removal of ROS (Moussa, 2008). It catalyzes the reaction of $O_2^{\bullet-}$ yielding molecular oxygen and H_2O_2 (Figure 2.9) (Shankar and Mehendale, 2014). Although H_2O_2 has been documented to be very harmful to cells at high concentrations, at low concentrations it controls physiological processes including thiol redox balance, cell proliferation, mitochondrial function, carbohydrate metabolism and cell death (Ighodaro and Akinloye, 2018). Various enzymes are capable of neutralizing H_2O_2; CAT, GPx and other peroxidases like cytochrome c peroxidase and NADH peroxidase are among these enzymes (Nandi *et al*., 2019). Catalase neutralizes H_2O_2 by converting it into water and oxygen (Figure 2.9) consequently ensuring that the molecule remains at its optimal level in the cell which is also essential for regulating physiological processes (Nandi *et al*., 2019, Asmat *et al*., 2016, Maritim *et al*., 2003, Kabel, 2014). CAT is extremely effective, as it can decompose millions of H_2O_2 molecules per second (Ighodaro and Akinloye, 2018, Kabel, 2014). GPx is responsible for the decomposition of H_2O_2 into water and oxygen (Figure 2.9) in mammalian cells' mitochondria since CAT is mostly found in peroxisomes (Ighodaro and Akinloye, 2018). The liver is the principal source of GSH and converts oxidized glutathione to active glutathione via glutathione reductase (Yaribeygi *et al*., 2020b, Gaucher *et al*., 2018). Furthermore, GSH, a co-substrate of GPx, detoxifies lipid peroxides and H_2O_2 to alcohol and water (Dare et al., 2021, Yaribeygi et al., 2020a). Mutations and deficiency of this enzyme are associated with a variety of abnormalities and diseases (Ighodaro and Akinloye, 2018, Nandi *et al*., 2019). NRF2 has been reported as a key regulator of transcriptional genes such as NADPH oxidase-1, oxygenase-1, GPx, SOD, GSH and CAT involved in metabolism and antioxidant defense pathway that protects cells from oxidative stress (Hussain *et al*., 2020, Ding *et al*., 2019, Yuan *et al*., 2019, Wang and Guo, 2019). A deficiency of NRF2 results in severe glucose intolerance decreased insulin signaling, and hyperglycemia (Ding *et al*., 2019).

2.4.1 Oxidative stress in T2DM complications

Hyperglycemia and hyperlipidemia induce the formation of excess ROS (Figure 2.10) by decreasing the production of antioxidants (Tang *et al*., 2017, Rahimi-Madiseh *et al*., 2017, Abo *et al*., 2008b). Increased ROS has been implicated in the development of microvascular complications of T2DM (Asmat *et al*., 2016). Oxidative phosphorylation is the main cause of ROS production in T2DM and its complications (Kumar *et al*., 2021; Moussa, 2008). Oxidative stress disturbs the uptake of glucose by peripheral tissues and insulin signaling, thereby inducing insulin resistance (Yaribeygi *et al*., 2020b). The formation of advanced

glycation end-products (AGEs), hexosamine pathway, diacylglycerol (DAG) and abnormal PKCβ1/2 kinase activation (Figure 2.10) are mechanisms activated by excess production of ROS causing microvascular diabetic complications, insulin resistance and dysfunction of β-cells (Bigagli and Lodovici, 2019, Tangvarasittichai, 2015a).

Long-term hyperglycemia damages kidney and liver tissue because the kidney filters and reabsorbs glucose and the liver is the primary organ that regulates blood glucose levels (Aslam *et al*., 2019). Hepatic antioxidant enzymes that scavenge free radicals decrease oxidative stress in the liver (Aslam *et al*., 2019). Oxidation of RNA and DNA has been observed at the onset of diabetic nephropathy (Wang *et al*., 2017). A recent study indicated that urinary oxidized 8-oxo-7,8-dihydro-2′-deoxyguanosine (8-oxoGuo) could be a potential diabetic nephropathy marker (Wang *et al*., 2017).

ROS triggers the expression of nuclear factor-*k*B (NF-*k*B) (Figure 2.10) which in turn promotes the production of inflammatory cytokines, resulting in the development of diabetic nephropathy (Galicia-Garcia *et al*., 2020, Lee *et al*., 2003). Production of ROS in diabetic nephropathy is induced by transforming growth factor- *β*1 (TGF-*β*1), angiotensin II and AGE, thereby activating elevated glucose signaling (Lee *et al*., 2003). Antioxidants are produced by the body and come from the food consumed (Sen *et al*., 2010). Plant antioxidants are well documented and can be used as therapeutic agents that can scavenge free radicals thereby preventing microvascular complications of DM and controlling normal blood glucose (Aslam *et al*., 2019, Sen *et al*., 2010).

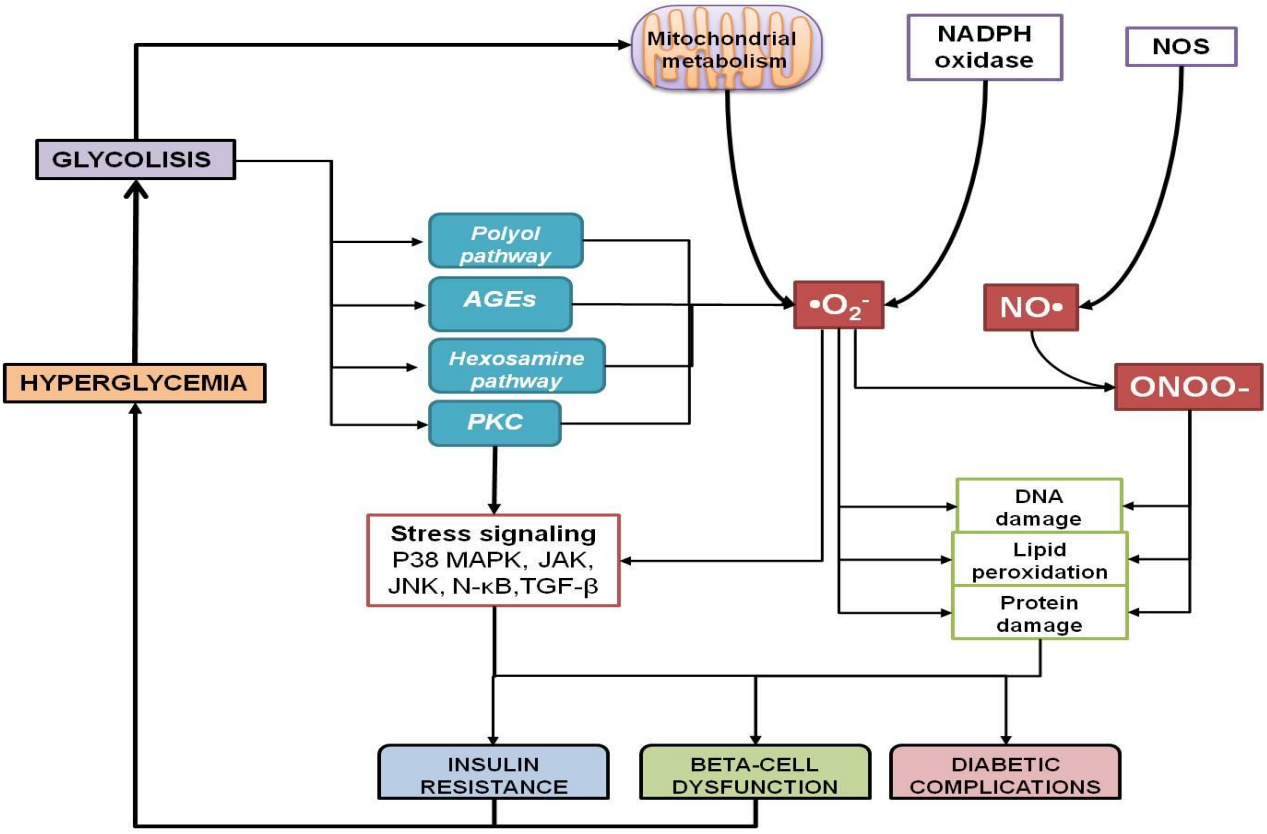

Figure 2.10: Mechanism of oxidative stress in type 2 diabetes mellitus complications. Hyperglycemia causes the production of ROS, which then activates the stress signaling pathway and disrupts DNA, lipid, and protein metabolism, resulting in insulin resistance, beta-cell dysfunction, and diabetes complications (Adapted from (Fernández-Mejía, 2013)).

CHAPTER 3: METHODOLOGY

3.1 Materials

The HepG2 cells were obtained from the Discipline of Medical Biochemistry at the University of KwaZulu-Natal. Cell culture media [Eagles Minimum Essential Medium (EMEM), L-glutamine, penstrep-fungizone, trypsin] were procured from Whitehead Scientific (Cape Town, South Africa (SA)), while plasticware including tissue culture plates, test tubes, micro-centrifuge tubes, 75cm² flasks and luminometer plates were purchased from Merck (Darmstadt, Germany). Foetal bovine serum (FBS) and Pierce™ protease/phosphatase inhibitor were acquired from ThermoFisher Scientific (Johannesburg, SA). Phosphate buffered saline (PBS), methylthiazol tetrazolium (MTT) salt and β-actin (#A3854) from Sigma (St. Louis, Missouri, USA), and dimethylsulfoxide (DMSO) from Merck (Johannesburg, SA). Cytobuster™ protein extraction reagent, bicinchoninic acid (BCA), thiobarbituric acid (TBA), malondialdehyde (MDA), butylated hydroxytoluene (BHT), copper sulphate, sodium nitrate, vanadium (III) chloride (VCl_3), sulphanilamide and N-1-Naphthyl ethylenediamine dihydrochloride (NEDD) were also purchased from Sigma (St. Louis, Missouri, USA). Western blot and PCR reagents were procured from Bio-Rad (Hercules, California, USA), while Cell Signalling Technology (CST, Danvers, Massachusetts, USA) antibodies and Promega products (Madison, Wisconsin, USA) were obtained from Anatech (Johannesburg, SA). The phosphoric acid (H_3PO_4), ethanol, hydrochloric acid (HCl) and butanol were from Merck (Darmstadt, Germany). Bovine serum albumin (BSA) and all primers were obtained from Inqaba Biotech (Johannesburg, SA). All other salts and solvents/acids were purchased from Lasec SA (Pty) Ltd unless stated otherwise.

3.2 Preparation of *M. foetida* aqueous extract

Fresh *M. foetida* leaves were harvested at Sheshe village (district) in Limpopo province and air-dried in the Medical Biochemistry laboratory (University of Kwazulu-Natal, Howard College). The leaves were blended with a laboratory blender at maximum speed to a fine powder. Thereafter, 50g of the leaf powder was added to a beaker containing 500ml of distilled water. The solution was boiled for 15 minutes and allowed to cool. After cooling, the solution was transferred to 10x 50ml falcon tubes. The tubes were centrifuged at 3220xg, 20˚C for 30 minutes. The supernatant was transferred to a freeze-dryer container and stored at -80˚C before being lyophilized using the freeze-dryer (VirTis SP Scientific Sentry 2.0). The

remaining dried extract was used to prepare a stock concentration in cell culture medium (CCM) (5mg/ml), from which all treatments were made.

3.3 Cell culture

The human hepatocellular carcinoma (HepG2) cells were maintained until approximately 80% confluent in a 75cm^2 flask containing CCM (EMEM supplemented with 10% FBS, 1% L-glutamine and 1% penstrep-fungizone) in a 5% CO_2 humidified atmosphere at 37˚C (NUAIRE, Plymouth, USA). To subculture cells, cells were examined under an inverted microscope for confluence and to ensure that no fungal or bacterial contamination occurred. The media was discarded, and the cells were rinsed 3 times with sterile 0.1M PBS. Cells were then trypsinized by adding 1ml of trypsin and monitoring under a microscope to check if the cells have dislodged. Once 90% of the cells were detached, the trypsin was discarded and 2ml of CCM was added to the flask to inactivate the trypsin. The flask was gently tapped on the palm of the hand to dislodge the cells. A cell counting solution was prepared by adding 150µl of CCM, 50µl of cell suspension, and 50µl of trypan blue to a microcentrifuge tube. Thereafter, 10µl of the counting solution was loaded onto a haemacytometer and the cells were counted using an inverted microscope. The number of cells in the cell suspension was determined ($\text{cells/ml} = \text{average cell count x dilution factor x } 10^4$). Thereafter, the cells were diluted as required for the respective assays, dispensed into cell culture plates or flasks, and incubated to allow cell attachment. Alternatively, the cells were stored (2 million cells, 10% DMSO:90% CCM).

3.4 3-(4,5-dimethylthiazol-2-yl)-2-5-diphenyltetrazolium bromide (MTT) assay

3.4.1 Principle

The MTT assay is a colorimetric assay that is commonly used to evaluate cytotoxicity and cell viability (van Meerloo *et al*., 2011, Stockert *et al*., 2018). This assay assesses mitochondrial activity by quantifying the reduction of the tetrazolium MTT salt (yellow) to insoluble formazan crystals (purple) by nicotinamide adenine dinucleotide phosphate (NADPH)-dependent oxidoreductase enzymes (Figure 3.1) (Stockert *et al*., 2018). The insoluble formazan crystals are then solubilized by adding a solubilizing solution such as acidified ethanol or dimethyl sulfoxide (DMSO) and measured using a spectrophotometer at 570nm/690nm (Kuete *et al*., 2017). The number of viable cells correlates with the amount of

formazan yielded; the mitochondrial activity and cell viability are higher as the solution becomes darker (Figure 3.1) (van Meerloo *et al*., 2011).

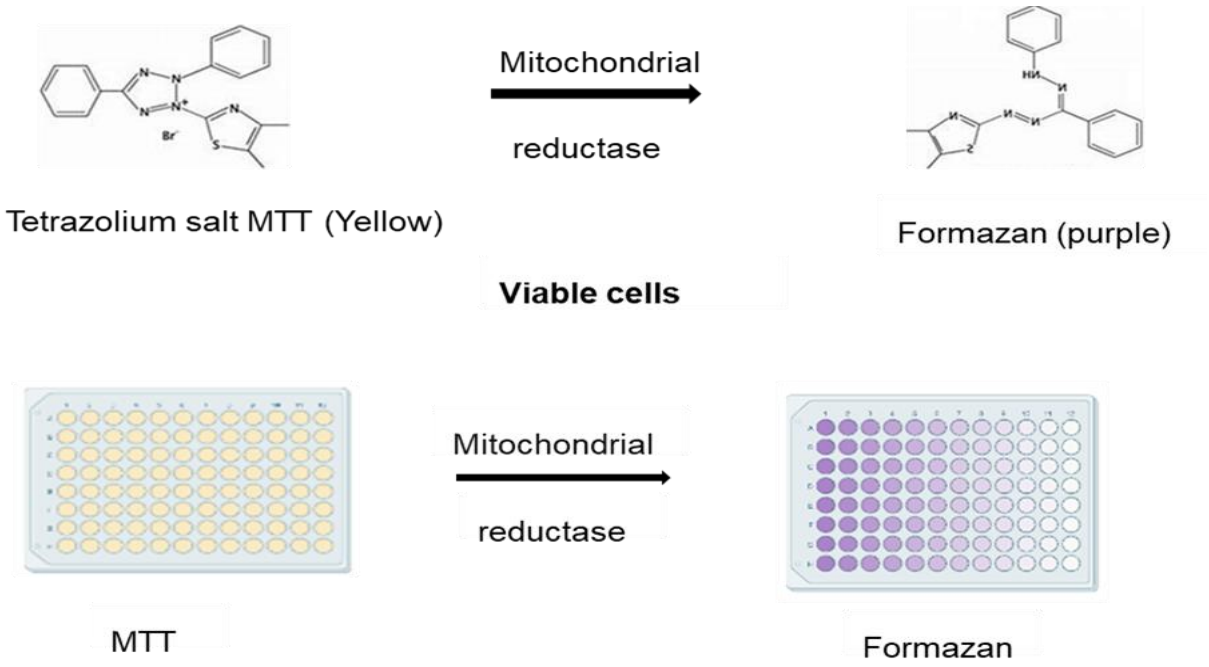

Figure 3.1: The MTT assay principle (adapted from ICBG Project). Tetrazolium salt MTT (yellow) is reduced to insoluble formazan (purple) by NADPH-dependent oxidoreductase enzymes in viable cells (Prepared by author).

3.4.2 Protocol

The MTT assay was used to determine the cytotoxicity of *M. foetida*, and to derive the treatment concentrations for subsequent assays. Confluent HepG2 cells were trypsinised and counted, then seeded into a 96-well microtiter plate (20000 cells / 200µl CCM / well). After adherence was achieved overnight, the CCM was discarded, and cells were starved for 1 hour in a serum-free, low glucose minimum essential medium. Thereafter, except for the control, all cells were equilibrated to hyperglycemic (HG) conditions by incubation in CCM containing 30mM glucose (HG-CCM) for 24 hours. The cells were then treated in triplicate with 125µg/ml, 500µg/ml and 1000 µg/ml *M. foetida* for 24 hours; control cells were untreated (normoglycemia CCM only), hyperglycemic control cells contained HG-CCM only and the positive control received metformin. Following treatment, MTT salt (5mg/ml in PBS) and CCM were mixed (1:4), then equal volumes (120µl) of the resultant MTT solution were pipetted into each well containing treated cells. The plate was incubated at 37˚C, 5% CO_2 (NUAIRE, Plymouth, USA) for 4 hours. After removal of the MTT salt solution, 100µl of DMSO was added to each well and incubated for 1 hour at 37˚C. The plate was then read

using BMG LABTECH SPECTROstar Nano (Ortenberg, Germany) microplate spectrophotometer at 570nm, and 690nm was used as a reference. The absorbance was used to calculate the percentage of cell viability ($\frac{\text{Average absorbance of treated cells}}{\text{Average absorbance of control cells}} \times 100$).

3.5 Treatment of cells

The HepG2 cells were treated in opaque microtiter plates for luminometry, and in flasks for western blotting and qPCR. For luminometry, confluent HepG2 cells were trypsinized and counted, then seeded into a 96-well white microtiter plate (20000 cells / 200µl CCM / well) in triplicate. The plate was incubated overnight to allow the cells to adhere before treatment. For western blotting and qPCR, six 75cm^2 flasks of HepG2 cells were maintained for 48 hours until cells reached approximately 80% confluence. The CCM was discarded from the plates and flasks, and the cells were treated as described below.

The cells were serum starved in serum free media for 1 hour, then hyperglycemia was induced by exposing the HepG2 cells to HG conditions (30mM D-glucose) for 24 hours, with exception of the control (low glucose CCM only). The cells were then treated with the *M. foetida* extract (125µg/ml, 500µg/ml and 1000 µg/ml in CCM) and metformin (100µg/ml; positive control) under HG conditions for 24 hours; the HG control was untreated. After 24 hours, the treatment medium was retained to determine glucose uptake, free radical production and LDH release. The treated cells were used in the luminometry, western blotting and qPCR assays.

3.6 Lactate Dehydrogenase (LDH) assay

3.6.1 Principle

The LDH assay is a colorimetric assay for evaluating cellular cytotoxicity by measuring the amount of LDH released (Aslantürk, 2018a). Lactate dehydrogenase is a stable and soluble cytosolic enzyme that is only released into the neighbouring environment of damaged cells; it is thus used as a cell death marker in a cell culture medium (Man, 2020). Released LDH activity is measured quantitatively in a coupled-enzymatic reaction where tetrazolium salt (INT) is reduced to red formazan salt (Figure 3.2) (Man, 2020). The LDH assay occurs in 2 steps (Figure 3.2); firstly, lactate is reduced to pyruvate thereby reducing NAD to NADH/H$^+$

(Aslantürk, 2018a). Subsequently, diaphorase, a catalyst, transfers H^+ from $NADH/H^+$ to tetrazolium salt (INT) producing red formazan salt (Aslantürk, 2018a). The number of damaged cells in the medium corresponds to the amount of colour produced (Man, 2020). Formazan is measured by spectroscopy at 490 nm (Man, 2020).

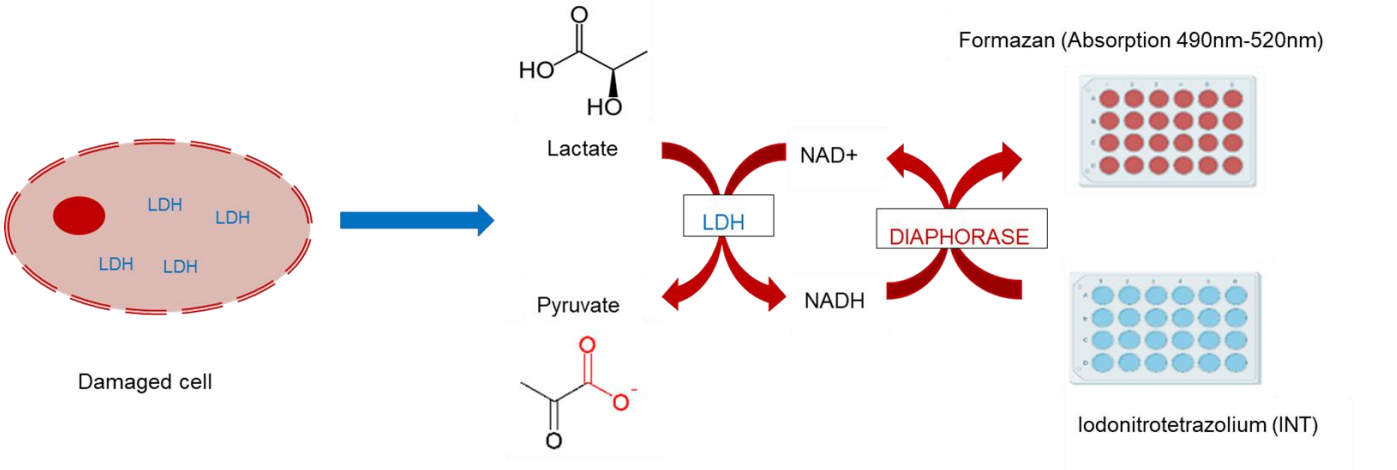

Figure 3.2: LDH cytotoxicity assay. The reaction is involved in the quantification of LDH activity. Reduced INT produces red-coloured formazan salt measured at 490nm by standard spectroscopy (Prepared by author)**.**

3.6.2 Protocol

To investigate cellular cytotoxicity, LDH was measured in the treatment medium using an LDH-Cytotoxicity assay kit (#J2380, Promega, Madison, Wisconsin, United States). Retained treatment medium containing released LDH was added into a 96-well plate in triplicate (50µl per well). A reconstituted reaction mix comprising the diaphorase/NAD^+ substrate and INT/sodium lactate dye solution was prepared as instructed by the manufacturer. The reaction mix was added to each well containing the transferred aliquots and the plate was covered with foil and incubated for 30 minutes at room temperature in the dark. The reaction was halted by adding 25µl of stop solution to the plate. The absorbance was then measured using a BMG LABTECH SPECTROstar Nano microplate spectrophotometer (Ortenberg, Germany) at 490nm, and 600nm was used as a reference. The results were expressed as the percentage of LDH released compared to the maximum LDH released from the untreated control cells.

3.7 Thiobarbituric acid reactive substances (TBARS) assay

3.7.1 Principle

Lipid peroxidation is a mechanism in which free radicals such as reactive nitrogen species (RNS) and reactive oxygen species (ROS) attack carbon-carbon double bonds in lipids (Ayala *et al*., 2014). This process results in a combination of products such as hydroperoxides and lipid peroxyl radicals as the main products, as well as 4-hydroxynonenal and malondialdehyde (MDA) as the predominant secondary products (Ayala *et al*., 2014). Malondialdehyde is a thiobarbituric acid reactive substance (TBARS) that is commonly used as an oxidative stress marker (De Leon and Borges, 2020). The TBARS assay is based on the reaction of the end product of lipid peroxidation, MDA with thiobarbituric acid (TBA) at a high temperature of 95˚C and low pH (1.5), yielding a pink-coloured adduct (Figure 3.3) that is quantified by spectrophotometry at 532nm (De Leon and Borges, 2020).

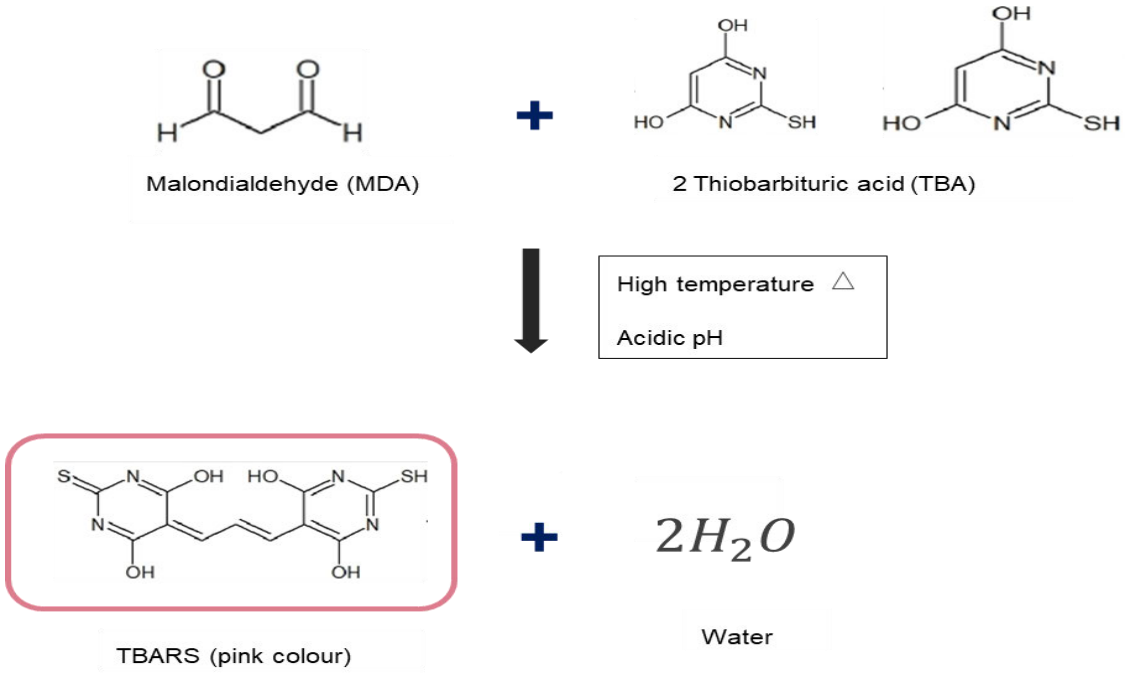

Figure 3.3: TBARS assay. Formation of TBARS by reaction of malondialdehyde with 2-thiobarbituric acid at high temperature and acidic conditions (Adapted from (Ghasemi *et al*., 2007)).

3.7.2 Protocol

Free radical production culminating in lipid peroxidation was measured using the TBARS assay to quantify MDA. A volume of 200µl of each retained treatment media of HepG2 cells [Control: CCM only, HG control, *M. foetida* (125µg/ml, 500µg/ml, and 1000µg/ml) and

metformin] was added into respective test tubes. Method controls were also prepared from fresh CCM; the positive control tube contained 200µl MDA solution (1.38µM), and the blank comprised 200µl CCM only. Thereafter, 200 µl of 7% phosphoric acid (H_3PO_4) was added to each tube, followed by the addition of 400µl of TBA/BHT (10mg/ml TBA in 50mM NaOH containing 0.1mM BHT, from 20mM BHT in ethanol) solution to each sample tube except to the blank, which received 400µl of 3mM HCL. All the glass tubes were then vortexed briefly for optimum mixing (VELP Scientifica Rx3). Thereafter, 200µl of 1M HCL was added to all tubes and boiled on a heating block set to 100˚C for 15 minutes. The samples were allowed to cool at room temperature for 15 minutes. Following the cooling step, 1500µl of butanol was added to all the tubes and the tubes were vortexed for 30 seconds (VELP Scientifica Rx3). The samples were allowed to settle until two distinct phases were observed. A volume of 500µl butanol phase (upper phase) was transferred to labelled microcentrifuge tubes, then 100µl of each sample was transferred into the 96-well microtiter plate in triplicate and the absorbance was measured at 532nm with a reference wavelength of 600nm using a spectrophotometer (BMG LABTECH SPECTROstar Nano, Ortenberg, Germany). The standard formula was used to calculate the mean MDA levels for each treatment as follows:

$$\text{MDA concentration (µM)} = \frac{Sample\ absorbance}{156mM^{-1}} \text{ X } 1000$$

3.8 Nitric oxide synthase (NOS) assay

3.8.1 *Principle*

The synthesis of nitric oxide (NO) from L-arginine is catalyzed by nitric oxide synthase (NOS). Nitric oxide plays an important role in pathological and physiological processes (Ghasemi *et al*., 2007). The low bioavailability of NO is correlated with the development of type 2 diabetes mellitus since NO is involved in the metabolism of carbohydrates (Bahadoran *et al*., 2020). It is hard to measure NO precisely since it is an unstable gas with a short life span (Ghasemi *et al*., 2007). Instead, the concentration of NO end products, nitrate (NOx) and nitrite are measured to estimate the entire NO activity (Ghasemi *et al*., 2007). Nitrate and NOx serve as indicators of NOS activity and could be quantified by ion-selective electrodes chromatography, mass spectroscopy, chemiluminescence, fluorescent and the colorimetric Griess assay (Ghasemi *et al*., 2007, Ghafourifar *et al*., 2008). The principle of this assay relies on the detection of nitrite after NOx has been reduced to nitrite by vanadium chloride (Ghafourifar *et al*., 2008). Nitrite then reacts with Griess reagents

(sulphanilamide and N-(1-naphthyl) ethylenediamine (NEDD)), forming a red-pink coloured that is quantified by a spectrophotometer at 546 nm (Figure 3.4) (Ghafourifar *et al*., 2008).

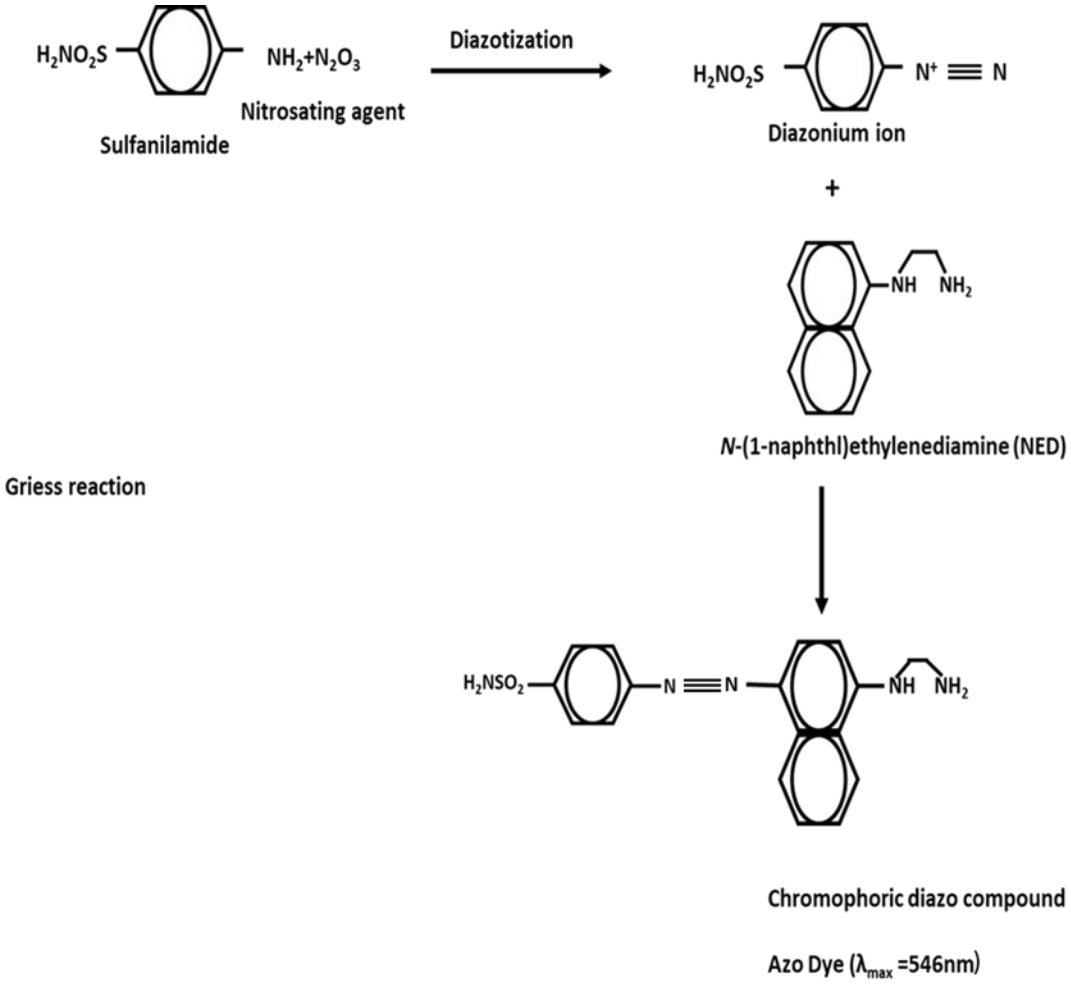

Figure 3.4: Griess reaction. Detection of NO concentration by reaction of nitrite with Griess reagents (Adapted from (Ghafourifar *et al*, 2008)).

3.8.2 Protocol

The NO produced by the HepG2 cells was determined by assaying the levels of NO_2^- using the Griess reagent. For this reaction, 50µl of treatment media was added to a 96-well plate, along with sodium nitrate standards [0; 25; 50; 75; 100; 125; 150; 175; 200µM] in triplicate for each standard and sample. This was followed by the addition of 50µl of vanadium chloride (100mg VCl_3 dissolved in 12.5ml of 1M HCl), 25µl of sulphanilamide (200mg sulphanilamide dissolved in 10ml of 5%HCl, wrapped with foil) and 50µl of N-1-Naphthyl ethylenediamine dihydrochloride (NEDD) (10mg NEDD dissolved in 10ml of dH_2O). After 30 minutes of incubation at room temperature (dark), the absorbance of the reaction mixture was read by a spectrophotometer (BMG LABTECH SPECTROstar Nano, Ortenberg, Germany) at 540nm and 690nm was used as reference. The means of standards were

calculated and used to construct a standard curve, which was used to estimate levels of nitrites and nitrates in the samples.

3.9 Luminometry

Bioluminescence is known as a mechanism of light emission from species and it reflects a chemical transfer of energy into light (Chollet and Ribault, 2012). A multi-step bioluminescence process involving the luciferase enzyme is a process that requires a substrate of luciferin, ATP, oxygen and magnesium cations (Mg^{2+}) (Chollet and Ribault, 2012). Luminometry was used to quantify ATP and GSH, and determine mitochondrial membrane potential ($\Delta\Psi m$); the HepG2 cells were prepared in the same way for each assay.

Briefly, the HepG2 cells (20,000 cells/well) were seeded into an opaque polystyrene 96-well luminometer plate and incubated at 37°C (NUAIRE, Plymouth, USA) overnight to facilitate adherence. The CCM was removed, and the attached cells were serum-starved for 1 hour, then hyperglycemia was induced by exposing the HepG2 cells to HG conditions (30mM D-glucose) for 24 hours, with exception of the control (low glucose CCM only). The cells were then treated with the *M. foetida* extract (125µg/ml, 500µg/ml and 1000 µg/ml in CCM) and Metformin (100µg/ml; positive control) under HG conditions for 24 hours; the HG control was untreated. After 24 hours, the treatment medium was removed, and wells were replenished with 50µl of 0.1M PBS before proceeding with the assays.

3.9.1 ATP assay

3.9.1.1 ***Principle***

Adenosine triphosphate (ATP) is found in all living species and serves as the cell's primary source of energy (Zheng *et al*., 2018). It is involved in signalling, cellular synthesis and mobility (Aslantürk, 2018b). The ATP assay is a rapid, reliable and sensitive assay to determine cell viability (Aslantürk, 2018b). It is based on the oxidation of luciferin by the enzyme luciferase in the presence of intracellular ATP to yield oxyluciferin (Kamiloglu *et al*., 2020; Chollet and Ribault, 2012). Intracellular ATP is directly proportional to the luminescence signal, which is measured by a luminometer (Kamiloglu *et al*., 2020; Chollet and Ribault, 2012).

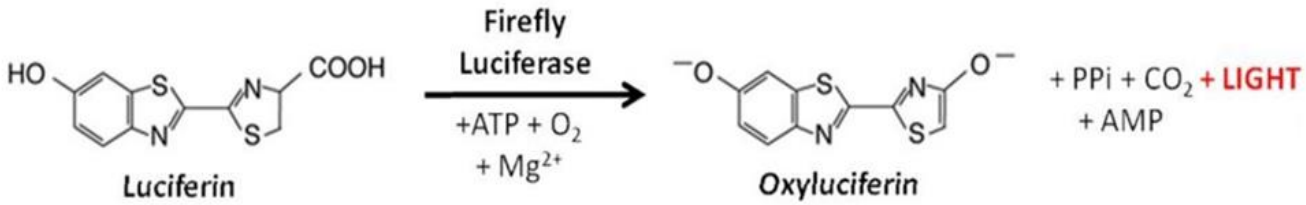

Figure 3.5: ATP-bioluminescence chemical reaction based on the luciferin/ luciferase method emits photons of yellow-green between 550-570 nm (Adapted from (Martin, 2022)).

3.9.1.2 ***Protocol***

The Promega CellTiter-Glo® Luminescent Cell Viability Assay Kit (#G7571) was used to determine ATP levels in HepG2 cells. The CellTiter-Glo® reagents were prepared according to the manufacturer's instructions (ATP detection buffer and ATP detection substrate mix). Thereafter, a 25µl ATP detection reagent was added to each well containing treated HepG2 cells in 0.1M PBS. The plate was incubated in the dark for 30 minutes at room temperature. After incubation, the plate was placed in a Turner BioSystems Modulus microplate luminometer (Sunnyvale, USA), and the luminescence was measured. The ATP concentration was directly proportional to the light emitted by the sample, which was presented as mean relative light units (RLU).

3.9.2 **Glutathione (GSH) assay**

3.9.2.1 ***Principle***

Glutathione is a tripeptide (γ-glutamyl cysteinyl glycine) involved in xenobiotic detoxification, apoptosis, gene expression and signal transduction (Ali *et al*., 2022, Rahman *et al*., 2006). Reduced GSH is the co-factor and electron donor for several antioxidant reactions, including GPx, thioredoxin, and glutaredoxin (Alisik *et al*., 2019, Rahman *et al*., 2006). In the process, the oxidized glutathione disulfide (GSSG) is produced. As a result, oxidized (GSSG) and reduced (GSH) forms serve as a good marker of oxidative stress (Alisik *et al*., 2019). The GSH assay is based on the conversion of Luciferin-NT to Luciferin in the presence of a glutathione-S-transferase enzyme (Figure 3.6) (Rahman *et al*., 2006). The amount of GSH in the sample is directly proportional to the luminescent signal produced (Mehdi *et al*., 2018).

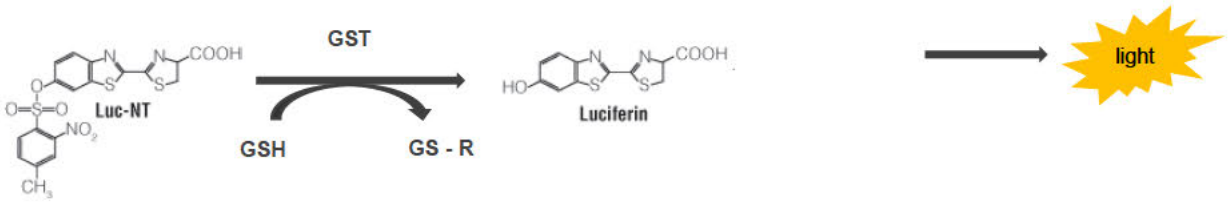

Figure 3.6: Mechanism of firefly luciferase. Glutathione-S-transferase catalyzes the conversion of Luciferin-NT and GSH probe to Luciferin. Adapted from (Promega, 2022).

3.9.2.2 ***Protocol***

The Promega GSH-Glo™ Glutathione Kit (#V6911) was used to detect and quantify GSH in HepG2 cells. The GSH-Glo™ reagent (Luciferin-NT substrate and glutathione-S-transferase in GSH-Glo™ Reaction Buffer) was prepared according to the manufacturer's instructions. Thereafter, 25µl/well of 2X GSH-Glo™ reagent was added to the treated cells in 50µl PBS. Following 30 minutes of incubation at room temperature, 12.5µl of luciferase detection reagent was added and the plate was incubated for 15 minutes at room temperature. The plate was placed in a Turner BioSystems Modulus microplate luminometer (Sunnyvale, USA), and the luminescence was measured. The results were reported as mean RLU.

3.9.3 Mitochondrial integrity

3.9.3.1 ***Principle***

Mitochondria are essential for the synthesis of ROS and ATP (Cowan *et al.*, 2019). This assay evaluates ATP levels as well as changes in cell membrane integrity. Mitochondrial integrity is assessed using a fluorogenic peptide substrate (bis-AAF-R110). A dead cell protease substrate in the media is cleaved by proteases released from cells with compromised membrane integrity (Figure 3.7). Thus, decreased membrane integrity correlates with increased fluorescence. The amount of ATP in the sample is determined by adding the ATP detection reagent, which causes cell lysis by diffusing into the mitochondrial matrix of healthy cells. The luminescent signal produced is proportional to the amount of ATP present (Figure 3.7).

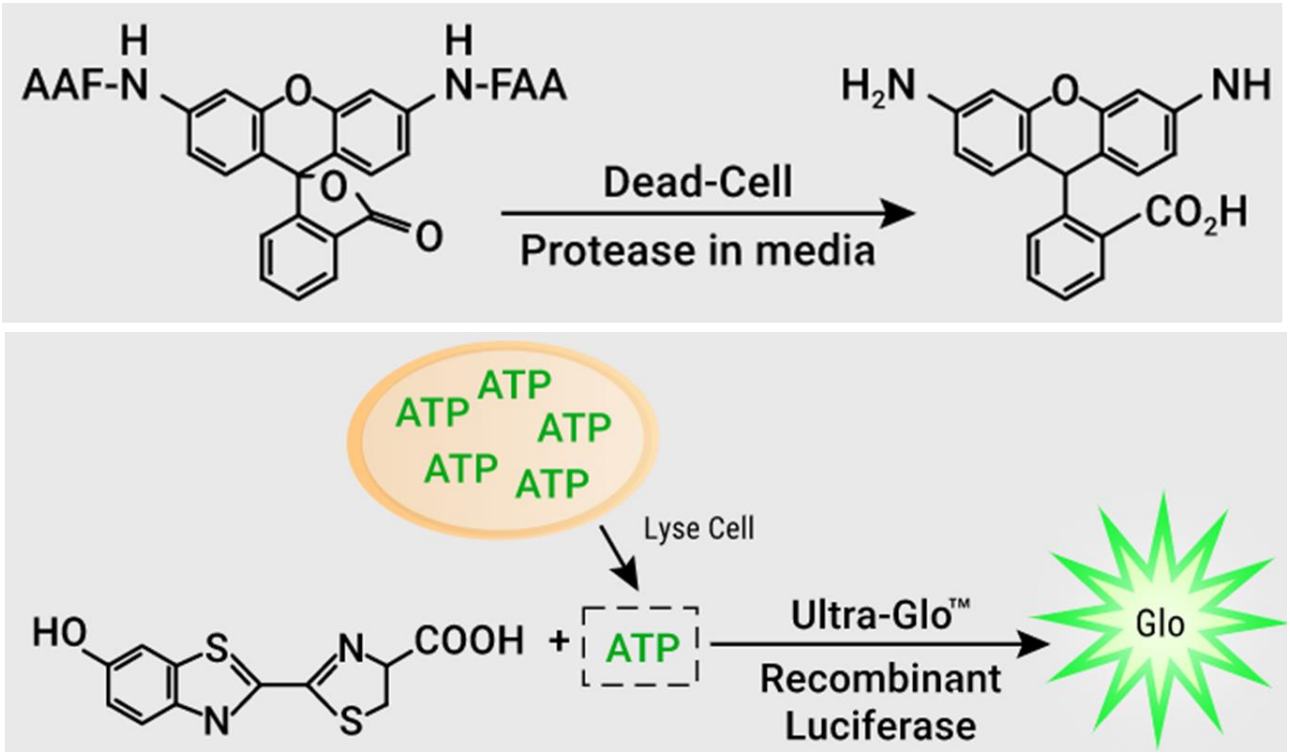

Figure 3.7: The mitochondrial membrane potential assay differentiates healthy from unhealthy cells based on the membrane integrity and ATP production (Adapted from (worldwide.promega.com, 2022)).

3.9.3.2 ***Protocol***

The Promega Mitochondrial ToxGlo™ Assay Kit (#G8000) was used to determine mitochondrial membrane integrity in HepG2 cells. The 5X cytotoxicity (5µl bis-AAF-R110 in 1ml assay buffer) and ATP detection reagents were prepared according to the manufacturer's instructions. Briefly, the treatment medium was replaced with 50µl PBS, then 25µl/well of 5X cytotoxicity reagent was added to the treated cells and incubated at room temperature for 30 minutes in the dark. Following incubation, fluorescence was measured at 485nm excitation and 525nm emission in a Turner BioSystems Modulus microplate luminometer (Sunnyvale, USA). The plate was then equilibrated for 10 minutes at room temperature. Thereafter, 25µl of ATP Detection Reagent was added to each sample. The plate was placed in a Turner BioSystems Modulus microplate luminometer (Sunnyvale, USA), and the luminescence was measured.

3.10 Western blot

3.10.1 Principle

Western blotting also known as immunoblotting is a commonly used assay for detecting proteins (Gwozdz and Dorey, 2017). Western blot uses antibody-based probes to extract precise target protein information from complex samples (Gwozdz and Dorey, 2017, Najafov and Hoxhaj, 2017). It is a very sensitive approach that even quantifies picogram amounts of targeted proteins because of the high affinities of antibodies towards their epitopes and the amplifying nature of western blotting (Najafov and Hoxhaj, 2017). Western blot is used to acquire details about post-translational modifications, quantity and molecular weight of proteins (Najafov and Hoxhaj, 2017). Sample protein is extracted, quantified using various assays such as Lowry and Bradford assays, and standardized (Roy *et al*., 2019). Sodium dodecyl sulfate-polyacrylamide gel electrophoresis (SDS-PAGE) is used to separate the proteins in the sample by molecular weight and isolated proteins are then transferred to a nitrocellulose or polyvinylidene difluoride membrane where the targeted proteins bind to specific antibodies (Figure 3.8) (Roy *et al*., 2019). The antigen-antibody reaction is visualized using a chemiluminescent substrate and the captured image is analysed to determine relative band density (RBD) (Bass *et al*., 2017). The RBD is normalized against housekeeping proteins such as β-actin (Bass *et al*., 2017).

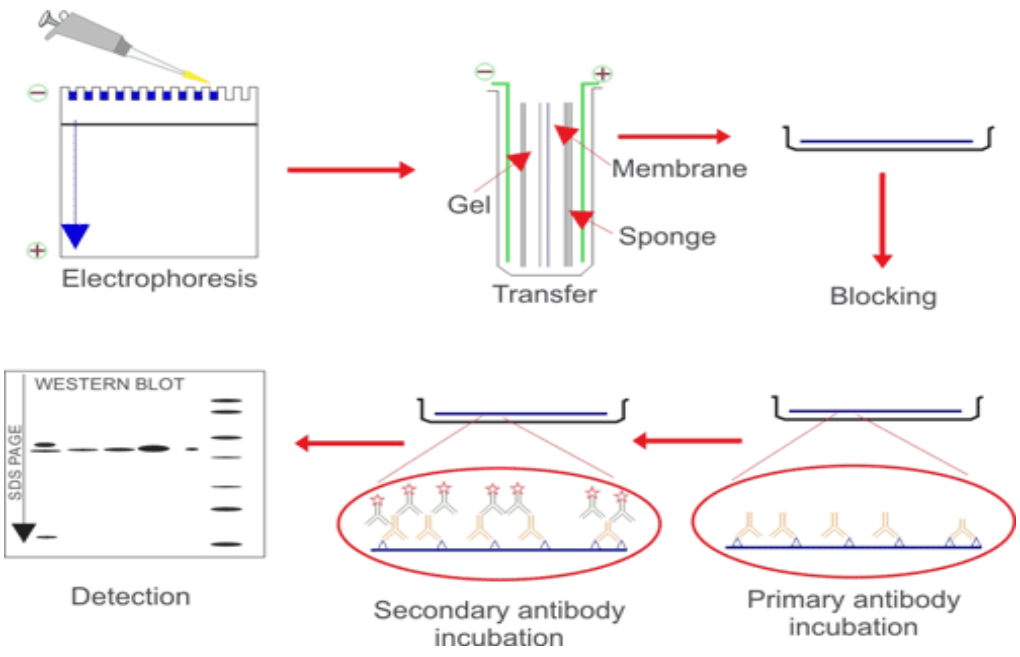

Figure 3.8: Overview of western blot protocol showing electrophoresis of the standardized protein, electro transfer and immunodetection steps (Adapted from (Cusabio, 2022)).

3.10.2 Protocol

3.10.2.1 Protein isolation

Treated cells were rinsed twice with PBS, followed by the addition of 200µl of Cytobuster™ protein extraction reagent (71009-3, Sigma-Aldrich, St. Louis, Missouri, USA) supplemented with protease and phosphatase inhibitors (Pierce™, ThermoScientific, Waltham, Massachusetts, USA). Cells were then lysed completely on ice for 30 minutes. The cells were scraped using a cell scraper and transferred to 1.5ml labelled microcentrifuge tubes. The lysate was then spun at 10000 × g for 10 minutes at 4℃ in a precooled centrifuge (Eppendorf Centrifuge 5804 R). The supernatant was transferred to new labelled tubes and samples were kept on ice.

3.10.2.2 Protein quantification and standardization

Proteins were quantified and standardized after isolation using the bicinchoninic acid (BCA) assay. The standards (0-1mg/ml) and samples were then plated in triplicates of 25µl in a 96-well plate, followed by the addition of 200µl BCA working solution (4µl $CuSO_4$ and 198µl BCA) into all samples and standards. The plate was then incubated for 10 minutes at 37°C, 5%CO_2 (NUAIRE). Using a spectrophotometer, the absorbance values were measured at 562nm after incubation (BMG LABTECH SPECTROstar Nano, Ortenberg, Germany). The absorbance readings of the standards were used to generate a curve from which the protein concentration of the various samples was estimated and standardized to 3.5mg/ml with the cytobuster.

3.10.2.3 Sample preparation for electrophoresis

A volume of 200µl of standardized protein samples were diluted in 50µl sample buffer [12ml Tris-HCl (pH 6.8, 0.5M), 20ml glycerol, 4g sodium dodecyl sulphate (SDS), β-mercaptoethanol, 8mg bromophenol blue]. Samples were boiled for 5 minutes at 100˚C and then allowed to cool at room temperature.

3.10.2.4 Protein separation by gel electrophoresis

Sodium dodecyl sulphate-polyacrylamide gel electrophoresis (SDS-PAGE) was used to separate proteins based on their molecular weight. The Mini-PROTEAN 3 SDS-PAGE apparatus were assembled according to manufacturer's instructions (Bio-Rad, Hercules, California). A 10% resolving gel [dH_2O, 1.5M Tris-HCl (pH 8.8), 10% (w/v) SDS, 30% bis-

acrylamide, 10% ammonium persulfate (APS), N, N, N', N'-tetramethylethylenediamine (TEMED)] was prepared and allowed to set for 1 hour at room temperature with water topped over the resolving gel to ensure a smooth interface. Following gel setting, dH_2O was removed and 4% stacking gel [dH_20, 0.5M Tris-HCl (pH 6.8), 10% SDS, 30% bis-acrylamide, 10% APS, TEMED] was prepared and added on the resolving gel with Bio-Rad plastic combs to create sample loading wells. The gel was allowed to set for 40 minutes, followed by transfer of the gel cassette sandwich from casting stands to the electrode assembly. The tank was filled with 1X running buffer [dH_2O, Tris, glycerine, SDS; (pH 8.3)]. An equal amount of protein (25 µl) was then loaded into wells of SDS-PAGE gel. The gel was run at a constant voltage of 150 V for 1 hour using a Bio-Rad power supplier (Hercules, California) to separate protein according to molecular weight.

3.10.2.5 Transfer the protein from the gel to the membrane

The electrophoresed gels were placed in 1x transfer buffer [25mM Tris, 192mM glycine, 20% methanol; pH 8.3] for 10 minutes to equilibrate. Blotting membranes, nitrocellulose and fibre pads were soaked in 1x transfer buffer and the transfer sandwich was assembled in the Bio-Rad Trans-Blot® Turbo™ Transfer System (Hercules, California) by sandwiching the nitrocellulose membrane and the equilibrated SDS-PAGE gel between the fibre pads. Proteins were transferred for 30 minutes at a constant voltage (25V, 2.5mA).

3.10.2.6 Antibody incubation

Following the transfer, the membranes were carefully placed in a 5ml blocking solution (5% BSA in Tween-20 Tris-buffered saline (TTBS)) and incubated on a shaker at room temperature for 1 hour. The membranes were incubated in primary antibody SOD2 (#13141), P-p38 (#4511), p38 (#8690), P-JNK (#9251), JNK (#9252), P-Erk (#8544), Erk (#4348), GPx-1(#3206), P-Stat3 (#9145), Stat3 (#4904) [1:1000 in 1% BSA in TTBS] for 1 hour on the shaker at room temperature and overnight incubation. Following overnight incubation, the membrane in the primary antibody was allowed to reach room temperature (1 hour on the shaker) and rinsed 5 times for 10 minutes in TTBS. The membranes were then probed with HRP-conjugated secondary antibody (1:2500 in 1% BSA in TTBS) for 2 hours at room temperature on a shaker. The membranes were rinsed 5 times for 10 minutes with TTBS.

3.10.2.7 Immunodetection

Following the second wash, membranes were viewed on the Chemidoc™ Imaging System (Bio-Rad, Hercules, California) using the chemiluminescent substrate (luminol and peroxidase buffer) which was applied according to the manufacturer's recommendation. The images were captured using Image Lab™ V6.0.1 build 34 Standard Edition © 2017, Bio-Rad Laboratories, Inc software, USA. The membranes were stripped with 5ml of H_2O_2 for 30 minutes at 37˚C, then probed for β-actin to normalize protein expression. The results were analysed using Image Lab™ V6.0.1 build 34 Standard Edition © 2017, Bio-Rad Laboratories, Inc software, USA to read the band intensity of the target proteins. The results were demonstrated as relative band intensity (RBI).

3.11 Quantitative real-time PCR (qPCR)

3.11.1 Principle

Real-time PCR, commonly known as quantitative PCR (qPCR), is a reliable and effective technique for detecting and quantifying DNA and mRNA (Fathurrahman *et al*., 2022, Jalali *et al*., 2017). The use of fluorescent assays to track the amplification process in real-time is a distinguishing feature of qPCR (Fathurrahman *et al*., 2022). Every qPCR cycle includes three main steps (figure 3.9): denaturing, annealing, and extension (Jalali *et al*., 2017). qPCR is based on the detection and quantification of target sequences in complementary DNA (cDNA) that is synthesised from extracted mRNA (Aryal, 2021, Jalali *et al*., 2017). As the amount of PCR products in the reaction increases, so will the fluorescent signal generated by the dye that is incorporated into the master mix (figure 3.9) (Fathurrahman *et al*., 2022). The advantage of qPCR over the traditional PCR method is that products are measured during each cycle in real time (Kadri, 2019, Arya *et al*., 2005). In addition, the quantity of templates at the beginning of the PCR reaction is directly proportional to the products produced (Kadri, 2019, Arya *et al*., 2005).

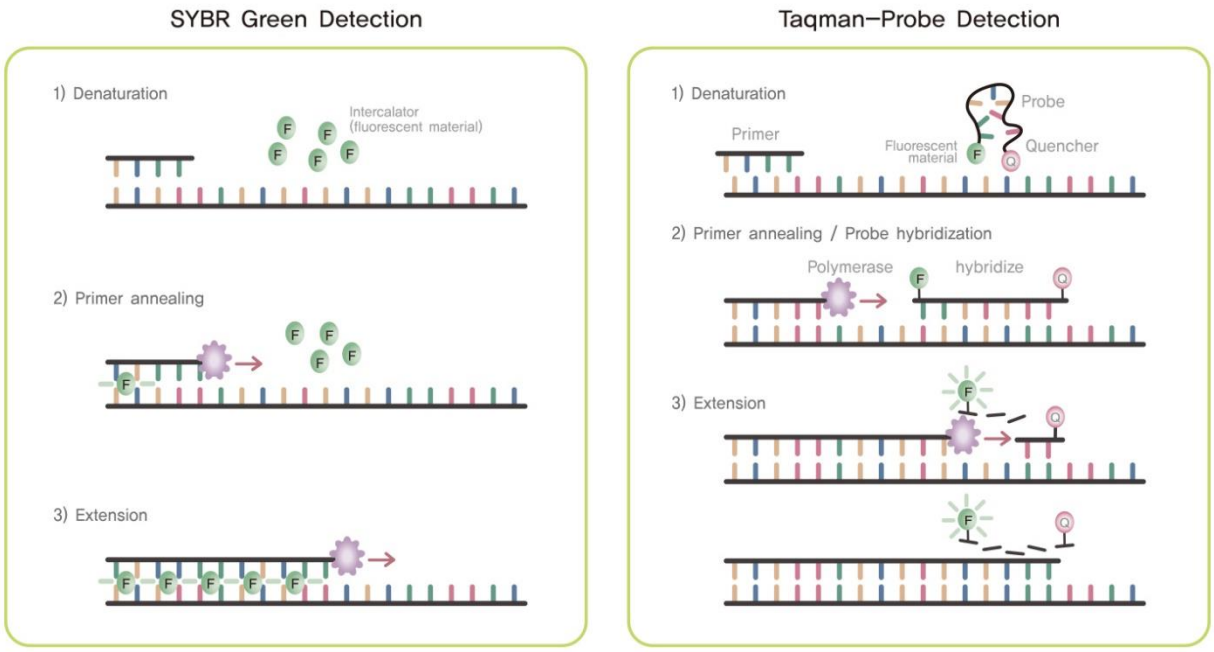

Figure 3.9: Fluorescent markers for use in qPCR. SYBR green solely fluoresce when it intercalates into dsDNA and in TaqMan probe detection, the fluorophore solely fluoresces when the quencher is released (Adapted from (Aryal, 2021)).

3.11.2 Protocol

3.11.2.1 mRNA isolation

Flasks of treated cells were washed with PBS. A volume of 500µl of Trizol and PBS each were added for the first step of mRNA isolation, followed by incubation for 5 minutes at room temperature. The homogenates were then transferred into 1.5ml microcentrifuge tubes and frozen overnight at -80°C. The samples were thawed and 100µl chloroform was added. The samples were then shaken vigorously for 15 seconds and incubated for 3 minutes at room temperature. Following incubation, samples were centrifuged for 15 minutes at 12000xg (Epperndorf Centrifuge 5804 R, Hamburg, Germany) 4˚C. The aqueous phase was then transferred to a new 1.5ml RNAse/DNAse-free microcentrifuge tube, followed by the addition of 250µl isopropanol. The samples were mixed by flicking and stored at -80˚C overnight. The samples were then thawed and centrifuged at 4˚C, 15 minutes, 12000xg (Epperndorf Centrifuge 5804 R, Hamburg, Germany). The supernatant was discarded, and the pellet was washed with 500µl cold ethanol (75%) and flicked to loosen the pellet. The samples were centrifuged at 4˚C, 15 minutes, 7400xg and then the ethanol was discarded. The samples were allowed to air dry for 1.5 hours. Following the air drying, the pellets were resuspended in 15µl nuclease free (NF) water and incubated at room temperature for 3

minutes. The RNA concentration was quantified using the Nanodrop 2000 spectrophotometer (ThermoScientific, Waltham, USA) and standardized to 900ng/ml using NF water and the purity ratio (A260/A280) was 2.

3.11.2.2 cDNA synthesis and Gene expression

The iScript cDNA Synthesis Kit (#1708891) was used for cDNA synthesis from template RNA. The cDNA synthesis was performed by mixing 2µl 5X iScript reaction mix, 0.5µl iScript reverse transcriptase (Bio-Rad, Hercules, California), 5.5µl NF water and 4µl Template RNA in a NF microcentrifuge tube. The GeneAMP PCR 97000 (Applied Biosystems, Waltham, Massachusetts) was utilized, with the following reaction conditions: 5 minutes at 25˚C, 30 minutes at 42˚C, and 5 minutes at 85˚C, 1 cycle. The expression of the genes *NRF2*, *PI3K*, *OGG1*, *p53*, *SOD2*, *Glycogen synthase*, *GLUT2*, *Glucokinase*, *AMPK2*α, *catalase* and housekeeping gene (*GAPDH*) (Table1) were evaluated, and master mixes were made by mixing 6.25µl iTaq Universal SYBR® Green Supermix (Bio-Rad, Hercules, California), 3.75µl NF water, 0.5µl each forward and reverse primers, and 1.5µl cDNA. For 40 cycles, the C1000 Touch Thermal Cycler CFX96 Real-Time System was used (Bio-Rad, Hercules, California), under the conditions listed in Table 2. The quantification cycle (Cq) values were obtained using the CFX Manager™ Software (Bio-Rad, Hercules, California), and gene expression was estimated using Livak and Schmittgen's 2-CT technique (Livak and Schmittgen, 2001).

Table1: Primers used to assess high glucose levels induce oxidative stress and alteration in glucose metabolism.

Gene	Primer sequence	Annealing temperature (°C)
Glycogen synthase	F:5'-GCCAGACACCTGACATTAAG-3' R:5'CTCCACTTCATCTTCCACATC-3'	55
AMPKα2	F:5'-GGGTGAAGATCGGACACTACGT-3' R:5'-TTGATGTTCAATCTTCACTTTG-3'	55
CAT	F:5'-TAAGACTGACCAGGGCATC-3' R:5'-CAACCTTGGTGAGATCGAA-3'	55
PI3K	F:5'-AACACAGAAGACCAATACTC-3' R:5'-TTCGCCATCTACCACTAC-3'	
GLUT2	F:5'-GGCTAATTTCAGGACTGGTT-3' R:5'-TTTCTTTGCCCTGACTTCCT-3'	59
Glucokinase	F:5'-GTCGAGCAGATCCTGGCAG-3' R:5'-ACTGTGTCGTTCACCATTGCC-3'	59
NRF2	F:5'-AGTGGATCTGCCAACTACTC-3' R:5'-CATCTACAAACGGGAATGTCTG-3'	53
OGG1	F:5'-GCATCGTACTCTAGCCTCCAC-3' R:5'-AGGACTTTGCTCCCTCCAC-3'	58
SOD2	F:5'-GAGATGTTACACGCCCAGATAGC-3' R:5'-AATCCCCAGCAGTGGAATAAGG-3'	60
p53	F:5'-CCACCATCCACTACAAACTACAT-3' R:5'-CAAACACGGACAGGACCC-3'	54,8
GAPDH	F:5'-TCCCTGAGCTGAACGGGAAG-3' R:5'-GGAGGAGTGGGTGTCGCTGT-3'	The temperature of the gene interest

Table 2: qPCR standard cycle conditions for 40 cycles

Steps	**Temperature (˚C)**	**Time**
Initial annealing	95	4 minutes
Denaturing	95	15 seconds
Annealing	Temperature at which the primer of interest is annealed	40 seconds
Extension	72	2 Seconds

3.12 Statistical analysis

Plating was performed in triplicates, and assays were repeated once for confirmation. Cells in CCM were used as a control, while cells in HG were used as a diabetes study model. GraphPad Prism 5 (La Jolla, California) was used to analyze the data. The *t*-test with Welch's correction was used to compare NG and HG data. A one-way analysis of variance (ANOVA) with Tukey post-test was used to analyze statistical differences between the samples compared to the hyperglycemic control. Data was represented as the standard error of the mean. Significant *p*-values were reported to be lower than 0.05.

CHAPTER 4: RESULTS

The cytoprotective effects of *M. foetida* on liver impaired glucose metabolism and oxidative stress damage were investigated in high glucose (HG) induced HepG2 cells, with Metformin as a positive drug control. The HepG2 cells were starved for 1 hour in a serum-free HG medium before treatment. Except for the normoglycemic control (NG-C), HepG2 cells were exposed to a HG concentration of 30mM for 24 hours after the fasting interval. Following a 24-hour HG treatment, HepG2 cells were treated with various *M. foetida* aqueous extract concentrations (125µg/ml (MF1), 500µg/ml (MF2) and 1000µg/ml (MF3)), with 100µg/ml Metformin as the positive control. The bar graph in the figures below contains the NG-C: untreated normoglycemic HepG2 cells; HG: high glucose; Met: Metformin; MF: *M. foetida*; MF1: 125µg/ml; MF2: 500µg/ml; MF3: 1000µg/ml. Error bars represent the standard error of the mean, the asterisk (*) above the error bars represents the statistically significant difference ($p < 0.05$) of the NG-C vs HG and the hash (#) represents the HG vs *M. foetida* and Metformin treatments (unpaired students *t*-test with Welch's corrections used to compare NG to HG and one-way ANOVA was used to compare treatments to HG).

4.1 Effects of *M. foetida* extracts on cellular cytotoxicity

The MTT assay was used to evaluate the effect of HG conditions and *M. foetida* on the metabolic activity of HepG2 cells. Figure 4.1A demonstrates that *M. foetida* extracts enhanced metabolic activity under NG and HG conditions, with an amplified metabolic response observed under HG conditions. Cell injury or death was not induced for any treatments, which corresponded with reduced extracellular LDH activity by *M. foetida* extracts (Figure 4.1B). The LDH concentration in HG-treated cells was significantly different when compared to the NG (ANOVA, $p = 0.0023$) and HG (ANOVA, $p = 0.0027$) control respectively (Figure 4.1B). The data shows that extracellular LDH increased from (0.10250±0.00450) under NG conditions to 0.12450±0.00350 in the HG control ($p = 0.0023$, Figure 4.1B). A significant decrease in LDH activity to similar levels was observed in Metformin (0.10100±0.00300), MF1 (0.09750±0.00050) and MF2 (0.09650±0.00550) treatments compared to the HG control ($p = 0.0027$). Interestingly, a significant decrease in LDH activity was noted at the highest concentration of *M. foetida* (Figure 4.1B), indicating that *M. foetida* inhibits cell cytotoxicity in a dose-dependent manner.

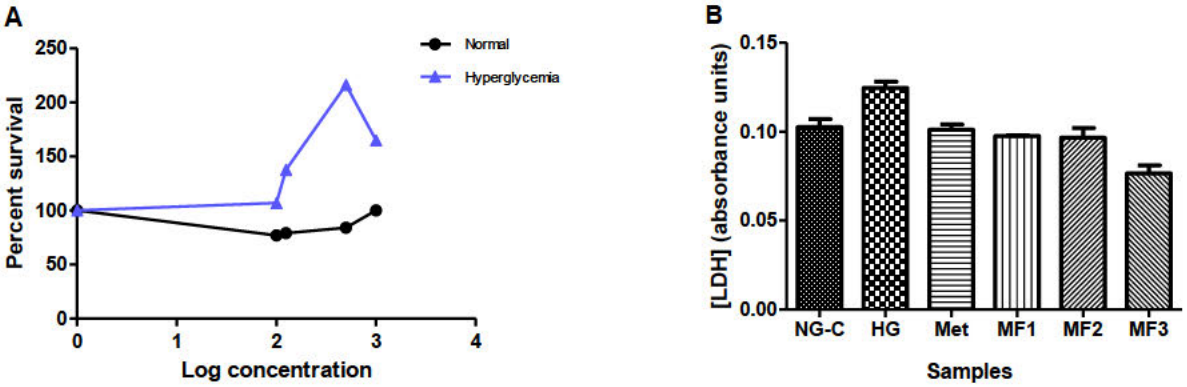

Figure 4.1: Effect of *M. foetida* leaf extracts on high glucose-induced cellular cytotoxicity in HepG2 cells. **(A)** *M. foetida* increased metabolic activity in both NG and HG conditions, with HG conditions showing the greatest increase. **(B)** LDH activity increased in HG condition, yet treatment with Metformin, MF1, MF2 and MF3 reduced LDH activity. NG- normoglycemia, HG- hyperglycemia, MF1- *M. foetida* 125µg/ml, MF2- *M. foetida* 500µg/ml, MF3- *M. foetida* 1000µg/ml and Met- Metformin. Error bars represent the standard error of the mean.

4.2 Effects of *M. foetida* extracts on high glucose induced mitochondrial membrane potential (ΔΨm) and ATP synthesis

Mitochondrial integrity is integral to metabolic activity and ATP production in cells. As shown in Figure 4.2A, the ΔΨm varied significantly between treatments when compared to the NG control (ANOVA, $p = 0.0139$) and HG control (ANOVA, $p = 0.0257$) respectively. The ΔΨm increased from 0.06169±0.00292 in the NG control to 0.07451±0.00775 in the HG control ($p = 0.3650$). Metformin and MF1 maintained ΔΨm within NG levels, but MF2 (0.08704±0.00309) and MF3 (0.11620±0.00171) concentrations increased ΔΨm non-significantly compared to HG control cells. The ATP concentration was decreased in HG-treated cells, compared to the NG (ANOVA, $p = 0.0071$) and HG (ANOVA, $p = 0.0171$) control (Figure 4.2B). ATP synthesis decreased almost 2-fold from 21350000±2250000 RLU in NG control cells to 11180000±775000 RLU in the HG control. Interestingly, ATP synthesis was slightly elevated in the MF1, MF2 and Metformin treated cells to 11750000±150000 RLU, 13980000±725000 RLU and 13280000±575000 RLU respectively in comparison to the HG control (Figure 4.2B), with the highest concentration of *M. foetida* (MF3) synthesizing the most ATP (18580000±1825000 RLU).

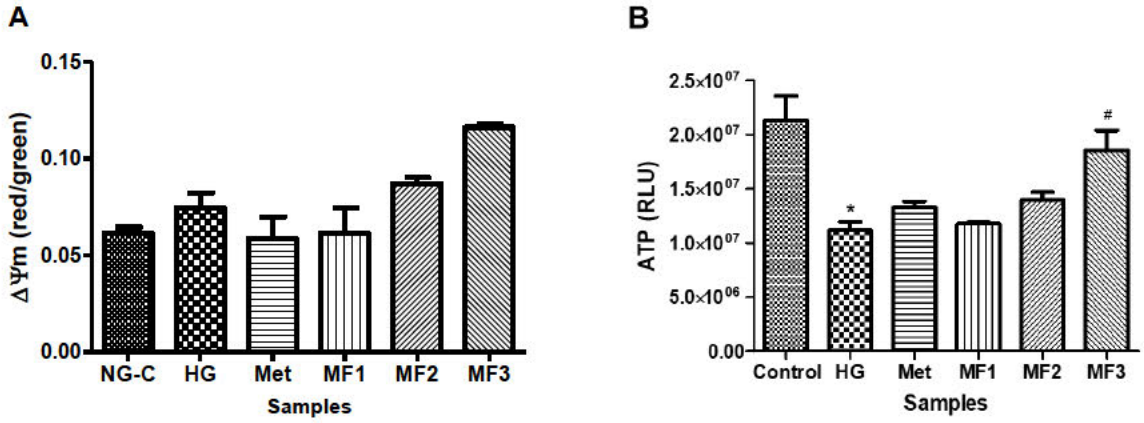

Figure 4.2: Effect of *M. foetida* leaf extracts on mitochondrial membrane potential **(A)** and ATP synthesis **(B)** in HepG2 cells. **(A)** Mitochondrial membrane potential increased in HG conditions; however, Metformin and MF1 reduced it back to the normal control level. MF2 and MF3 increased more than in HG conditions. **(B)** In HG conditions, ATP concentration decreased, but Metformin, MF1, MF2 and MF3 counteracted this effect. NG- normoglycemia, HG- hyperglycemia, MF1- *M. foetida* 125µg/ml, MF2- *M. foetida* 500µg/ml, MF3- *M. foetida* 1000µg/ml and Met- Metformin. Error bars represent the standard error of the mean.

4.3 Effects of *M. foetida* extracts on high glucose-induced pro-oxidant production

To investigate pro-oxidant production, lipid peroxidation (MDA) and NO (nitrate and nitrite) production were measured in HG-induced HepG2 cells. The MDA concentration (Figure 4.3A) in HG-treated cells increased significantly when compared to the NG (ANOVA, $p < 0.0001$) and HG (ANOVA, $p < 0.0001$) control. The MDA level was increased a significant 1.4-fold to 0.02205±0.00005 µM in the HG control compared to 0.01550±0.00050 µM in the NG control (Figure 4.3A, $p = 0.0487$). While Metformin treatment induced a further increase in lipid peroxidation to 0.03750±0.00050 µM ($p = 0.0207$), lipid peroxidation decreased to NG levels at the lowest concentration of *M. foetida* (0.01505±0.00005 µM, $p = 0.0064$) compared to the HG control. In addition, MDA concentration for MF2 (0.02101±0.00001 µM) and MF3 (0.02200±0.00100 µM) treatments was similar to the HG HepG2 cells (Figure 4.3A). The RNS concentration (Figure 4.3B) was significantly different from the NG ($p < 0.0001$) and HG ($p < 0.0001$) control. The NO concentration in NG HepG2 cells (4.01200±0.22230 µM) was decreased 1.4-fold to 2.96300±0.00003 µM ($p = 0.0421$) in HG HepG2 cells. Similar RNS concentration was observed in Metformin-treated cells (2.90100±0.12330 µM). All *M. foetida* treatments (MF1, MF2 and MF3) significantly increased NO production to 5.4940±0.06200 µM ($p = 0.0006$), 11.61000±0.24700 µM ($p = 0.00086$) and 19.26000±0.59530 µM ($p = 0.0013$) respectively in comparison with the HG control (Figure 4.3B). In addition, the highest NO production was observed for MF3-treated cells compared to the lower concentrations of the *M. foetida* extracts.

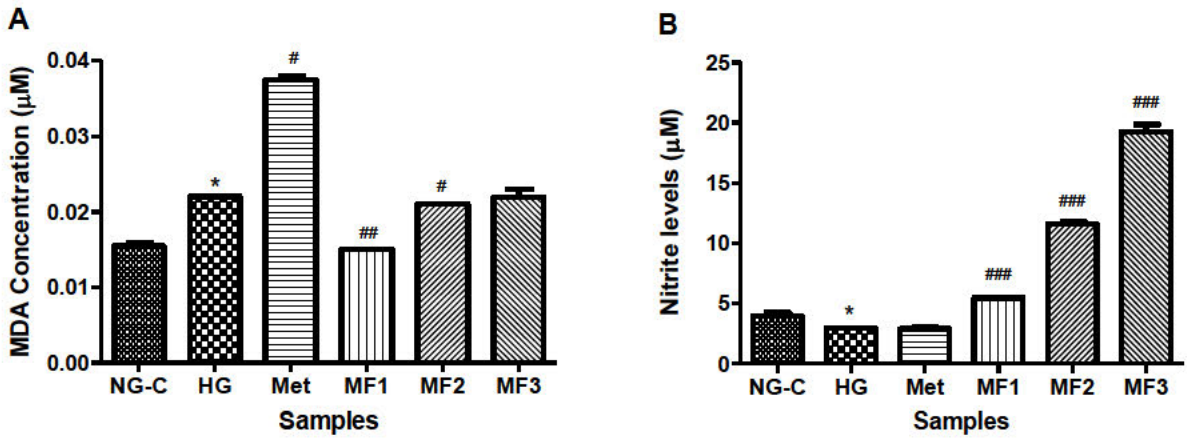

Figure 4.3: Effect of *M. foetida* leaf extracts on high glucose-induced lipid peroxidation **(A)** and **(B)** Nitric Oxide in HepG2 cells. **(A)** MDA levels increased in HG conditions similarly to MF2 and MF3. On the other hand, metformin treatment increased MDA concentration more than HG conditions, whereas MF1 treatment decreased MDA concentration back to normal control levels. **(B)** NO production decreased in HG control in a similar manner as Metformin. However, MF1, MF2 and MF3 increased the production of NO. NG- normoglycemia, HG- hyperglycemia, MF1- *M. foetida* 125µg/ml, MF2- *M. foetida* 500µg/ml, MF3- *M. foetida* 1000µg/ml and Met- Metformin. Error bars represent the standard error of the mean. The asterisk (*) above the error bars represents the statistically significant difference ($p < 0.05$) of the NG-C vs HG and the hash (#) represents the HG vs *M. foetida* and Metformin treatments.

4.4 Effects of *M. foetida* extracts on high glucose-induced antioxidant system

Antioxidants were assessed to determine the response to oxidant production. Figure 4.4A demonstrates a significant difference in the protein expression of SOD2 in the HG treatments compared to the NG (ANOVA, $p = 0.0004$) and HG (ANOVA, $p = 0.0316$) control. The expression of SOD2 was increased 1.5-fold in HG control cells to 18360000±384000 RBD compared to the NG control (12690000±209200 RBD) ($p = 0.0010$). While Metformin (15180000±1163000 RBD) and MF2 (16370000±257200 $p = 0.0230$) decreased the expression of SOD2 toward control levels, no significant difference was observed for the MF1 (19310000±989900 RBD) and MF3 (18010000±876500 RBD) treatment compared to the HG control (Figure 4.4A). Data for GPx1 was statistically different when compared to the NG (ANOVA, $p < 0.0001$) and HG (ANOVA, $p < 0.0001$) control (Figure 4.4B). *HG* induced a slight decrease in the expression of GPx1 compared to the NG control (23340000±228300 RBD and 24950000±712100 RBD respectively) (Figure 4.4B). As shown in Figure 4.4B, MF1 (28080000±34820 RBD, $p = 0.0310$), MF3 (28910000±372400 RBD, $p = 0.0498$) and Metformin (31340000±20140 RBD, $p = 0.0182$) increased GPx1 protein expression significantly compared to the induced HG control. Moreover, Metformin increased GPx1 expression more than *M. foetida* extracts (Figure 4.4B). No significant difference was observed in GPx1 expression in cells treated with MF2 (23390000±201700 RBD) compared

to the HG control (Figure 4.4B). HG significantly decreased the gene expression of *catalase* ($p < 0.0001$) compared to the NG control (Figure 4.4C). The *CAT* expression decreased to 0.32500±0.01500 fold in the HG control compared to the NG control ($p = 0.0141$). A more than 6-fold increase was observed following Metformin treatment ($p < 0.0001$), with similar increases noted for MF2 ($p < 0.0001$) and MF3 ($p < 0.0001$) treatment in comparison with the induced HG control. At the lowest *M. foetida* concentration (MF1) *catalase* expression was only slightly increased towards NG control levels (0.72000±0.03000 fold). Metformin increased catalase expression less than MF2 and MF3. Reduced glutathione (GSH) levels were recorded as 52810±45170 RLU for the NG control and were only slightly increased to 622700±73190 RLU for the HG control. The GSH concentration remained the same at MF1 (657900±107000 RLU) and MF3 (628500±78250 RLU) in the induced HG control, whereas Metformin and MF2 similarly decreased GSH levels by 1.4-fold (460500±31980 RLU) and 1.3-fold (484300±66650 RLU) respectively (Figure 4.4D). As shown in Figure 4.4E, HG treatments significantly altered the expression of *NRF2* compared to the NG ($p < 0.0001$) and HG ($p < 0.0001$) control. The expression of *NRF2* significantly increased by 1.7–fold ($p = 0.0314$) in MF2 treated HepG2 cells compared to the HG control, but no significant difference was observed in MF1. In contrast, Metformin ($p = 0.0092$) and MF3 ($p = 0.0041$) significantly decreased the expression of *NRF2* by 1.3-fold and 2.4-fold respectively compared to the HG control. Moreover, MF3 treatment reduced *NRF2* expression more than Metformin treatment.

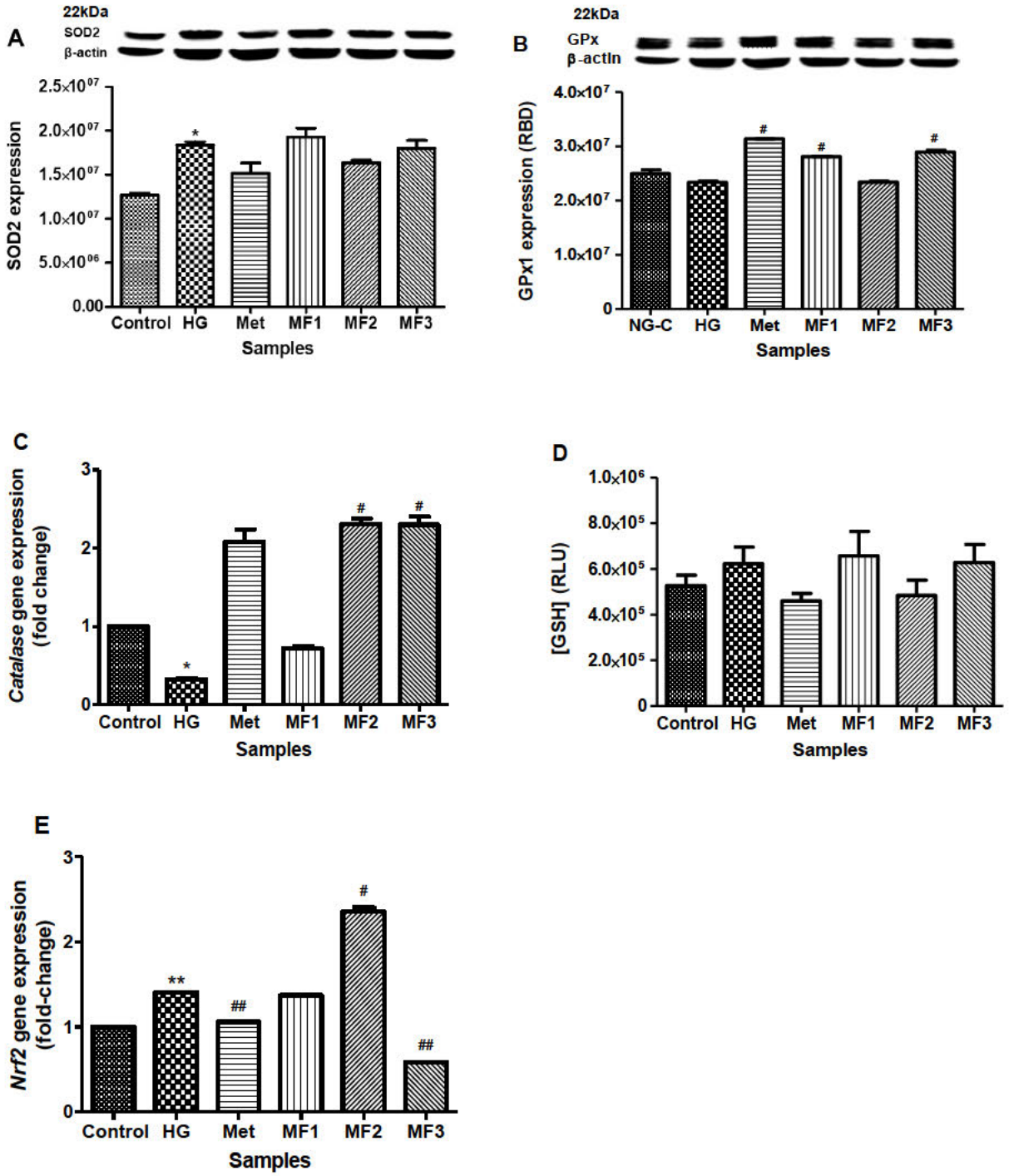

Figure 4.4: Effect of *M. foetida* leaf extracts on high glucose-induced antioxidant expression in HepG2 cells. Protein expression is represented by **A** and **B**, while gene expression is represented by **C**, **D**, and **E**. **(A)** SOD2 expression increased in HG conditions more than in normal control. Metformin, MF3 and MF2 could not improve the effects of high glucose on SOD2 expression. MF1 increased the expression of SOD2. **(B)** Gpx1 expression decreased in HG conditions and MF2. However, Metformin, MF1 and MF3 increased Gpx1 expression back to normal control **(C)** In HG conditions, CAT expression decreased, and Metformin, MF1, MF2, and MF3 counteract the effect of HG by increasing *CAT* expression. **(D)** GSH increased in HG condition, MF1 and MF3 treatment. However, Metformin and MF2 reduced GSH expression less than the NG control. **(E)** *NRF2* expression increased in HG condition and MF1 treatment. Metformin and MF3 reduced the effect of HG on *NRF2* expression in comparison to a NG control. MF3 increased *Nfr2* above HG levels. NG- normoglycemia, HG- hyperglycemia, MF1- *M. foetida* 125µg/ml, MF2- *M. foetida* 500µg/ml, MF3- *M. foetida* 1000µg/ml and Met- Metformin. Error bars represent the standard error of the mean. The asterisk (*) above the error bars represents the statistically significant difference ($p < 0.05$) of the NG-C vs HG and the hash (#) represents the HG vs *M. foetida* and Metformin treatments

4.5 Effects of *M. foetida* on high glucose induced MAPK pathway

To investigate the effects of HG-induced oxidative stress on the intracellular signalling transduction pathway, mitogen-activated protein kinases (MAPK) such as ERK1/2, Stress-activated Protein Kinase (SAPK)/-c-Jun N-terminal kinases (JNK) and p38, as well as signal transducer and activator of transcription 3 (STAT3) were investigated. A significant difference in the MAPK expression ratio for pERK1/2 and ERK1/2 (Figure 4.5A), pJNK/JNK (Figure 4.5B) and p-p38/p38 (Figure 4.5C) was observed between the HG treatments and the NG control (ANOVA, $p < 0.0001$). The expression ratio of pERK1/2 and ERK1/2 was decreased from 14.46000±0.06320 in the NG control to 13.22000±0.19270 in the HG control ($p = 0.0256$, Figure 4.5A). While Metformin significantly increased the expression ratio of pERK1/2 and ERK1/2 (16.44000±0.62670, $p = 0.0256$), MF1 ($p = 0.0015$) and MF2 ($p = 0.0061$) significantly decreased the expression of pERK1/2 and ERK1/2 to 8.14000±0.05377 and 7.84200±0.37400 respectively (Figure 4.5A). Interestingly, the MF3 treatment maintained the expression of pERK1/2 and ERK1/2 at similar levels to the NG control (14.67000±0.27390). As demonstrated in Figure 4.5B, pJNK/JNK expression decreased from 0.7448±0.02181 in the NG control to 0.50540±0.00575 in the HG control ($p = 0.00088$). Interestingly, phosphorylation of JNK was enhanced by Metformin (1.69800±0.01389, $p = 0.0002$), MF1 (1.63200±0.12870, $p = 0.00128$), MF2 (3.55100±0.02330, $p < 0.0001$) and MF3 (2.67400±0.10930, $p = 0.0025$) as noted by the increased pJNK/JNK expression ratio when compared to the HG control (Figure 4.5B). MF2 and MF3 increased the ratio of pJNK/JNK expression more than Metformin, whereas MF1 and Metformin increased the ratio of pJNK/JNK expression in a similar manner. *HG* significantly decreased the expression ratio of p-p38/p38 (2.24100±0.11740) compared to the normal control (4.58200±0.30740) (Figure 4.5C, $p = 0.0192$). All treatments reduced phosphorylation of p-p38/p38; Metformin significantly reduced the p-p38/p38 expression ratio compared to the HG control (1.65100±0.11360, $p = 0.0364$), and the MF1 (2.27600±0.08853), MF2 (1.91300±0.07288) and MF3 (1.9500±0.11210) treatments (Figure 4.5C). When MF1, MF2 and MF3 treatments were compared to the HG control, no significant changes in the expression of p-p38/p38 expression were observed. Figure 4.5D indicates that HG treatments significantly varied the expression of pSTAT3/STAT3 when compared to the NG (ANOVA, $p < 0.0001$) and HG (ANOVA, $p < 0.0001$) control. The pSTAT3/STAT3 expression ratio decreased from 0.28940±0.01348 in the NG control to 1.84400±0.05171 in the HG control ($p = 0.0012$). Metformin (0.94630±0.09726, $p = 0.0039$), MF1 (1.26600±0.06953, $p = 0.0069$), MF2 (1.15500±0.01496, $p = 0.0061$) and MF3 (0.99150±0.07890, $p = 0.0029$) significantly decreased the expression ratio of pSTAT3/STAT3 relative to the HG control,

but all were higher than the NG control (Figure 4.5D). Although *M. foetida* concentrations reduced pSTAT3/STAT3 expression, Metformin reduced pSTAT3/STAT3 expression more than *M. foetida*.

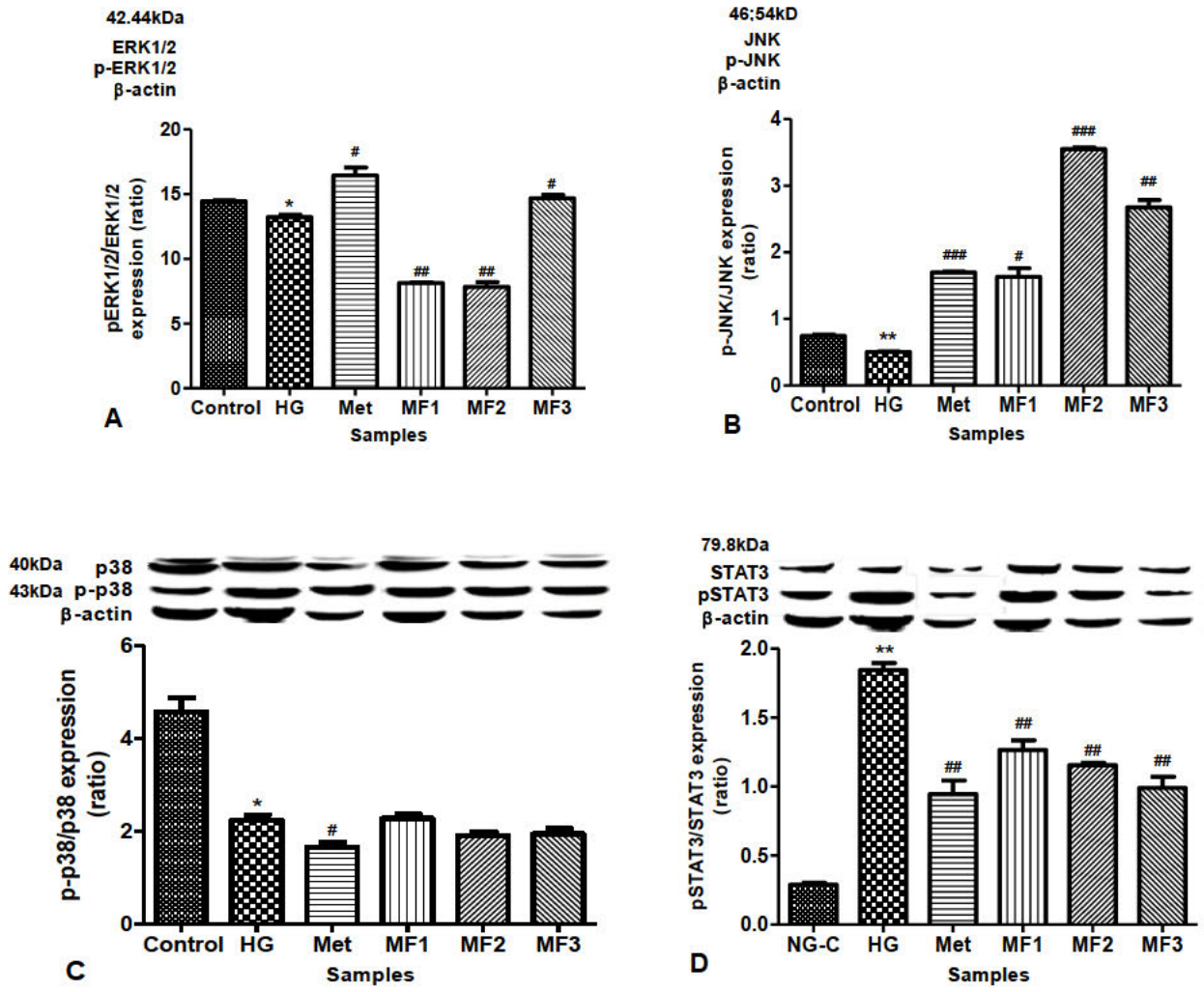

Figure 4.5: Effect of *M. foetida* leaf extracts on high glucose-induced oxidative stress signaling pathway in HepG2 cells. **(A)** Under hyperglycemic conditions, pERK1/2/ERK1/2 expression decreased. Metformin and MF3 increased the expression of pERK1/2/ERK1/2 back to normal control, whilst MF1 and MF2 decreased the expression of pERK1/2/ERK1/2 more than in hyperglycemic conditions. **(B)** Expression of p-JNK/JNK decreased more than the normal control in hyperglycemic conditions. Metformin, like MF1, increased p-JNK/JNK expression when compared to hyperglycemic conditions. MF2 and MF3 increased p-JNK/JNK expression when compared to hyperglycemic conditions. **(C)** p-p38/p38 expression decreased in hyperglycemic conditions as well as in MF2 and MF3. Metformin on the other had decreased p-p38/p38 expression more than in the hyperglycemic condition, whereas MF1 increased p-p38/p38 expression more than in the hyperglycemic condition but less than normal control. **(D)** pSTAT3/STAT3 expression increased in hyperglycemic conditions. Metformin, MF1, MF2 and MF3 decreased pSTAT3/STAT3 expression. NG- normoglycemia, HG- hyperglycemia, MF1- *M. foetida* 125µg/ml, MF2- *M. foetida* 500µg/ml, MF3- *M. foetida* 1000µg/ml and Met- Metformin. Error bars represent the standard error of the mean. the asterisk (*) above the error bars represents the statistically significant difference ($p < 0.05$) of the NG-C vs HG and the hash (#) represents the HG vs *M. foetida* and Metformin treatments.

4.6 Effects of *M. foetida* on high glucose-induced oxidative damage

To assess the repair of high glucose-induced oxidative damage, *OGG1* and *p53* gene expression were evaluated. As shown in Figure 4.6A, HG treatments varied *OGG1* expression when compared to the NG (ANOVA, $p < 0.0001$) and HG (ANOVA, $p < 0.0001$) control. The *OGG1* expression in the HG control decreased to 0.28860±0.01097 fold of the NG control ($p = 0.0002$), while a significant increase in *OGG1* expression was induced by Metformin (3.38700±0.02603, $p < 0.0001$), MF1 (1.18000±0.00000, $p = 0.0002$), MF2 (3.66000±0.02887, $p < 0.0001$) and MF3 (1.80000±0.147300, $p = 0.0094$) in comparison with the induced HG control (Figure 4.6A). The data for p53 gene expression varied from the NG (ANOVA, $p < 0.0001$) and HG (ANOVA, $p < 0.0001$) control (Figure 4.6B). In addition, both the NG and HG control expressed similar *p53* levels. The expression of *p53* increased significantly for Metformin (3.31700±0.16750-fold, $p = 0.0052$), MF1 (1.21700±0.01453 ($p = 0.0045$), MF2 (4.36300±0.11260, $p = 0.0011$) and MF3 (2.68300±0.12410, $p = 0.0054$) in comparison with the HG control (Figure 4.6B). In addition, MF2 increased *p53* expression more than Metformin, whereas MF1 and MF3 increased the expression of *p53* less than Metformin.

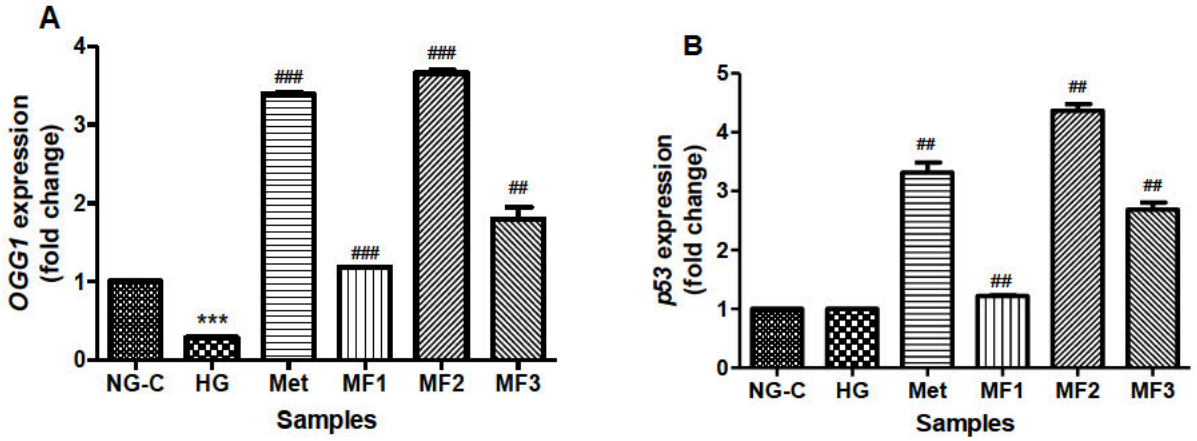

Figure 4.6: Effects of *M. foetida* in high glucose-induced DNA repair in HepG2 cells. **(A)** In hyperglycemic conditions, OGG1 expression decreased. Metformin, MF1, MF2 and MF3 increased OGG1 expression significantly. **(B)** There was no change in p53 expression in hyperglycemic conditions, however, Metformin, MF2 and MF3 increased the expression of p53. There was a slight increase in p53 expression after MF1 treatment. NG- normoglycemia, HG- hyperglycemia, MF1- *M. foetida* 125µg/ml, MF2- *M. foetida* 500µg/ml, MF3- *M. foetida* 1000µg/ml and Met- Metformin. Error bars represent the standard error of the mean. The asterisk (*) above the error bars represents the statistically significant difference ($p < 0.05$) of the NG-C vs HG and the hash (#) represents the HG vs *M. foetida* and Metformin treatments.

4.7 Effects of *M. foetida* on high glucose-induced hepatic glucose uptake

An increase in glucose consumption was observed in all *M. foetida* treatments and Metformin in comparison with the HG control (Table 3). Figure 4.7A shows a 1.76500±0.02500-fold increase in *AMPKα2* in the HG control compared to the NG control ($p = 0.0208$). However, Metformin and *M. foetida* treatments decreased *AMPKα2* relative to the NG and HG control (ANOVA, $p < 0.0001$). All *M. foetida* concentrations ($p = 0.0128$, $p = 0.0244$ and $p = 0.0137$ for MF1, MF2 and MF3 respectively) and Metformin ($p = 0.0153$) had lower *AMPKα2* expression that was similar to the NG control (Figure 4.7A). Similarly, a 3.00000±0.01732-fold elevation in *PI3K* expression was observed in HG-treated HepG2 cells compared to the NG control (Figure 4.7B, $p < 0.0001$), while Metformin and *M. foetida* treatments decreased *PI3K* expression. Figure 4.7B shows that Metformin ($p < 0.0001$), MF1 ($p = 0.0002$), MF2 ($p = 0.0006$) and MF3 ($p = 0.0004$) decreased *PI3K* when compared to the HG control, with similar *PI3K* expression noted for the Metformin and MF3 treatments. In contrast, *GLUT2* (ANOVA, $p < 0.0001$), *GK* (ANOVA, $p < 0.0001$) and *GS* (ANOVA, $p < 0.0001$) gene expressions varied when compared to the NG control and HG control (Figure 4.7C-E). *GLUT2* was decreased in the HG control to 0.17500±0.04500 fold of NG levels ($p = 0.0347$). Similarly, Metformin ($p = 0.0296$) and MF2 ($p = 0.0309$) increased the expression of *GLUT2* to levels similar to the NG control, whereas for MF1 ($p = 0.0489$) and MF3 ($p = 0.0513$) the *GLUT2* expression of was higher than the HG control (Figure 4.7C). Figure 4.7D demonstrates a significant decrease in the expression of *GK* to 0.11460±0.00466 fold for the HG control ($p = 0.0034$), while MF2 ($p = 0.0011$), MF3 ($p = 0.0005$) and Metformin ($p = 0.0067$) upregulated *GK* expression. The MF3 had the highest amount of *GK* expression ($p = 0.0005$) and MF1 ($p = 0.0013$) was not as effective at raising the expression of *GK*. *GS* expression decreased to 0.62000±0.00000 fold for the HG control ($p < 0.0001$, Figure 4.7E). The MF1 treatment was similar to the HG control (Figure 4.7E), while the expression of *GS* increased for Metformin ($p < 0.0001$), MF2 ($p < 0.0001$) and MF3 ($p = 0.0005$) treatments compared to the HG control.

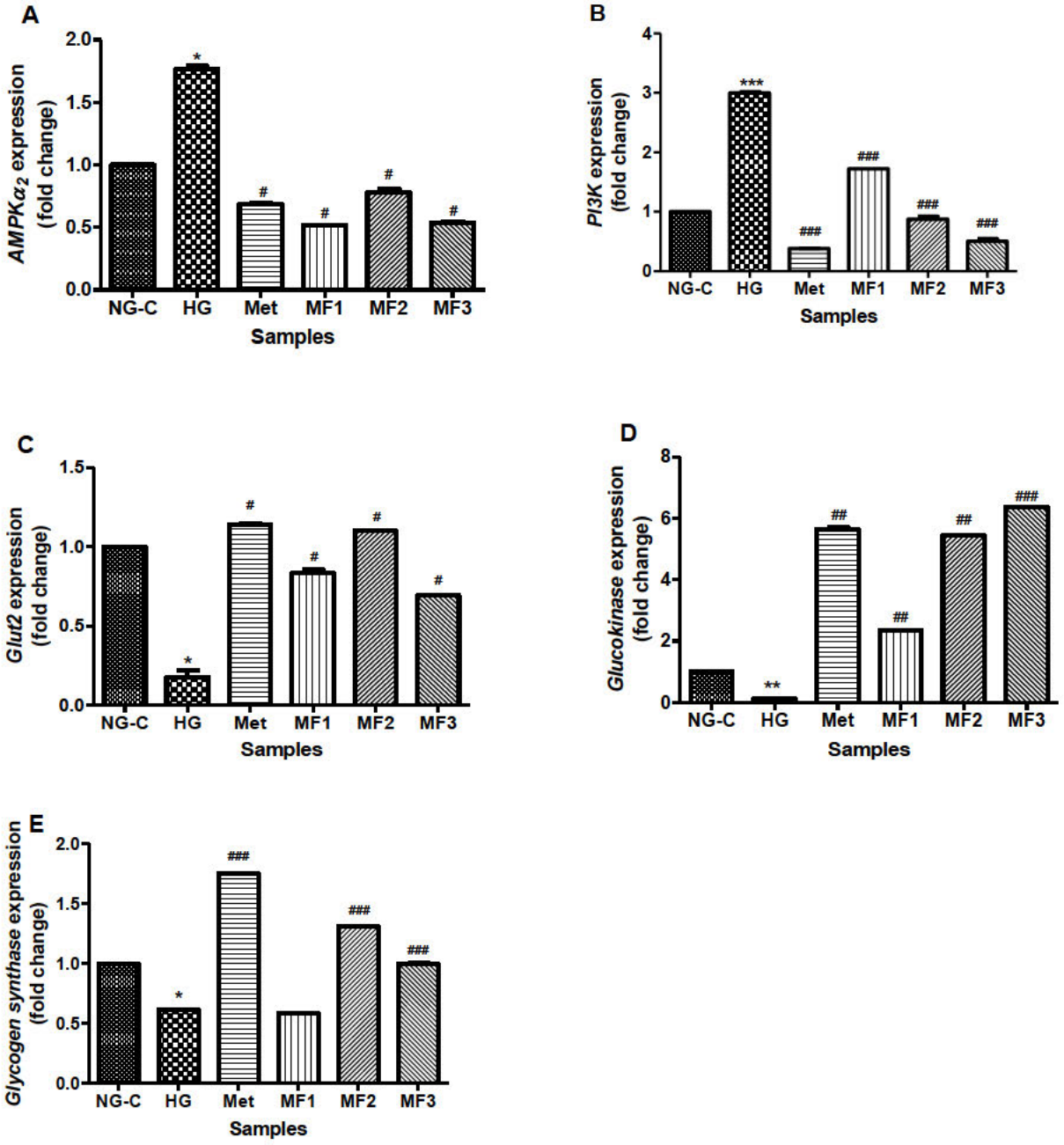

Figure 4.7: Effect of *M. foetida* leaf extracts on hepatic glucose uptake pathway. **(A)** In hyperglycemic conditions, AMPKα2 expression increased. Metformin, MF1, MF2 and MF3 treatments reduced the expression of AMPKα2 back to the normal control range. **(B)** PI3K expression increased in hyperglycemic conditions. Expression of PI3K increased in MF1 whilst Metformin, MF2 and MF3 reduced it back to the normal control level **(C)** In hyperglycemic conditions, GLUT2 expression decreased, however, treatment with Metformin, MF1, MF2 and MF3 enhanced GLUT2 expression back to normal. **(D)** Glucokinase expression decrease in hyperglycemic condition. Metformin, MF1, MF2 and MF3 increased the expression of glucokinase. **(E)** Glycogen synthase expression decreased in hyperglycemic conditions, yet, Metformin, MF2 and MF3 treatment brought back glycogen synthase expression to normal control. MF1 reduced glycogen synthase expression. NG- normoglycemia, HG- hyperglycemia, MF1- *M. foetida* 125µg/ml, MF2- *M. foetida* 500µg/ml, MF3- *M. foetida* 1000µg/ml and Met- Metformin. Error bars represent the standard error of the mean. the asterisk (*) above the error bars represents the statistically significant difference ($p < 0.05$) of the NG-C vs HG and the hash (#) represents the HG vs *M. foetida* and Metformin treatments.

CHAPTER 5: DISCUSSION

The incidence and mortality associated with type 2 diabetes mellitus (T2DM) is increasing at an alarming rate (Motala *et al*., 2022, Sun *et al*., 2022, Williams *et al*., 2020). Characterised by chronic hyperglycemia, T2DM may affect multiple organs through complications associated with its pathogenesis (Lee *et al*., 2021, Galicia-Garcia *et al*., 2020). Insulin therapy is vital to control T2DM when pancreatic β-cells fail to compensate for insulin resistance (van de Venter *et al*., 2008). However, in cases where β-cells continue to produce insulin, the primary goal of T2DM treatment is to keep blood glucose levels stable, which can be accomplished through the use of, but not limited to, oral hypoglycaemic drugs and lifestyle changes (Adenike, 2020, van de Venter *et al*., 2008). The principal oral hypoglycaemic drug used to treat T2DM, metformin, works well to decrease blood glucose levels but presents with a few undesirable side effects such as prolonged gastrointestinal disturbances (Yang *et al*., 2019). The aetiology of T2DM and its complications are exacerbated by hyperglycemia-induced oxidative stress (Yarahmadi *et al*., 2021). In both the microvascular and cardiovascular systems, oxidative stress plays a major role in the pathogenesis of diabetes complications (Pieme *et al.*, 2017). Studies have suggested that antioxidants be used as a supplementary strategy to prevent diabetic complications and diabetes mellitus (Bourebaba *et al*., 2021, Atchan Nwakiban *et al*., 2020, Safarzad *et al*., 2020, Unuofin and Lebelo, 2020). Thus, screening medicinal plants for anti-diabetic efficacy has become popular because they have fewer adverse effects and plants naturally possess antioxidants (Adenike, 2020). Several studies have highlighted the significance of *M. foetida* leaf extract as a powerful antioxidant, however the mechanism by which *M. foetida* induces glucose absorption and restores the antioxidant system has yet to be investigated (Soh *et al*., 2020, Molehin and Adefegha, 2014, Acquaviva *et al*., 2013, Oloyede and Aluko, 2012). The present study evaluated *M. foetida's* ability to protect HepG2 cells from high glucose-induced oxidative stress. The mechanism of action of *M. foetida* serves as the foundation for this study.

While the liver is pivotal to glucose homeostasis, the mitochondria are the metabolic hub of the cell (Degli Esposti *et al*., 2012). These organelles are vital for oxidative metabolism and cell viability. Viable cells sustain metabolic activity by maintaining mitochondrial membrane potential (ΔΨm), ATP production and plasma membrane integrity. In this study, *M. foetida*

extracts-maintained cell viability in NG-treated HepG2 cells and promoted metabolic activity in HG-treated HepG2 cells (Figure 4.1A). Previous *in vitro* drug metabolism studies indicate that the acceptable toxicity criterion of plant extract should be 20% or less (Olwenyi *et al*., 2021, Lan *et al*., 2010, van de Venter *et al*., 2008). The toxicity threshold in this study was less than 20% at all *M. foetida* concentrations, suggesting that the aqueous extract of *M. foetida* is not toxic to HepG2 cells. This study thus demonstrated that *M. foetida* was not cytotoxic to HepG2 cells, which contrasted with previous observations that *M. foetida* leaf has anti-proliferative action in HepG2 cells (Nkambule, 2017). The reduced cytotoxic effect of *M. foetida* was validated by the LDH assay, which showed reduced lysis of the plasma membrane in a dose-dependent manner; HG enhanced LDH activity compared to the NG control, whereas *M. foetida* and Metformin significantly reduced this impact (Figure 4.1B). The loss of plasma membrane integrity and consequent release of LDH from the cytoplasm is one of the main events after cell death and is assumed to be an indicator of necrosis or apoptosis (Parhamifar *et al*., 2019). The current findings are comparable with those of Subraminiyan and kumar Natarajan, 2017, who found that citral, a phytochemical from a citrus medicinal herb, significantly protected HepG2 cells from HG-induced apoptosis at a concentration of 30mM. On the other hand, Yarahmadi *et al.* (2021) found that HepG2 cells cultured in 30mM and 50mM D-glucose for 48 and 72 hours did not affect cell viability when treated with quercetin (Yarahmadi *et al*., 2021).

The cell viability assay used in this study is dependent on a functioning electron transport chain (ETC), since the conversion of the MTT salt to formazan is performed by mitochondrial (NADPH)-dependent cellular oxidoreductase enzymes (Subramaniyan and Natarajan, 2017). In particular, succinate dehydrogenase from complex II of the ETC is implicated in the conversion of MTT to formazan; the successful formation of formazan suggests that this complex was stimulated by the *M. foetida* in HG-induced cells. Complex I, III and IV of the ETC work together to generate a ΔΨm that is utilized by ATP synthase (complex V) to generate ATP during oxidative phosphorylation (Zorova *et al*., 2018). Suppression of ETC complexes reduces ATP synthesis, resulting in a rise in cellular AMP and ADP production and a change in the AMP/ATP ratio (Apostolova *et al*., 2020). Although HG-induced HepG2 cells raised ΔΨm slightly, it lowered ATP levels thus implying that metabolite exchange between the cytosol and mitochondria was reduced (Figure 4.2A, B). The result is comparable to the Ramesh (2021) study, where ΔΨm and ATP were decreased in diabetic rats (Ramesh, 2021). The decrease in ΔΨm in HG Metformin-treated HepG2 cells to NG

levels (Figure 4.2A) may be attributed to ΔΨm-driven mitochondrial import; when Metformin is recruited into mitochondria, its gradual build-up induces a reduction in ΔΨm (Vial *et al.*, 2019). Treatment of HG HepG2 cells with *M. foetida* increased ΔΨm and ATP levels (Figure 4.2A, B), suggesting its potential to increase electron flux in the ETC to restore ATP to the normal range. Similar findings were observed in a study where treatment with Asiatic acid restored ATP levels and ETC function in diabetic rats to the normal range (Ramesh, 2021). In obese mice, quercetin raised ATP levels and mitochondria complexes II, IV, and V, thereby regulating the mitochondrial oxidative phosphorylation system (Sharma *et al*., 2015). It has been reported that polyphenols and flavonoids in *M. foetida* aqueous extracts scavenge free radicals in human adipose mesenchymal stem cells (Acquaviva *et al*., 2013). This may suggest that the increased ATP and ΔΨm in the current study is due to the presence of polyphenol flavonoids in *M. foetida*.

Since impaired glucose metabolism during hyperglycemia reverses the flow of electrons to complex I and II, the raised ΔΨm may be accompanied by the generation of free radicals that subject the hepatocytes to oxidative damage (Ramesh, 2021, Yaribeygi *et al*., 2020a). The principal free radical produced by mitochondria is superoxide ($O_2^{\bullet-}$), which may form other ROS as part of the detoxification process. Alternatively, excess $O_2^{\bullet-}$ reacts with NO to produce RNS, increasing oxidative stress (Azizi *et al*., 2021). Since NO plays a significant role in carbohydrate metabolism, impaired NO pathways contribute to T2DM pathogenesis (Bahadoran *et al*., 2020). Recent studies demonstrated that serum NO levels were reduced in T2DM (Azemi *et al*., 2021, Azizi *et al*., 2021, Majeed *et al*., 2021). Similar findings were found in a study by Mishra and Mishra (2017), who observed that nitrite levels in diabetics and diabetics with complication groups were significantly lower than in the control group; this decrease in NO was linked to endothelial abnormalities in T2DM (Mishra and Mishra, 2017). In this study, HG and Metformin reduced nitrate concentration but *M. foetida* induced an increase in nitrite (Figure 4.3B); thus, *M. foetida* may contain inorganic nitrate which could have been converted to NO. Inorganic nitrate compounds, found in green leafy vegetables can be converted to form nitrite and then NO without the involvement of nitric oxide synthases (Lundberg *et al*., 2018, Bahadoran *et al*., 2015). Therefore, dietary nitrate and nitrite may have therapeutic benefits for T2DM because they can function as a substrate for endogenous non-enzymatic NO production and could restore NO homeostasis, thus improving glucose uptake and the insulin signaling pathway (Lundberg *et al*., 2018, Bahadoran *et al*., 2015).

Increased ROS and RNS are potent oxidants that induce damage to cellular macromolecules, including carbohydrates, lipids, protein and DNA (Liguori *et al*., 2018, Nita and Grzybowski, 2016). As the product of lipid peroxidation, MDA is a biomarker of cellular damage induced by free radicals; increased MDA levels indicate an increase in lipid peroxidation and DNA damage (Bassey *et al*., 2020). Recent *in vivo* studies have shown elevated MDA levels in T2DM (Azemi *et al*., 2021, Azizi *et al*., 2021, Majeed *et al*., 2021). Previous studies also demonstrated an increase in lipid peroxidation in HepG2 cells treated with 50mM glucose concentration for 24 -72 hours (Subramaniyan and Natarajan, 2017, Shokrzadeh *et al*., 2016). Similar results were observed in this study, with MDA levels increasing in the study model compared to the control, indicating oxidative cellular damage to the lipid membrane (Figure 4.3A). The lowest concentration of *M. foetida* significantly reduced the level of MDA (Figure 4.3A), corresponding to an *in vivo* study where *M. foetida* leaf extract inhibited lipid peroxidation induced by iron II sulphate in the liver and brain (Oloyede and Aluko, 2012). Other studies also reported that the leaf extract of *M. foetida* inhibited lipid peroxidation due to its antioxidant content (Adenike, 2020, Puškárová *et al*., 2017, Khoza *et al*., 2016, Acquaviva *et al*., 2013, Oloyede and Aluko, 2012). Polyphenols and flavonoids are antioxidant phytochemicals that have been reported to exert hepatoprotection on HepG2 cells and mice liver injury (Farhood *et al*., 2019). Quercetin and kaempferol, polyphenolic and flavonoid compounds extracted from *M. foetida* leaves were found to have anti-inflammatory, antioxidant and blood pressure-lowering properties (Khoza *et al*., 2016). Indeed, quercetin has potent antioxidant capacity that may protect HepG2 cells from hyperglycemia-induced oxidative stress (Yarahmadi *et al*., 2021).

Guanine's lower redox potential makes it susceptible to oxidative damage from ROS, forming 8-oxo-7,8-dihydro-2′-deoxyguanosine (8-oxodG) (Szewczuk *et al*., 2020). This mutagenic base is removed by 8-Oxoguanine Glycosylase (OGG1), another biomarker for ROS-induced cellular damage (Tao *et al*., 2021). The DNA damage in hyperglycemia, caused by an imbalance between the DNA repair system and DNA damage, could contribute to the further development of T2DM complications (Tao *et al*., 2021, Pang *et al*., 2012). A previous study reported that in HepG2 cells, HG treatment reduced OGG1 mRNA levels, resulting in DNA damage (Pang *et al*., 2012). Similarly, HG-treated HepG2 cells significantly decreased *OGG1* expression; however, *M. foetida* extracts and Metformin upregulated the expression of *OGG1* expression (Figure 4.6A); it is, therefore, possible that any oxidative DNA damage induced by ROS was repaired by OGG1. The finding in Figure

4.6A is in accordance with a study that showed that HG decreased *OGG1* expression in endothelial cells, but Metformin increased OGG1 protein and mRNA levels (Tao *et al*., 2021). According to Scheffler *et al*. (2018), mitochondrial ETC activity was reduced in the hepatocytes of OGG1-/- knockout mice due to reduced glycolysis during the absorptive state (feeding state) (Scheffler *et al*., 2018).

Tumor protein 53 is a transcription factor that responds to cellular stimuli and controls genes involved in metabolism, DNA repair, apoptosis, and cell cycle arrest (Itahana and Itahana, 2018). Given that p53 plays an important role in regulating glucose homeostasis, p53 dysregulation due to stimuli such as oxidative stress results in T2DM (Itahana and Itahana, 2018, Sliwinska *et al*., 2017). Interestingly, p53 is activated under oxidising conditions. In addition, its pleiotropic properties mean that at low-stress levels it may serve as an antioxidant protein, inhibiting ROS generation, yet at high-stress levels it acts as a pro-apoptotic protein, activating both the senescence and apoptotic pathways (Turacli *et al*., 2018). The HG treatment had minimal effect on *p53* gene expression in the current study, while the *M. foetida* extract and Metformin increased *p53* expression (Figure 4.7B). This observation is consistent with the findings of Turacli *et al.* (2018) that showed that administering Metformin to T2DM patients significantly enhanced p53 expression, which may contribute to the antioxidant response in treated cells (Turacli *et al*., 2018). In addition, *Solanum melongena* green calyx upregulated *p53* gene expression in diabetic rat liver (Roshankhah *et al*., 2020). Thus, *p53* upregulation by *M. foetida* could contribute to the antioxidant response.

To regulate and decrease oxidative damage in diabetes, the plant extract is used as an antioxidant therapeutic agent (Balakrishnan *et al*., 2019). The primary intracellular antioxidants that form part of the antioxidant defense system are superoxide dismutase (SOD), catalase (CAT), glutathione peroxidase (GPx) and reduced glutathione (GSH) (Javid *et al*., 2020). Literature shows that hyperglycemia impairs antioxidant function in hepatic cells by lowering GPx, CAT and SOD activity, resulting in the persistence of free radicals that are connected to the development of T2DM (Yaribeygi *et al*., 2020a, Abdulmalek *et al*., 2021, Apostolova *et al*., 2020). Scientific exploration has demonstrated that HG increased the expression of SOD2 and GSH, while decreasing expression of *CAT* and GPx (Yarahmadi *et al*., 2021, Shokrzadeh *et al*., 2016, Gounden *et al*., 2015), as was evident in

this study (Figure 4.4A, D). Thus, SOD2 was available to catalyse the breakdown of $O_2^{\bullet-}$ into O_2 and H_2O_2, which should be detoxified by CAT or GPx into O_2 and H_2O (Yarahmadi *et al*., 2021, Iftikhar *et al*., 2020). However, HG decreased the expression of GPx and *CAT* (Figure 4.4B, C) potentially, allowing H_2O_2 to persist; the H_2O_2 would be shunted to the Fenton reaction producing the highly reactive $^{\bullet}OH$ radical and consequently increasing lipid peroxidation (Figure 4.2A). In this study, Metformin decreased SOD2 and GSH, but Metformin and *M. foetida* increased the expression GPx and *CAT* (Figure 4.4B, C). Metformin is known to act as an antioxidant by increasing NADPH oxidase and boosting the endogenous antioxidant system (Apostolova *et al*., 2020). The result is consistent with the findings by Yarahmadi *et al.* (2021) who showed that CAT and GPx activity decreased after 72 hours of HG treatment, while quercetin increased the expression of CAT and GPx (Yarahmadi *et al*., 2021). The livers of alloxan-induced HG rats showed similar results, with decreasing CAT and GPx levels that were restored by polyphenol extracts of *Caesalpinia bonduc* (Iftikhar *et al*., 2020).

In the current study, HG increased the expression of GSH (Figure 4.4D), which is consistent with previous studies in T2DM patients and or HG-treated cells (Pieme *et al*., 2017, Yarahmadi *et al*., 2021, Shokrzadeh *et al*., 2016, Gounden *et al*., 2015). However, GSH was decreased by the Metformin and *M. foetida* treatments (Figure 4.4D). This could be attributed to the increase in GPx activity, which uses GSH to detoxify H_2O_2 to water (Pieme *et al*., 2017). Detoxification of lipid radicals (Figure 4.2A) is also accomplished by GSH, which may further deplete the GSH. The master regulator of the antioxidant response is NRF2. The findings of this study suggest that *NRF2* up-regulation may play a role in SOD, GPx and GSH homeostasis in HG conditions (Farhood *et al*., 2019). However, the Metformin and *M. foetida* antioxidant defense is not dependent on NRF2.

Studies have shown that NO and p53 could influence hepatic glucose uptake (de la Torre *et al*., 2013, Bahadoran *et al*., 2020). In fasting rats, foetidin from *M. foetida* has been shown to lower blood sugar levels (Muronga *et al*., 2021). It is anticipated that this could be facilitated by increased glucose uptake, which has been linked to 5' AMP-activated protein kinase (AMPK) activation, and the downregulation of this protein kinase has been linked to the pathogenesis of DM (Yuan *et al*., 2019). The phosphorylation of threonine172 on the catalytic α1/2 subunits of AMPK has been shown to modulate its activity (Zhou *et al*., 2021).

In diabetic mice, upregulating AMPK in hepatocytes reduced HG levels and gluconeogenic genes. In T2DM, treatment with Metformin is mainly utilized to regulate blood glucose levels by activating *AMPKα2*, thereby inhibiting hepatic gluconeogenesis (Tao *et al*., 2021, Day *et al*., 2017). The decreased *AMPK2*α expression by Metformin in this study was unexpected; however, gene expression was measured in this study, while other studies have quantified protein expression. In addition, in this study increased AMPK2α expression in HG HepG2 cells was decreased with *M. foetida* leaf extracts to levels equivalent to Metformin (Figure 4.7A), suggesting that *M. foetida* does not affect glucose absorption via AMPK2α.

Glucose transporter 2 (GLUT2) is the primary glucose transporter expressed in hepatocytes, facilitating glucose uptake during meals, preventing postprandial hyperglycemia and releasing glucose into the bloodstream during the fasting state (Kinsella *et al*., 2021). Glucose enters liver cells through GLUT2 and is converted to glucose-6-phosphate by glucokinase in the liver during the first step of glycolysis (Lodhi and Kori, 2021). Inhibition of hepatic GLUT2 has been correlated to the long-term progression of glucose intolerance (Kinsella *et al*., 2021). In the current study, HG decreased *GLUT2* gene expression in comparison with normal control (Figure 4.7C). However, treatment of HG HepG2 cells with *M. foetida* restrained this by upregulating *GLUT2* expression significantly to levels comparable to Metformin (Figure 4.7C), by restoring *GLUT2* expression, and is supported by a previous study which reported that the Cocoa phenolic (epicatechin and cocoa phenolic extract) extract was able to restore GLUT2 expression in HepG2 cells (Cordero-Herrera *et al*., 2015). Given that *M. foetida* contains catechin, a cis isomer of epicatechin, it is thus feasible to suggest that *M. foetida* phenolics act in a similar manner to restore GLUT2 expression (Nantia *et al*., 2018, Colomer *et al*., 2017, Acquaviva *et al*., 2013). Furthermore, Metformin enhanced hepatic *GLUT2* levels in insulin-resistant mice implying that hepatic insulin tolerance had been restored (Cordero-Herrera *et al*., 2015). Zhu *et al.* (2020) also demonstrated that *Pea*-derived peptides might stimulate GLUT2 protein and gene expression in HepG2 cells (Zhu *et al.*, 2020). The data implies that *M. foetida* induced glucose absorption via *GLUT2* was not dependent on *AMPK2α*, since *GLUT2* upregulation did not correlate with increased *AMPK2α* expression as observed in diabetic rats treated with *Bactris setosa* Mart. (Heibel *et al*., 2018).

Glucose that enters the cells is phosphorylated by GK to commit it to glycolysis, and excess glucose is directed to glycogen synthesis by GS. HG lowered the expression of *GK* and *GS* in the current study; however, treatment of HG-induced HepG2 cells with *M. foetida* leaf extracts restored *GK* (Figure 4.7E) and *GS* (Figure 4.7D) gene expression to levels similar to Metformin. The data suggest that *M. foetida* enhanced GK and GS expression and could restore glycogen synthesis in T2DM patients who have limited capacity to store glycogen when GS is inactivated (Hussain *et al*., 2020). The above results are consistent with a study that demonstrated that injecting quercetin in streptozotocin-induced diabetic rats improved hepatic GK activity and glucose sensitivity in hyperglycemia (Al-Ishaq *et al*., 2019). These findings can be ascribed to glycogen synthesis in the liver. Quercetin also restored GS activity in human HepG2 and murine H4IIE cells (Eid *et al*., 2015). Hussain *et al*. (2020) found ingestion of sodium butyrate improved the GS activity in db/db mice (Hussain *et al*., 2020). Oral administration of ferulic acid has been shown to significantly improve plasma insulin levels by lowering blood glucose levels in T2DM mice, thereby increasing GK activity and hepatic glycogen synthesis (Odeyemi and Dewar, 2020). The current data suggest that *M. foetida* possesses a mechanism in hepatic glucose uptake that is comparable to Metformin, resulting in the upregulation of genes involved in glucose uptake and storage. As a result, this effect promoted glucose absorption in hepatocytes and stimulated glucose storage (Hussain *et al*., 2020).

Interestingly, the current data demonstrated that *M. foetida* significantly upregulated *GK* and *GLUT2* activity and notably decreased PI3K expression (Figure 4.7B). This is in contrast to a study by Dihingia *et al.* (2018) where vitamin K1 treatment stimulated glucose absorption in HG HepG2 cells and up-regulated *GK*, *p-AMPK* and *PI3K* expression while decreasing *GLUT2* expression (Dihingia *et al*., 2018).

The PI3K/AKT pathway plays an important role in the cell response to insulin. Intracellular signal transduction becomes dysfunctional due to increased HG levels mediated by ROS (Bourebaba *et al*., 2021). Although ROS inhibits the PI3K/AKT pathway, it stimulates the mitogen-activated protein kinase (MAPK pathway), which lowers glucose metabolism and NOS activity (Yuan *et al*., 2019). Thus, suppression of ROS stress-mediated MAPK is a critical strategy for preventing oxidative stress development in hepatocytes (Subramaniyan and Natarajan, 2017). The MAPK pathways that include extracellular signal-

regulated kinase 1/2 (ERK1/2), p38-MAPK and c-Jun N-terminal kinase (JNK) are associated with inflammation, cell proliferation, the modulation of phosphorylation intermediates, apoptosis and oxidative stress (Abdulmalek *et al*., 2021). In the current study, HG modulated the expression of p-p38, p-JNK and p-ERK1/2 in HepG2 cells (Figure 4A-C). Interestingly, Metformin further decreased p-p38 while *M. foetida* maintained p-p38 (MF2 and MF3) expression to levels comparable to the HG control (Figure 4.5C). *M. foetida* also inhibited the expression of p-ERK1/2 (MF1 and MF2), but an increased expression was observed for MF3 and Metformin (Figure 4.5A). The results are consistent with data that showed that treatment of HG-induced HepG2 cells with citral significantly downregulated the expression of p-p38 and p-ERK1/2 (Subramaniyan and Natarajan, 2017). Similarly, the expression of p38 MAPK in the liver of T2D-induced rats was decreased by the treatment of curcumin and zinc oxide nanoparticles, as well as Metformin (Abdulmalek *et al*., 2021). Due to the importance of p-p38 and p-ERK1/2 in various pathways, the response in HG-treated HepG2 cells may ultimately impact inflammatory signalling, cell survival and protection against oxidative stress (Das *et al*., 2020, Cordero-Herrera *et al*., 2015).

Interestingly, while HG non-significantly decreased the expression of p-JNK, pSTAT3 was elevated (Figure 4.5B, D). In addition, treatment of HG-HepG2 cells with *M. foetida* upregulated the expression of p-JNK similar to Metformin (Figure 4.5B), but *M. foetida* and Metformin dramatically reduced pSTAT3 (Figure 4.5D). This is important since activation of the oxidative stress-induced p-JNK pathway is associated with insulin resistance (Iftikhar *et al*., 2020). The expression of p-STAT3 in HepG2 cells is known to increase following treatment with HG, but the effect was attenuated by pre-treatment of HG HepG2 cells with Stattic or knockdown with STAT3 (Kuo *et al*., 2020). Also, in a manner similar to nifuroxazide in palmitic acid-treated HepG2 cells, suppressed STAT3 activation by Metformin and *M. foetida* could inhibit insulin resistance and gluconeogenesis, and improve dysregulated glucose metabolism and glycogen content (Figure 4.7E) (Liu *et al*., 2019).

CHAPTER 6: CONCLUSION

The purpose of this study was to investigate the effect of hyperglycemic conditions on the induction of oxidative stress in HepG2 cells, as well as the ability of *M. foetida* (in comparison to Metformin) to counteract it. In this study, associated cytotoxicity was evident by increased LDH and decreased ATP, as well as oxidative and nitrosative stress. Free radical production was attributed to increased $\Delta\Psi m$ and corresponding MDA and nitrites in HG-HepG2 cells. An antioxidant response by *NRF2*, GSH and SOD2 was noted in the HG-HepG2 cells, but catalase, GPx1 and the MAPK pathway were not induced. The data suggest that the high flavonoid and polyphenol content of *M. foetida* confers potent antioxidant potential that may alleviate oxidative stress induced by HG levels, while also lowering blood glucose to normal levels. In this study, *M. foetida* was not cytotoxic as indicated by the MTT and LDH assays. In contrast to Metformin, the HG-induced increase in $\Delta\Psi m$ was amplified by *M. foetida* to ensure ATP production and preserve cell viability. Interestingly, the expected increase in free radical production was counteracted by an antioxidant response that relied on catalase to facilitate the detoxification of H_2O_2, thus reducing lipid peroxidation as indicated by the decreased MDA and LDH levels. The heightened JNK response by Metformin and *M. foetida* noted in accordance with increased catalase activity was expected since JNK induces protective genes in response to oxidative stress; both ERK1/2 and p38 were not activated by *M. foetida* in response to the prevailing oxidative stress (Figure 6.1). However, the JNK response facilitated Metformin and *M. foetida* modulation of *NRF2*, GPx1, GSH and SOD2 to a minimal extent in the endogenous antioxidant system, by increasing *OGG1* and *p53* expression. Furthermore, the associated suppressed STAT3 influenced glucose homeostasis and glycogen production, while NO increased glucose uptake by increasing *glucokinase* expression. However, the data suggests that Metformin and *M. foetida's* influence on glucose metabolism in HepG2 cells is independent of AMPKα2 and PI3K gene expression. As a result, *M. foetida* can regulate glucose uptake and glycogenesis in the liver by upregulating *GLUT2*, *glycogen synthase* and *glucokinase* expression similar to Metformin; in HG-treated cells glucose homeostasis was disrupted by downregulation of *GLUT2*, *GS* and *GK* (Figure 6.1). Thus, *M. foetida* demonstrates the potential to be a valuable therapeutic agent in the treatment and management of T2DM. Most importantly, these data provide evidence for its long-standing traditional usage in diabetes treatment. Further studies should be conducted in a rat or mouse model to corroborate these findings.

In addition, the phytochemical composition of the aqueous leaf crude extracts needs to be investigated, and compounds should be individually assessed for their effect on hyperglycemia-induced oxidative stress.

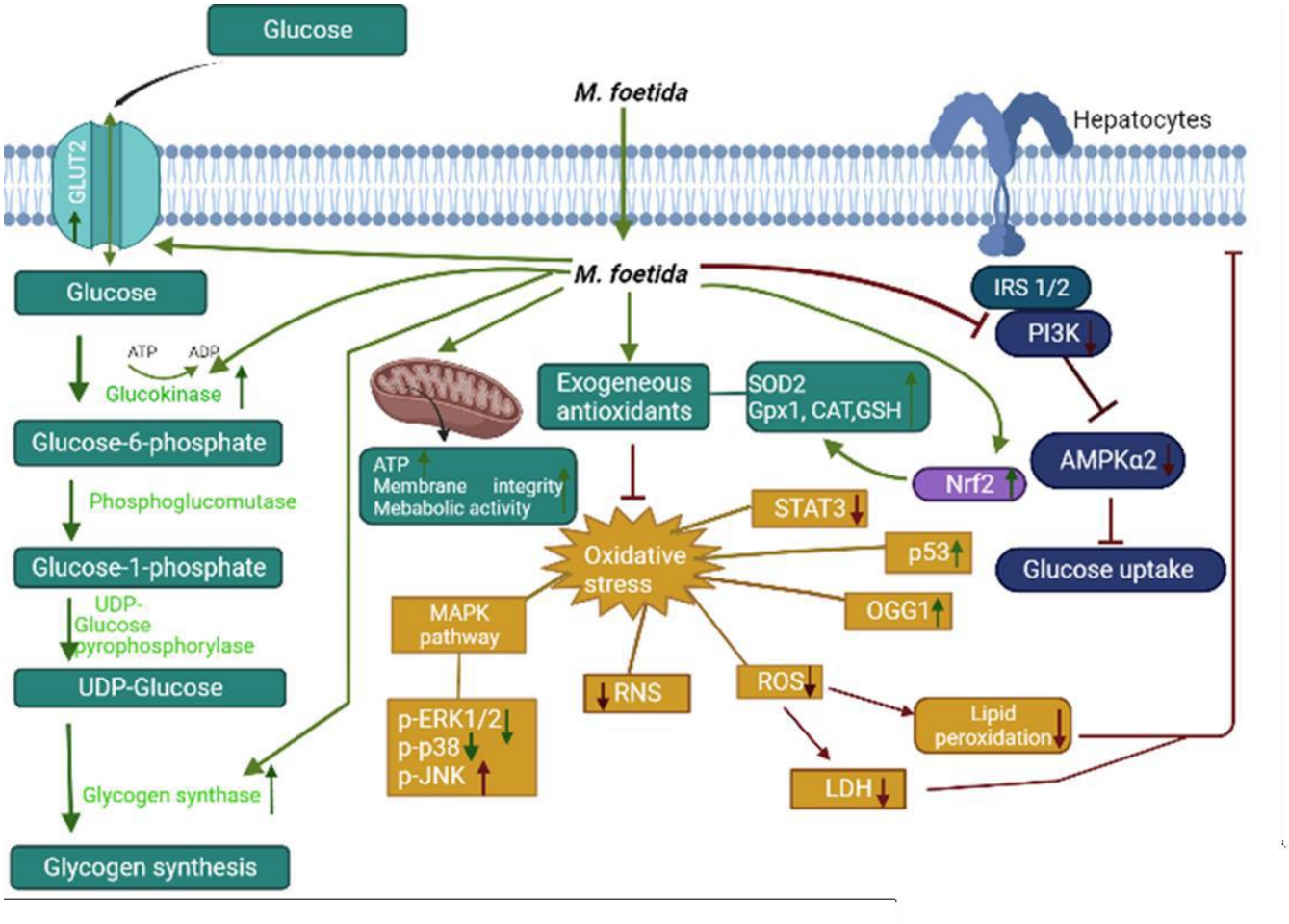

Figure 6.1: Summary diagram showing the pathways affected by *M. foetida* treatment of HepG2 cells under hyperglycemic conditions (prepared by author).

REFERENCES

ABDOLLAHI, S., MESHKINI, F., CLARK, C. C., HESHMATI, J. & SOLTANI, S. 2021. The Effect of Probiotics/synbiotics Supplementation on Renal and Liver Biomarkers in Patients with Type 2 Diabetes: A Systematic Review and Meta-Analysis of Randomized-Controlled Trials. *British Journal of Nutrition*, 1-31.

ABDULMALEK, S., ELDALA, A., AWAD, D. & BALBAA, M. 2021. Ameliorative effect of curcumin and zinc oxide nanoparticles on multiple mechanisms in obese rats with induced type 2 diabetes. *Scientific reports,* 11, 1-22.

ABO, K., FRED-JAIYESIMI, A. & JAIYESIMI, A. J. J. O. E. 2008a. Ethnobotanical studies of medicinal plants used in the management of diabetes mellitus in South Western Nigeria. 115, 67-71.

ABO, K. A., FRED-JAIYESIMI, A. A. & JAIYESIMI, A. E. 2008b. Ethnobotanical studies of medicinal plants used in the management of diabetes mellitus in South Western Nigeria. *J Ethnopharmacol,* 115, 67-71.

ACQUAVIVA, R., DI GIACOMO, C., VANELLA, L., SANTANGELO, R., SORRENTI, V., BARBAGALLO, I., GENOVESE, C., MASTROJENI, S., RAGUSA, S. & IAUK, L. 2013. Antioxidant activity of extracts of Momordica foetida Schumach. et Thonn. *Molecules,* 18, 3241-3249.

ADENIKE, A. O. 2020. In vitro antioxidant, α-amylase and α-glucosidase activities of methanol extracts from three Momordica species.

AGIUS, L. 2016. Hormonal and Metabolite Regulation of Hepatic Glucokinase. *Annu Rev Nutr,* 36, 389-415.

AKOMOLAFE, S. A., OYELEYE, S. I., OLASEHINDE, T. A. & OBOH, G. 2018. Phenolic characterization, antioxidant activities, and inhibitory effects of Physalis angulata and Newbouldia laevis on enzymes linked to erectile dysfunction. *International Journal of Food Properties,* 21, 645-654.

AL-GOBLAN, A. S., AL-ALFI, M. A. & KHAN, M. Z. 2014. Mechanism linking diabetes mellitus and obesity. *Diabetes, metabolic syndrome and obesity: targets and therapy,* 7, 587.

AL-ISHAQ, R. K., ABOTALEB, M., KUBATKA, P., KAJO, K. & BÜSSELBERG, D. 2019. Flavonoids and their anti-diabetic effects: cellular mechanisms and effects to improve blood sugar levels. *Biomolecules,* 9, 430.

ALAM, M. M., MEERZA, D. & NASEEM, I. 2014. Protective effect of quercetin on hyperglycemia, oxidative stress and DNA damage in alloxan induced type 2 diabetic mice. *Life sciences,* 109, 8-14.

ALAMRI, Z. Z. 2018. The role of liver in metabolism: an updated review with physiological emphasis.

ALBERTI, K. G. M. M. & ZIMMET, P. Z. 1998a. Definition, diagnosis and classification of diabetes mellitus and its complications. Part 1: diagnosis and classification of diabetes mellitus. Provisional report of a WHO consultation. *Diabetic medicine,* 15, 539-553.

ALBERTI, K. G. M. M. & ZIMMET, P. Z. J. D. M. 1998b. Definition, diagnosis and classification of diabetes mellitus and its complications. Part 1: diagnosis and classification of diabetes mellitus. Provisional report of a WHO consultation. 15, 539-553.

ALI, S. S., AHSAN, H., ANSARI, S., ABDULLAH, K. M. & KHAN, F. H. 2022. Photo-illuminated Glutathione Inactivates Alpha-2-macroglobulin: Spectroscopic and Thermodynamic Studies. *Molecular and Cellular Biomedical Sciences,* 6, 35-42.

ALISIK, M., NESELIOGLU, S. & EREL, O. 2019. A colorimetric method to measure oxidized, reduced and total glutathione levels in erythrocytes. *Journal of Laboratory Medicine,* 43, 269-277.

ALKAHTANI, S., ALARIFI, S., ALKAHTANE, A. A., ALBASHER, G., MOHAMMED, A.-Z., ALHOSHANI, N. M., AL-JOHANI, N. S., ALJARBA, N. H. & HASNAIN, M. S. 2021. Pyrroloquinoline quinone alleviates oxidative damage induced by high glucose in HepG2 cells. *Saudi Journal of Biological Sciences,* 28, 6127-6132.

AMERICANDIABETESASSOCIATION 2004. Gestational diabetes mellitus. *Diabetes care,* 27, s88-s90.

AMERICANDIABETESASSOCIATION 2017. 2. Classification and diagnosis of diabetes. *Diabetes care,* 40, S11-S24.

AMERICANDIABETESASSOCIATION 2019. 2. Classification and diagnosis of diabetes: standards of medical care in diabetes—2019. *Diabetes care,* 42, S13-S28.

AMINI, M., SABOORY, E., POURHEYDAR, B., BAGHERI, M. & NADERI, R. 2020. Involvement of endocannabinoid system, inflammation and apoptosis in diabetes induced liver injury: role of 5-HT3 receptor antagonist. *International immunopharmacology,* 79, 106158.

APOSTOLOVA, N., IANNANTUONI, F., GRUEVSKA, A., MUNTANE, J., ROCHA, M. & VICTOR, V. M. 2020. Mechanisms of action of metformin in type 2 diabetes: Effects on mitochondria and leukocyte-endothelium interactions. *Redox biology,* 34**,** 101517.

ARYA, M., SHERGILL, I. S., WILLIAMSON, M., GOMMERSALL, L., ARYA, N. & PATEL, H. R. 2005. Basic principles of real-time quantitative PCR. *Expert review of molecular diagnostics,* 5**,** 209-219.

ARYAL, S. 2021. *Real Time PCR- Principle, Process, Markers, Advantages, Uses* [Online]. Available: https://microbenotes.com/real-time-pcr-principle-process-markers-advantages-applications/ [Accessed].

ASCHNER, P., KARURANGA, S., JAMES, S., SIMMONS, D., BASIT, A., SHAW, J. E., WILD, S. H., OGURTSOVA, K. & SAEEDI, P. 2021. The International Diabetes Federation's guide for diabetes epidemiological studies. *Diabetes Research and Clinical Practice,* 172.

ASLAM, F., IQBAL, S., NASIR, M. & ANJUM, A. A. 2019. White sesame seed oil mitigates blood glucose level, reduces oxidative stress, and improves biomarkers of hepatic and renal function in participants with type 2 diabetes mellitus. *Journal of the American College of Nutrition,* 38**,** 235-246.

ASLANTÜRK, Ö. S. 2018a. *In vitro cytotoxicity and cell viability assays: principles, advantages, and disadvantages*, InTech.

ASLANTÜRK, Ö. S. 2018b. In vitro cytotoxicity and cell viability assays: principles, advantages, and disadvantages. *Genotoxicity-A predictable risk to our actual world,* 2**,** 64-80.

ASMAT, U., ABAD, K. & ISMAIL, K. 2016. Diabetes mellitus and oxidative stress—A concise review. *Saudi pharmaceutical journal,* 24**,** 547-553.

ASNAKE, S., TEKLEHAYMANOT, T., HYMETE, A., ERKO, B. & GIDAY, M. 2016. Antimalarial medicinal plants used by Gumuz people of mandura woreda, benishangul-gumuz regional state, Ethiopia.

ATCHAN NWAKIBAN, A. P., CICOLARI, S., PIAZZA, S., GELMINI, F., SANGIOVANNI, E., MARTINELLI, G., BOSSI, L., CARPENTIER-MAGUIRE, E., DEUTOU TCHAMGOUE, A. & AGBOR, G. A. 2020. Oxidative stress modulation by cameroonian spice extracts in hepg2 cells: Involvement of nrf2 and improvement of glucose uptake. *Metabolites,* 10**,** 182.

ATKINSON, M. A., EISENBARTH, G. S. & MICHELS, A. W. 2014. Type 1 diabetes. *The Lancet,* 383**,** 69-82.

ATLAS, D. 2021. IDF Diabetes Atlas. 10th ed.

AYALA, A., MUÑOZ, M. F. & ARGÜELLES, S. 2014. Lipid peroxidation: production, metabolism, and signaling mechanisms of malondialdehyde and 4-hydroxy-2-nonenal. *Oxidative medicine and cellular longevity,* 2014.

AZEMI, A. K., MOKHTAR, S. S., HOU, L. J., SHARIF, S. E. T. & RASOOL, A. H. G. 2021. Model for type 2 diabetes exhibits changes in vascular function and structure due to vascular oxidative stress and inflammation. *Biotechnic & Histochemistry,* 96**,** 498-506.

AZIZI, S., EBRAHIMI-MAMEGHANI, M., MOBASSERI, M., KARAMZAD, N. & MAHDAVI, R. 2021. Oxidative stress and nitrate/nitrite (NOx) status following citrulline supplementation in type 2 diabetes: a randomised, double-blind, placebo-controlled trial. *Journal of Human Nutrition and Dietetics,* 34**,** 64-72.

BADAL, S. S. & DANESH, F. R. 2014. New insights into molecular mechanisms of diabetic kidney disease. *American Journal of Kidney Diseases,* 63**,** S63-S83.

BAHADORAN, Z., GHASEMI, A., MIRMIRAN, P., AZIZI, F. & HADAEGH, F. 2015. Beneficial effects of inorganic nitrate/nitrite in type 2 diabetes and its complications. *Nutrition & metabolism,* 12**,** 1-9.

BAHADORAN, Z., MIRMIRAN, P. & GHASEMI, A. 2020. Role of nitric oxide in insulin secretion and glucose metabolism. *Trends in Endocrinology & Metabolism,* 31**,** 118-130.

BAHARVAND-AHMADI, B., BAHMANI, M., TAJEDDINI, P., NAGHDI, N. & RAFIEIAN-KOPAEI, M. 2016a. An ethno-medicinal study of medicinal plants used for the treatment of diabetes. *J Nephropathol,* 5**,** 44-50.

BAHARVAND-AHMADI, B., BAHMANI, M., TAJEDDINI, P., NAGHDI, N. & RAFIEIAN-KOPAEI, M. J. J. O. N. 2016b. An ethno-medicinal study of medicinal plants used for the treatment of diabetes. 5**,** 44.

BAHMANI, M., ZARGARAN, A., RAFIEIAN-KOPAEI, M. & SAKI, K. 2014. Ethnobotanical study of medicinal plants used in the management of diabetes mellitus in the Urmia, Northwest Iran. *Asian Pacific Journal of Tropical Medicine,* 7**,** S348-S354.

BALAKRISHNAN, B. B., KRISHNASAMY, K., MAYAKRISHNAN, V. & SELVARAJ, A. 2019. Moringa concanensis Nimmo extracts ameliorates hyperglycemia-mediated oxidative stress and upregulates PPARγ and GLUT4 gene expression in liver and pancreas of streptozotocin-nicotinamide induced diabetic rats. *Biomedicine & pharmacotherapy,* 112**,** 108688.

BANERJEE, J., MISHRA, N., DAMLE, G. & DHAS, Y. 2019. Beyond LDL-c: The importance of serum oxidized LDL in predicting risk for type 2 diabetes in the middle-aged Asian Indians. *Diabetes & Metabolic Syndrome: Clinical Research & Reviews,* 13**,** 206-213.

BASS, J. J., WILKINSON, D. J., RANKIN, D., PHILLIPS, B. E., SZEWCZYK, N. J., SMITH, K. & ATHERTON, P. J. 2017. An overview of technical considerations for Western blotting applications to physiological research. *Scandinavian journal of medicine & science in sports,* 27**,** 4-25.

BASSEY, I. E., INYANG, I. E., AKPAN, U. O., ISONG, I. K. P., ICHA, B. E., AYAWAN, V. M., PETER, R. E., ITITA, H. A., ODUMUSOR, P. U. & EKANEM, E. G. 2020. Cardiovascular disease risk factors and markers of oxidative stress and DNA damage in leprosy patients in Southern Nigeria. *PLoS neglected tropical diseases,* 14**,** e0008749.

BATISTA, T. M., HAIDER, N. & KAHN, C. R. 2021. Defining the underlying defect in insulin action in type 2 diabetes. *Diabetologia,* 64**,** 994-1006.

BIGAGLI, E. & LODOVICI, M. 2019. Circulating oxidative stress biomarkers in clinical studies on type 2 diabetes and its complications. *Oxidative Medicine and Cellular Longevity,* 2019.

BIRBEN, E., SAHINER, U. M., SACKESEN, C., ERZURUM, S. & KALAYCI, O. 2012. Oxidative stress and antioxidant defense. *World Allergy Organization Journal,* 5**,** 9-19.

BLAHOVA, J., MARTINIAKOVA, M., BABIKOVA, M., KOVACOVA, V., MONDOCKOVA, V. & OMELKA, R. 2021. Pharmaceutical drugs and natural therapeutic products for the treatment of type 2 diabetes mellitus. *Pharmaceuticals,* 14**,** 806.

BOUREBABA, N., KORNICKA-GARBOWSKA, K., MARYCZ, K., BOUREBABA, L. & KOWALCZUK, A. 2021. Laurus nobilis ethanolic extract attenuates hyperglycemia and hyperinsulinemia-induced insulin resistance in HepG2 cell line through the reduction of oxidative stress and improvement of mitochondrial biogenesis–Possible implication in pharmacotherapy. *Mitochondrion,* 59**,** 190-213.

BUCHANAN, T. A. & XIANG, A. H. 2005. Gestational diabetes mellitus. *The Journal of clinical investigation,* 115**,** 485-491.

CHADT, A. & AL-HASANI, H. 2020. Glucose transporters in adipose tissue, liver, and skeletal muscle in metabolic health and disease. *Pflügers Archiv-European Journal of Physiology***,** 1-26.

CHAMI, M. A. & KHALED, M. B. 2022. Epidemiology, diagnosis, and assessment of diabetes mellitus in the elderly population: a purposive review. *The North African Journal of Food and Nutrition Research,* 6**,** 9-21.

CHATTERJEE, S., KHUNTI, K. & DAVIES, M. J. 2017. Type 2 diabetes. *The Lancet,* 389**,** 2239-2251.

CHAUDHARI, H. J., RAVAT, M. K., VANIYA, V. H. & BHEDI, A. N. 2017. Morphological Study of Human Liver and Its Surgical Importance. *J Clin Diagn Res,* 11**,** AC09-AC12.

CHEN, R. J., ZHANG, G., GARFIELD, S. H., SHI, Y. J., CHEN, K. G., ROBEY, P. G. & LEAPMAN, R. D. 2015. Variations in Glycogen Synthesis in Human Pluripotent Stem Cells with Altered Pluripotent States. *PLoS One,* 10**,** e0142554.

CHIANG, J. 2014. Liver Physiology: Metabolism and Detoxification. *Pathobiology of Human Disease.*

CHIANG, J. Y. & FERRELL, J. M. J. G. E. 2018. Bile acid metabolism in liver pathobiology. 18**,** 71.

CHO, K.-H. & WOLKENHAUER, O. 2003. Analysis and modelling of signal transduction pathways in systems biology. Portland Press Ltd.

CHOLKAR, K., RAY, A., AGRAHARI, V., PAL, D. & MITRA, A. K. 2013. Transporters and receptors in the anterior segment of the eye. *Ocular Transporters and Receptors.* Elsevier.

CHOLLET, R. & RIBAULT, S. 2012. Use of ATP bioluminescence for rapid detection and enumeration of contaminants: the milliflex rapid microbiology detection and enumeration system. *Bioluminescence-Recent Advances in Oceanic Measurements and Laboratory Applications.* IntechOpen.

COCK, I., NDLOVU, N. & VAN VUUREN, S. 2021. The use of South African botanical species for the control of blood sugar. *Journal of Ethnopharmacology,* 264**,** 113234.

COLOMER, R., SARRATS, A., LUPU, R. & PUIG, T. 2017. Natural polyphenols and their synthetic analogs as emerging anticancer agents. *Current drug targets,* 18**,** 147-159.

CORDERO-HERRERA, I., MARTÍN, M. A., GOYA, L. & RAMOS, S. 2015. Cocoa flavonoids protect hepatic cells against high-glucose-induced oxidative stress: Relevance of MAPKs. *Molecular nutrition & food research,* 59**,** 597-609.

COWAN, K., ANICHTCHIK, O. & LUO, S. 2019. Mitochondrial integrity in neurodegeneration. *CNS neuroscience & therapeutics,* 25**,** 825-836.

CUNNINGHAM, C. C. 2003. Energy availability and alcohol-related liver pathology. *Alcohol Research & Health,* 27**,** 291.

CUSABIO. 2022. *Western Blotting (WB) Protocol* [Online]. Available: https://www.cusabio.com/m-244.html [Accessed].

DABELEA, D., MAYER-DAVIS, E. J., SAYDAH, S., IMPERATORE, G., LINDER, B., DIVERS, J., BELL, R., BADARU, A., TALTON, J. W. & CRUME, T. 2014. Prevalence of type 1 and type 2 diabetes among children and adolescents from 2001 to 2009. *Jama,* 311**,** 1778-1786.

DARE, A., CHANNA, M. L. & NADAR, A. 2021. L-ergothioneine and metformin alleviates liver injury in experimental type-2 diabetic rats via reduction of oxidative stress, inflammation, and hypertriglyceridemia. *Canadian journal of physiology and pharmacology,* 99**,** 1137-1147.

DAS, N. A., CARPENTER, A. J., BELENCHIA, A., AROOR, A. R., NODA, M., SIEBENLIST, U., CHANDRASEKAR, B. & DEMARCO, V. G. 2020. Empagliflozin reduces high glucose-induced oxidative stress and miR-21-dependent TRAF3IP2 induction and RECK suppression, and inhibits human renal proximal tubular epithelial cell migration and epithelial-to-mesenchymal transition. *Cellular signalling,* 68**,** 109506.

DAY, E. A., FORD, R. J. & STEINBERG, G. R. 2017. AMPK as a therapeutic target for treating metabolic diseases. *Trends in Endocrinology & Metabolism,* 28**,** 545-560.

DE LA TORRE, A. J., ROGOFF, D. & WHITE, P. C. 2013. P53 and cellular glucose uptake. *Endocrine research,* 38**,** 32-39.

DE LEON, J. A. D. & BORGES, C. R. 2020. Evaluation of Oxidative Stress in Biological Samples Using the Thiobarbituric Acid Reactive Substances Assay. *JoVE (Journal of Visualized Experiments)***,** e61122.

DEAVALL, D. G., MARTIN, E. A., HORNER, J. M. & ROBERTS, R. 2012. Drug-induced oxidative stress and toxicity. *Journal of toxicology,* 2012.

DEGLI ESPOSTI, D., HAMELIN, J., BOSSELUT, N., SAFFROY, R., SEBAGH, M., POMMIER, A., MARTEL, C. & LEMOINE, A. 2012. Mitochondrial roles and cytoprotection in chronic liver injury. *Biochemistry research international,* 2012.

DEMIR, S., NAWROTH, P. P., HERZIG, S. & EKIM ÜSTÜNEL, B. 2021. Emerging targets in type 2 diabetes and diabetic complications. *Advanced Science,* 8**,** 2100275.

DEVASAGAYAM, T., TILAK, J., BOLOOR, K., SANE, K. S., GHASKADBI, S. S. & LELE, R. 2004. Free radicals and antioxidants in human health: current status and future prospects. *Japi,* 52**,** 4.

DEWANJEE, S., DAS, A. K., SAHU, R. & GANGOPADHYAY, M. 2009. Antidiabetic activity of Diospyros peregrina fruit: effect on hyperglycemia, hyperlipidemia and augmented oxidative stress in experimental type 2 diabetes. *Food Chem Toxicol,* 47**,** 2679-85.

DHATARIYA, K. 2019. Diabetic ketoacidosis and hyperosmolar crisis in adults. *Medicine,* 47**,** 46-51.

DIHINGIA, A., OZAH, D., GHOSH, S., SARKAR, A., BARUAH, P. K., KALITA, J., SIL, P. C. & MANNA, P. 2018. Vitamin K1 inversely correlates with glycemia and insulin resistance in patients with type 2 diabetes (T2D) and positively regulates SIRT1/AMPK pathway of glucose metabolism in liver of T2D mice and hepatocytes cultured in high glucose. *The Journal of nutritional biochemistry,* 52**,** 103-114.

DING, X., JIAN, T., WU, Y., ZUO, Y., LI, J., LV, H., MA, L., REN, B., ZHAO, L. & LI, W. 2019. Ellagic acid ameliorates oxidative stress and insulin resistance in high glucose-treated HepG2 cells via miR-223/keap1-Nrf2 pathway. *Biomedicine & Pharmacotherapy,* 110**,** 85-94.

DUTTA, S., MISHRA, S. P., SAHU, A. K., MISHRA, K., KASHYAP, P. & SAHU, B. 2021. Hepatocytes and Their Role in Metabolism. *Drug Metabolism***,** 3.

EID, H. M., NACHAR, A., THONG, F., SWEENEY, G. & HADDAD, P. S. 2015. The molecular basis of the antidiabetic action of quercetin in cultured skeletal muscle cells and hepatocytes. *Pharmacognosy magazine,* 11**,** 74.

ELUJOBA, A. A., ODELEYE, O., OGUNYEMI, C. J. A. J. O. T., COMPLEMENTARY & MEDICINES, A. 2005. Traditional medicine development for medical and dental primary health care delivery system in Africa. 2**,** 46-61.

FARHOOD, H. B., BALAS, M., GRADINARU, D., MARGINA, D. & DINISCHIOTU, A. 2019. Effects of chlorogenic acid on the liver cell metabolism under high glucose conditions. *Rom Biotechnol Lett,* 24**,** 883-892.

FATHURRAHMAN, I., KUSUMAWATI, A., RAHMAN, A., ULVIANI, Y., PRIHANTOKO, K. & UNSUNNIDHAL, L. Molecular sexing in Bos taurus using quantitative polymerase chain reaction (qPCR) method. IOP Conference Series: Earth and Environmental Science, 2022. IOP Publishing, 012002.

FERN, K. 2014. *Useful Tropical Plants Database* [Online]. Available: https://tropical.theferns.info/viewtropical.php?id=Momordica+foetida [Accessed].

FERNÁNDEZ-MEJÍA, C. 2013. Oxidative stress in diabetes mellitus and the role of vitamins with antioxidant actions. *Oxidative stress and chronic degenerative diseases-a role for antioxidants,* 209.

FODEN, W. P., L. 2005. *Momordica foetida Schumach. National Assessment: Red List of South African Plants* [Online]. Available: http://redlist.sanbi.org/species.php?species=1930-8 [Accessed 2021].

FOWLER, M. J. 2008. Microvascular and macrovascular complications of diabetes. *Clinical diabetes,* 26**,** 77-82.

FROELICH, S., ONEGI, B., KAKOOKO, A., SIEMS, K., SCHUBERT, C. & JENETT-SIEMS, K. 2007. Plants traditionally used against malaria: phytochemical and pharmacological investigation of Momordica foetida. *Revista Brasileira de Farmacognosia,* 17**,** 1-17.

FRÖJDÖ, S., VIDAL, H. & PIROLA, L. 2009. Alterations of insulin signaling in type 2 diabetes: a review of the current evidence from humans. *Biochimica et Biophysica Acta (BBA)-Molecular Basis of Disease,* 1792**,** 83-92.

GALICIA-GARCIA, U., BENITO-VICENTE, A., JEBARI, S., LARREA-SEBAL, A., SIDDIQI, H., URIBE, K. B., OSTOLAZA, H. & MARTÍN, C. J. I. J. O. M. S. 2020. Pathophysiology of type 2 diabetes mellitus. 21**,** 6275.

GAUCHER, C., BOUDIER, A., BONETTI, J., CLAROT, I., LEROY, P. & PARENT, M. 2018. Glutathione: antioxidant properties dedicated to nanotechnologies. *Antioxidants,* 7**,** 62.

GERMOUSH, M. O., ELGEBALY, H. A., HASSAN, S., KAMEL, E. M., BIN-JUMAH, M. & MAHMOUD, A. M. 2019. Consumption of terpenoids-rich padina pavonia extract attenuates hyperglycemia, insulin resistance and oxidative stress, and upregulates pparγ in a rat model of type 2 diabetes. *Antioxidants,* 9**,** 22.

GHAFOURIFAR, P., PARIHAR, M. S., NAZAREWICZ, R., ZENEBE, W. J. & PARIHAR, A. 2008. Detection assays for determination of mitochondrial nitric oxide synthase activity; advantages and limitations. *Methods in enzymology,* 440**,** 317-334.

GHASEMI, A., HEDAYATI, M. & BIABANI, H. 2007. Protein precipitation methods evaluated for determination of serum nitric oxide end products by the Griess assay. *Jmsr,* 2**,** 29-32.

GOUNDEN, S., PHULUKDAREE, A., MOODLEY, D. & CHUTURGOON, A. 2015. Increased SIRT3 expression and antioxidant defense under hyperglycemic conditions in HepG2 cells. *Metabolic syndrome and related disorders,* 13**,** 255-263.

GRYSZCZYŃSKA, B., FORMANOWICZ, D., BUDZYŃ, M., WANIC-KOSSOWSKA, M., PAWLICZAK, E., FORMANOWICZ, P., MAJEWSKI, W., STRZYŻEWSKI, K. W., KASPRZAK, M. P. & ISKRA, M. 2017. Advanced oxidation protein products and carbonylated proteins as biomarkers of oxidative stress in selected atherosclerosis-mediated diseases. *BioMed Research International,* 2017.

GWOZDZ, T. & DOREY, K. 2017. Western blot. *Basic science methods for clinical researchers.* Elsevier.

HAN, H. S., KANG, G., KIM, J. S., CHOI, B. H. & KOO, S. H. 2016. Regulation of glucose metabolism from a liver-centric perspective. *Exp Mol Med,* 48**,** e218.

HEIBEL, A. B., DA CUNHA, M. D. S. B., FERRAZ, C. T. S. & ARRUDA, S. F. 2018. Tucum-do-cerrado (Bactris setosa Mart.) may enhance hepatic glucose response by suppressing gluconeogenesis and upregulating Slc2a2 via AMPK pathway, even in a moderate iron supplementation condition. *Food Research International,* 113**,** 433-442.

HUSSAIN, T., TAN, B., MURTAZA, G., LIU, G., RAHU, N., KALHORO, M. S., KALHORO, D. H., ADEBOWALE, T. O., MAZHAR, M. U. & UR REHMAN, Z. 2020. Flavonoids and type 2 diabetes: Evidence of efficacy in clinical and animal studies and delivery strategies to enhance their therapeutic efficacy. *Pharmacological research,* 152**,** 104629.

HYDE, M. A., WURSTEN, B.T., BALLINGS, P. & COATES PALGRAVE, M. 2002. *Momordica foetida Schumach.* [Online]. Available: https://www.zimbabweflora.co.zw/speciesdata/species.php?species_id=157210 [Accessed 7 July 2020 2020].

IBRAHIM, M., PARVEEN, B., ZAHIRUDDIN, S., GAUTAM, G., PARVEEN, R., KHAN, M. A., GUPTA, A. & AHMAD, S. 2021. Analysis of polyphenols in Aegle marmelos leaf and ameliorative efficacy against diabetic mice through restoration of antioxidant and anti-inflammatory status. *Journal of Food Biochemistry***,** e13852.

IFTIKHAR, A., ASLAM, B., IFTIKHAR, M., MAJEED, W., BATOOL, M., ZAHOOR, B., AMNA, N., GOHAR, H. & LATIF, I. 2020. Effect of Caesalpinia bonduc polyphenol extract on alloxan-induced diabetic rats in attenuating hyperglycemia by upregulating insulin secretion and inhibiting JNK signaling pathway. *Oxidative medicine and cellular longevity,* 2020.

IGHODARO, O. & AKINLOYE, O. 2018. First line defence antioxidants-superoxide dismutase (SOD), catalase (CAT) and glutathione peroxidase (GPX): Their fundamental role in the entire antioxidant defence grid. *Alexandria journal of medicine,* 54**,** 287-293.

INZUCCHI, S. E., BERGENSTAL, R. M., BUSE, J. B., DIAMANT, M., FERRANNINI, E., NAUCK, M., PETERS, A. L., TSAPAS, A., WENDER, R. & MATTHEWS, D. R. 2015. Management of hyperglycaemia in type 2 diabetes, 2015: a patient-centred approach. Update to a position statement of the American Diabetes Association and the European Association for the Study of Diabetes. *Diabetologia,* 58**,** 429-442.

ITAHANA, Y. & ITAHANA, K. 2018. Emerging roles of p53 family members in glucose metabolism. *International journal of molecular sciences,* 19**,** 776.

JALALI, M., ZABOROWSKA, J. & JALALI, M. 2017. The polymerase chain reaction: PCR, qPCR, and RT-PCR. *Basic science methods for clinical researchers.* Elsevier.

JAVID, A. Z., HOSSEINI, S. A., GHOLINEZHAD, H., MORADI, L., HAGHIGHI-ZADEH, M. H. & BAZYAR, H. 2020. Antioxidant and anti-inflammatory properties of melatonin in patients with type 2 diabetes mellitus with periodontal disease under non-surgical periodontal therapy: a double-blind, placebo-controlled trial. *Diabetes, metabolic syndrome and obesity: targets and therapy,* 13**,** 753.

JOSHI, S. R., PARIKH, R. M. & DAS, A. 2007. Insulin-history, biochemistry, physiology and pharmacology. *Journal-association of physicians of India,* 55**,** 19.

KABEL, A. M. 2014. Free radicals and antioxidants: role of enzymes and nutrition. *World Journal of Nutrition and Health,* 2**,** 35-38.

KADRI, K. 2019. Polymerase chain reaction (PCR): principle and applications. *Synthetic Biology-New Interdisciplinary Science*.

KARIGIDI, K. O., AKINTIMEHIN, E. S., OMOBOYOWA, D. A., ADETUYI, F. O. & OLAIYA, C. O. 2020. Effect of Curculigo pilosa supplemented diet on blood sugar, lipid metabolism, hepatic oxidative stress and carbohydrate metabolism enzymes in streptozotocin-induced diabetic rats. *Journal of Diabetes & Metabolic Disorders,* 19**,** 1173-1184.

KASANGANA, P. B., EID, H. M., NACHAR, A., STEVANOVIC, T. & HADDAD, P. S. 2019. Further isolation and identification of anti-diabetic principles from root bark of Myrianthus arboreus P. Beauv.: The ethyl acetate fraction contains bioactive phenolic compounds that improve liver cell glucose homeostasis. *J Ethnopharmacol,* 245**,** 112167.

KHARROUBI, A. T. & DARWISH, H. M. 2015. Diabetes mellitus: The epidemic of the century. *World journal of diabetes,* 6**,** 850.

KHOZA, B., DUBERY, I., BYTH-ILLING, H.-A., STEENKAMP, P., CHIMUKA, L. & MADALA, N. 2016. Optimization of pressurized hot water extraction of flavonoids from Momordica foetida using UHPLC-qTOF-MS and multivariate chemometric approaches. *Food Analytical Methods,* 9**,** 1480-1489.

KIM, M. K., KO, S.-H., KIM, B.-Y., KANG, E. S., NOH, J., KIM, S.-K., PARK, S.-O., HUR, K. Y., CHON, S., MOON, M. K. J. D. & JOURNAL, M. 2019. 2019 Clinical practice guidelines for type 2 diabetes mellitus in Korea. 43**,** 398-406.

KINSELLA, G. K., CANNITO, S., BORDANO, V., STEPHENS, J. C., ROSA, A. C., MIGLIO, G., GUASCHINO, V., IANNACCONE, V., FINDLAY, J. B. & BENETTI, E. 2021. GPR21 Inhibition Increases Glucose-Uptake in HepG2 Cells. *International journal of molecular sciences,* 22**,** 10784.

KLISIĆ, A., ISAKOVIĆ, A., KOCIĆ, G., KAVARIĆ, N., JOVANOVIĆ, M., ZVRKO, E., SKEROVIĆ, V. & NINIĆ, A. 2018. Relationship between oxidative stress, inflammation and dyslipidemia with fatty liver index in patients with type 2 diabetes mellitus. *Experimental and Clinical Endocrinology & Diabetes,* 126**,** 371-378.

KOK, A., HARIRAM, A., WEBB, D. & AMOD, A. 2021. Patterns of diabetes management in South Africa: baseline and 24-month data from the South African cohort of the DISCOVER study. *Journal of Endocrinology, Metabolism and Diabetes in South Africa,* 26**,** 60-65.

KOMAKECH, R. 2017. *Plants & Herbs: Momordica Foetida – A Very Versatile Plant* [Online]. Available: https://combonimissionaries.ie/2017/11/16/plants-herbs-momordica-foetida-a-very-versatile-plant/ [Accessed 21-03-2021 2021].

KUETE, V., KARAOSMANOĞLU, O. & SIVAS, H. 2017. Anticancer activities of African medicinal spices and vegetables. *Medicinal Spices and Vegetables from Africa.* Elsevier.

KUMAR, K. S., LIN, C., TSENG, Y.-H. & WANG, S.-Y. 2021. Fruits of Rosa laevigata and its bio-active principal sitostenone facilitate glucose uptake and insulin sensitivity in hepatic cells via AMPK/PPAR-γ activation. *Phytomedicine Plus,* 1**,** 100109.

KUO, F. Y., CHENG, K.-C., LI, Y., CHENG, J.-T. & TSAI, C.-C. 2020. Promotion of Adropin Expression by Hyperglycemia Is Associated with STAT3 Activation in Diabetic Rats. *Diabetes, Metabolic Syndrome and Obesity: Targets and Therapy,* 13**,** 2269.

LAN, S.-F., SAFIEJKO-MROCZKA, B. & STARLY, B. 2010. Long-term cultivation of HepG2 liver cells encapsulated in alginate hydrogels: a study of cell viability, morphology and drug metabolism. *Toxicology in Vitro,* 24**,** 1314-1323.

LEE, H. B., YU, M.-R., YANG, Y., JIANG, Z. & HA, H. 2003. Reactive oxygen species-regulated signaling pathways in diabetic nephropathy. *Journal of the American Society of Nephrology,* 14**,** S241-S245.

LEE, S., WASHBURN, D. J., COLWELL, B., GWARZO, I. H., KELLSTEDT, D., AHENDA, P., MADDOCK, J. E. J. D. R. & PRACTICE, C. 2021. Examining social determinants of undiagnosed diabetes in Namibia and South Africa using a behavioral model of health services use. 175**,** 108814.

LENNICKE, C. & COCHEMÉ, H. M. 2021. Redox regulation of the insulin signalling pathway. *Redox Biology,* 42**,** 101964.

LENNICKE, C., RAHN, J., LICHTENFELS, R., WESSJOHANN, L. A. & SELIGER, B. 2015. Hydrogen peroxide–production, fate and role in redox signaling of tumor cells. *Cell Communication and Signaling,* 13**,** 1-19.

LEUTI, A., MACCARRONE, M. & CHIURCHIÙ, V. 2019. Proresolving lipid mediators: endogenous modulators of oxidative stress. *Oxidative medicine and cellular longevity,* 2019.

LI, C. & HU, Z. 2020. Is liver glycogen fragility a possible drug target for diabetes? *The FASEB Journal,* 34**,** 3-15.

LI, C., YANG, J., LIU, C., WANG, X. & ZHANG, L. 2020. Long Non-Coding RNAs in Hepatocellular Carcinoma: Ordering of the Complicated lncRNA Regulatory Network and Novel Strategies for HCC Clinical Diagnosis and Treatment. *Pharmacological Research***,** 104848.

LI, M., DANG, Y., LI, Q., ZHOU, W., ZUO, J., YAO, Z., ZHANG, L. & JI, G. 2019. Berberine alleviates hyperglycemia by targeting hepatic glucokinase in diabetic db/db mice. *Scientific reports,* 9**,** 1-12.

LIGUORI, I., RUSSO, G., CURCIO, F., BULLI, G., ARAN, L., DELLA-MORTE, D., GARGIULO, G., TESTA, G., CACCIATORE, F. & BONADUCE, D. 2018. Oxidative stress, aging, and diseases. *Clinical interventions in aging,* 13**,** 757.

LIU, J.-Y., ZHANG, Y.-C., SONG, L.-N., ZHANG, L., YANG, F.-Y., ZHU, X.-R., CHENG, Z.-Q., CAO, X. & YANG, J.-K. 2019. Nifuroxazide ameliorates lipid and glucose metabolism in palmitate-induced HepG2 cells. *RSC Advances,* 9**,** 39394-39404.

LIVAK, K. J. & SCHMITTGEN, T. D. 2001. Analysis of relative gene expression data using real-time quantitative PCR and the 2− ΔΔCT method. *methods,* 25**,** 402-408.

LODHI, S. & KORI, M. L. 2021. Structure–Activity Relationship and Therapeutic Benefits of Flavonoids in the Management of Diabetes and Associated Disorders. *Pharmaceutical Chemistry Journal,* 54**,** 1106-1125.

LÓPEZ-SOLDADO, I., BERTINI, A., ADROVER, A., DURAN, J. & GUINOVART, J. J. 2020. Maintenance of liver glycogen during long-term fasting preserves energy state in mice. *FEBS letters,* 594**,** 1698-1710.

LORENTE, S., HAUTEFEUILLE, M. & SANCHEZ-CEDILLO, A. 2020. The liver, a functionalized vascular structure. *Sci Rep,* 10**,** 16194.

LUNDBERG, J. O., CARLSTRÖM, M. & WEITZBERG, E. 2018. Metabolic effects of dietary nitrate in health and disease. *Cell metabolism,* 28**,** 9-22.

MAANDA, M. & BHAT, R. 2010. Wild vegetable use by Vhavenda in the Venda region of Limpopo Province, South Africa. *Phyton (Buenos Aires),* 79**,** 189-194.
MAGKOS, F., WANG, X. & MITTENDORFER, B. 2010. Metabolic actions of insulin in men and women. *Nutrition,* 26**,** 686-693.
MAGWEDE, K., VAN WYK, B. E. & VAN WYK, A. E. 2019. An inventory of Vhavenda useful plants. *South African Journal of Botany,* 122**,** 57-89.
MAHADEVAN, V. 2020. Anatomy of the liver. *Surgery (Oxford),* 38**,** 427-431.
MAJEED, H. J., IBRAHIM, G. I., YOUSIF, P. A. & ABDULKAREEM, S. M. 2021. Association between some serum oxidative stress biomarkers and lipid profile in type 2 diabetic patients in Erbil City. *Zanco Journal of Pure and Applied Sciences,* 33**,** 107-112.
MAN, T. P. 2020. *The Role of LDH in Cellular Cytotoxicity* [Online]. Available: https://info.gbiosciences.com/blog/the-role-of-ldh-in-cellular-cytotoxicity [Accessed 7 September 2020].
MANCUSI, C., IZZO, R., DI GIOIA, G., LOSI, M. A., BARBATO, E. & MORISCO, C. 2020. Insulin resistance the hinge between hypertension and type 2 diabetes. *High Blood Pressure & Cardiovascular Prevention,* 27**,** 515-526.
MARITIM, A., SANDERS, A. & WATKINS III, J. 2003. Diabetes, oxidative stress, and antioxidants: a review. *Journal of biochemical and molecular toxicology,* 17**,** 24-38.
MARTIN, K. 2022. *A Quick and Helpful Introduction to the ATP Bioluminescence Assay* [Online]. Gold Biotechnology. Available: https://www.goldbio.com/articles/article/Quick-Helpful-Introduction-to-ATP-Bioluminescence-Assay [Accessed].
MCCUNE, L. M. & JOHNS, T. 2002. Antioxidant activity in medicinal plants associated with the symptoms of diabetes mellitus used by the indigenous peoples of the North American boreal forest. *Journal of Ethnopharmacology,* 82**,** 197-205.
MEENAKSHI, P., BHUVANESHWARI, R., RATHI, M. A., THIRUMOORTHI, L., GURAVAIAH, D. C., JIJI, M. J. & GOPALAKRISHNAN, V. K. 2010. Antidiabetic activity of ethanolic extract of Zaleya decandra in alloxan-induced diabetic rats. *Applied biochemistry and biotechnology,* 162**,** 1153-1159.
MEHDI, M., MENON, M., SEYOUM, N., BEKELE, M., TIGENEH, W. & SEIFU, D. 2018. Blood and tissue enzymatic activities of GDH and LDH, index of glutathione, and oxidative stress among breast cancer patients attending Referral Hospitals of Addis Ababa, Ethiopia: hospital-based comparative cross-sectional study. *Oxidative medicine and cellular longevity,* 2018.
MISHRA, S. & MISHRA, B. B. 2017. Study of lipid peroxidation, nitric oxide end product, and trace element status in type 2 diabetes mellitus with and without complications. *International Journal of Applied and Basic Medical Research,* 7**,** 88.
MOHAMED, J., NAFIZAH, A. N., ZARIYANTEY, A. & BUDIN, S. 2016. Mechanisms of diabetes-induced liver damage: the role of oxidative stress and inflammation. *Sultan Qaboos University Medical Journal,* 16**,** e132.
MOKGANYA, M. & TSHISIKHAWE, M. 2019. Medicinal uses of selected wild edible vegetables consumed by Vhavenda of the Vhembe District Municipality, South Africa. *South African Journal of Botany,* 122**,** 184-188.
MOLEHIN, O. & ADEFEGHA, S. 2014. Comparative study of the aqueous and ethanolic extract of Momordica foetida on the phenolic content and antioxidant properties. *International Food Research Journal,* 21**,** 401.
MORÓN, Ú. M. & CASTILLA-CORTÁZAR, I. J. A. E. 2012. Protection against oxidative stress and "IGF-I deficiency conditions". 89.
MOTALA, A. A., MBANYA, J. C., RAMAIYA, K., PIRIE, F. J. & EKORU, K. 2022. Type 2 diabetes mellitus in sub-Saharan Africa: challenges and opportunities. *Nature Reviews Endocrinology***,** 1-11.
MOUSSA, S. 2008. Oxidative stress in diabetes mellitus. *Romanian J biophys,* 18**,** 225-236.
MU, W., CHENG, X.-F., LIU, Y., LV, Q.-Z., LIU, G.-L., ZHANG, J.-G. & LI, X.-Y. 2019. Potential nexus of non-alcoholic fatty liver disease and type 2 diabetes mellitus: insulin resistance between hepatic and peripheral tissues. *Frontiers in pharmacology,* 9**,** 1566.
MUKHTAR, Y., GALALAIN, A. & YUNUSA, U. 2020. A modern overview on diabetes mellitus: a chronic endocrine disorder. *European Journal of Biology,* 5**,** 1-14.

MULHOLLAND, D. A., SEWRAM, V., OSBORNE, R., PEGEL, K. H. & CONNOLLY, J. D. 1997a. Cucurbitane triterpenoids from the leaves of Momordica foetida. *Phytochemistry,* 45**,** 391-395.

MULHOLLAND, D. A., SEWRAM, V., OSBORNE, R., PEGEL, K. H. & CONNOLLY, J. D. J. P. 1997b. Cucurbitane triterpenoids from the leaves of Momordica foetida. 45**,** 391-395.

MURONGA, M., QUISPE, C., TSHIKHUDO, P. P., MSAGATI, T. A., MUDAU, F. N., MARTORELL, M., SALEHI, B., ABDULL RAZIS, A. F., SUNUSI, U. & KAMAL, R. M. 2021. Three Selected Edible Crops of the Genus Momordica as Potential Sources of Phytochemicals: Biochemical, Nutritional, and Medicinal Values. *Frontiers in Pharmacology,* 12**,** 1123.

MURONGA, M., TSHIKHUDO, P. P., MSAGATI, T. A. & MUDAU, F. N. 2020. Three Selected Edible Crops of the Genus Momordica as a Potential Source of Phytochemicals: From Production to Pharmaceutical Usage. *Preprints*.

MYKONIATIS, I., GRAMMATIKOPOULOU, M. G., BOURAS, E., KARAMPASI, E., TSIONGA, A., KOGIAS, A., VAKALOPOULOS, I., HAIDICH, A.-B. & CHOURDAKIS, M. 2018. Sexual dysfunction among young men: overview of dietary components associated with erectile dysfunction. *The Journal of Sexual Medicine,* 15**,** 176-182.

NAICKER, N., NAGIAH, S., PHULUKDAREE, A. & CHUTURGOON, A. 2016. Trigonella foenum-graecum seed extract, 4-hydroxyisoleucine, and metformin stimulate proximal insulin signaling and increase expression of glycogenic enzymes and GLUT2 in HepG2 cells. *Metabolic syndrome and related disorders,* 14**,** 114-120.

NAJAFOV, A. & HOXHAJ, G. 2017. *Western Blotting Guru*, Academic Press.

NANDI, A., YAN, L.-J., JANA, C. K. & DAS, N. 2019. Role of catalase in oxidative stress-and age-associated degenerative diseases. *Oxidative medicine and cellular longevity,* 2019.

NANTIA, A., SOH, D., CHOUMESSI, T., NGUM, N., CHI, H. & KENFACK, A. 2018. In vitro antioxidant property of the methanol extracts of the whole plant and fruit of Momordica foetida (Cucurbitaceae). *The Pharmaceutical and Chemical Journal,* 5**,** 117-125.

NARENDHIRAKANNAN, R., SUBRAMANIAN, S. & KANDASWAMY, M. 2005a. Mineral content of some medicinal plants used in the treatment of diabetes mellitus. *Biological trace element research,* 103**,** 109-115.

NARENDHIRAKANNAN, R., SUBRAMANIAN, S. & KANDASWAMY, M. J. B. T. E. R. 2005b. Mineral content of some medicinal plants used in the treatment of diabetes mellitus. 103**,** 109-115.

NAVALE, A. M. & PARANJAPE, A. N. 2016. Glucose transporters: physiological and pathological roles. *Biophysical reviews,* 8**,** 5-9.

NAZARIAN-SAMANI, Z., SEWELL, R. D. E., LORIGOOINI, Z., AND & RAFIEIAN-KOPAEI, M. 2018. Medicinal plants with multiple effects on diabetes mellitus and its complications: a systematic review. *Current diabetes reports,* 18**,** 1-13.

NDHLALA, A., FINNIE, J. & VAN STADEN, J. 2011. Plant composition, pharmacological properties and mutagenic evaluation of a commercial Zulu herbal mixture: Imbiza ephuzwato. *Journal of Ethnopharmacology,* 133**,** 663-674.

NITA, M. & GRZYBOWSKI, A. 2016. The role of the reactive oxygen species and oxidative stress in the pathomechanism of the age-related ocular diseases and other pathologies of the anterior and posterior eye segments in adults. *Oxidative medicine and cellular longevity,* 2016.

NKAMBULE, T. 2017. *Evaluation of Momordica balsamina and Momordica foetida from Swaziland for their antimicrobial activity, anti-proliferative properties and biochemical composition.* University of Nottingham.

NOUMI, E. & DJEUMEN, C. 2007. Abortifacient plants of the Buea region, their participation in the sexuality of adolescent girls.

NOZAKI, Y., PETERSEN, M. C., ZHANG, D., VATNER, D. F., PERRY, R. J., ABULIZI, A., HAEDERSDAL, S., ZHANG, X.-M., BUTRICO, G. M. & SAMUEL, V. T. 2020. Metabolic control analysis of hepatic glycogen synthesis in vivo. *Proceedings of the National Academy of Sciences,* 117**,** 8166-8176.

ODELEYE, O. M. & OYEDEJI, A. O. 2008. Antibacterial Activity of Crude and Fractions of Momordica foetida Leaf Extracts. *International Journal of Biomedical and Pharmaceutical Sciences,* 2**,** 75-78.

ODEYEMI, S. & DEWAR, J. 2020. In vitro antidiabetic activity affecting glucose uptake in hepg2 cells following their exposure to extracts of Lauridia tetragona (Lf) RH Archer. *Processes,* 8**,** 33.

OGURTSOVA, K., GUARIGUATA, L., BARENGO, N. C., RUIZ, P. L.-D., SACRE, J. W., KARURANGA, S., SUN, H., BOYKO, E. J. & MAGLIANO, D. J. 2022. IDF diabetes Atlas: Global estimates of undiagnosed diabetes in adults for 2021. *Diabetes research and clinical practice,* 183**,** 109118.

OLIVARES-REYES, J. A., ARELLANO-PLANCARTE, A. & CASTILLO-HERNANDEZ, J. R. 2009a. Angiotensin II and the development of insulin resistance: implications for diabetes. *Molecular and cellular endocrinology,* 302**,** 128-139.

OLIVARES-REYES, J. A., ARELLANO-PLANCARTE, A., CASTILLO-HERNANDEZ, J. R. J. M. & ENDOCRINOLOGY, C. 2009b. Angiotensin II and the development of insulin resistance: implications for diabetes. 302**,** 128-139.

OLOYEDE, O. & ALUKO, O. 2012. Determination of antioxidant potential of Momordica Foetida leaf extract on tissue homogenate. *Science Journal of Medicine and Clinical Trial,* 2012.

OLWENYI, O. A., ASINGURA, B., NALUYIMA, P., ANYWAR, G. U., NALUNGA, J., NAKABUYE, M., SEMWOGERERE, M., BAGAYA, B., CHAM, F. & TINDIKAHWA, A. 2021. In-vitro Immunomodulatory activity of Azadirachta indica A. Juss. Ethanol: water mixture against HIV associated chronic CD4+ T-cell activation/exhaustion. *BMC complementary medicine and therapies,* 21**,** 1-14.

OMOKHUA-UYI, A. G. & VAN STADEN, J. 2020a. Phytomedicinal relevance of South African Cucurbitaceae species and their safety assessment: A review. *Journal of Ethnopharmacology***,** 112967.

OMOKHUA-UYI, A. G. & VAN STADEN, J. 2020b. Phytomedicinal relevance of South African Cucurbitaceae species and their safety assessment: A review. *Journal of Ethnopharmacology,* 259**,** 112967.

OYEDEMI, S., BRADLEY, G. & AFOLAYAN, A. 2009. Ethnobotanical survey of medicinal plants used for the management of diabetes mellitus in the Nkonkobe municipality of South Africa. *Journal of Medicinal Plants Research,* 3**,** 1040-1044.

PANG, J., XI, C., DAI, Y., GONG, H. & ZHANG, T.-M. 2012. Altered expression of base excision repair genes in response to high glucose-induced oxidative stress in HepG2 hepatocytes. *Medical science monitor: international medical journal of experimental and clinical research,* 18**,** BR281.

PAREEK, H., SHARMA, S., KHAJJA, B. S., JAIN, K. & JAIN, G. 2009a. Evaluation of hypoglycemic and anti-hyperglycemic potential of Tridax procumbens (Linn.). *BMC complementary and alternative medicine,* 9**,** 48.

PAREEK, H., SHARMA, S., KHAJJA, B. S., JAIN, K., JAIN, G. J. B. C. & MEDICINE, A. 2009b. Evaluation of hypoglycemic and anti-hyperglycemic potential of Tridax procumbens (Linn.). 9**,** 1-7.

PARHAMIFAR, L., ANDERSEN, H. & MOGHIMI, S. M. 2019. Lactate dehydrogenase assay for assessment of polycation cytotoxicity. *Nanotechnology for Nucleic Acid Delivery.* Springer.

PHEIFFER, C., PILLAY-VAN WYK, V., TURAWA, E., LEVITT, N., KENGNE, A. P., BRADSHAW, D. J. I. J. O. E. R. & HEALTH, P. 2021. Prevalence of Type 2 Diabetes in South Africa: A Systematic Review and Meta-Analysis. 18**,** 5868.

PIEME, C. A., TATANGMO, J. A., SIMO, G., NYA, P. C. B., MOOR, V. J. A., MOUKETTE, B. M., NZUFO, F. T., NONO, B. L. N. & SOBNGWI, E. 2017. Relationship between hyperglycemia, antioxidant capacity and some enzymatic and non-enzymatic antioxidants in African patients with type 2 diabetes. *BMC research notes,* 10**,** 1-7.

POSTIC, C., DENTIN, R. & GIRARD, J. 2004. Role of the liver in the control of carbohydrate and lipid homeostasis. *Diabetes & Metabolism,* 30**,** 398-408.

PRASAD, S. H., SUBBAIAH, G. V., RAVI, S., REDDY, B. V. G., SHANMUGAM, B. & REDDY, K. S. J. P. M. 2020. Preclinical study on effects of Acalypha indica on streptozotocin-induced liver damage in diabetic rats. 16**,** 722.

PROMEGA. 2022. *A Luminescent-Based Assay for the Detection and Quantification of Glutathione (GSH)* [Online]. Available: https://worldwide.promega.com/products/cell-health-assays/oxidative-stress-assays/gsh_glo-glutathione-assay/?catNum=V6911 [Accessed].

PUŠKÁROVÁ, A., BUČKOVÁ, M., KRAKOVÁ, L., PANGALLO, D. & KOZICS, K. 2017. The antibacterial and antifungal activity of six essential oils and their cyto/genotoxicity to human HEL 12469 cells. *Scientific reports,* 7**,** 1-11.

RAHIMI-MADISEH, M., HEIDARIAN, E., KHEIRI, S. & RAFIEIAN-KOPAEI, M. 2017. Effect of hydroalcoholic Allium ampeloprasum extract on oxidative stress, diabetes mellitus and dyslipidemia in alloxan-induced diabetic rats. *Biomedicine & pharmacotherapy,* 86**,** 363-367.

RAHMAN, I., KODE, A. & BISWAS, S. K. 2006. Assay for quantitative determination of glutathione and glutathione disulfide levels using enzymatic recycling method. *Nature protocols,* 1**,** 3159.

RAINS, J. L. & JAIN, S. K. 2011. Oxidative stress, insulin signaling, and diabetes. *Free Radical Biology and Medicine,* 50**,** 567-575.

RAJENDIRAN, D., PACKIRISAMY, S. & GUNASEKARAN, K. 2018. A review on role of antioxidants in diabetes. *Asian journal of pharmaceutical and clinical research,* 11**,** 48-53.

RAMESH, T. 2021. Oxidative stress and hepatocellular mitochondrial dysfunction attenuated by asiatic acid in streptozotocin-induced diabetic rats. *Journal of King Saud University-Science,* 33**,** 101369.

RINES, A. K., SHARABI, K., TAVARES, C. D. & PUIGSERVER, P. J. N. R. D. D. 2016. Targeting hepatic glucose metabolism in the treatment of type 2 diabetes. 15**,** 786-804.

ROCHETTE, L., ZELLER, M., COTTIN, Y. & VERGELY, C. 2014a. Diabetes, oxidative stress and therapeutic strategies. *Biochimica et Biophysica Acta (BBA)-General Subjects,* 1840**,** 2709-2729.

ROCHETTE, L., ZELLER, M., COTTIN, Y. & VERGELY, C. 2014b. Diabetes, oxidative stress and therapeutic strategies. *Biochim Biophys Acta,* 1840**,** 2709-29.

RODER, P. V., WU, B., LIU, Y. & HAN, W. 2016. Pancreatic regulation of glucose homeostasis. *Exp Mol Med,* 48**,** e219.

ROSENBLOOM, A. L., SILVERSTEIN, J. H., AMEMIYA, S., ZEITLER, P. & KLINGENSMITH, G. J. 2009. Type 2 diabetes in children and adolescents. *Pediatric diabetes,* 10**,** 17-32.

ROSHANKHAH, S., SHABANIZADEH, A., ABDOLMALEKI, A., GHOLAMI, M. R. & SALAHSHOOR, M. R. 2020. Evaluation of biomarkers in liver following Solanum melongena green calyx administration in diabetic rats. *Journal of Diabetes & Metabolic Disorders,* 19**,** 1115-1127.

ROY, J., JAIN, N., SINGH, G., DAS, B. & MALLICK, B. 2019. Small RNA proteome as disease biomarker: An incognito treasure of clinical utility. *AGO-Driven Non-Coding RNAs.*

SAFARZAD, M., MARJANI, A., JAZI, M. S., QUJEQ, D., MIR, S. M., MARJANI, M. & KALDEHI, A. N. 2020. Effect of Rubus anatolicus leaf extract on glucose metabolism in HepG2, CRI-D2 and C2C12 cell lines. *Diabetes, Metabolic Syndrome and Obesity: Targets and Therapy,* 13**,** 1109.

SAGBO, I. J., VAN DE VENTER, M., KOEKEMOER, T. & BRADLEY, G. 2018. In vitro antidiabetic activity and mechanism of action of Brachylaena elliptica (Thunb.) DC. *Evidence-Based Complementary and Alternative Medicine,* 2018.

SALEHI, B., ATA, A., V. ANIL KUMAR, N., SHAROPOV, F., RAMIREZ-ALARCON, K., RUIZ-ORTEGA, A., ABDULMAJID AYATOLLAHI, S., VALERE TSOUH FOKOU, P., KOBARFARD, F. & AMIRUDDIN ZAKARIA, Z. 2019. Antidiabetic potential of medicinal plants and their active components. *Biomolecules,* 9**,** 551.

SALLEH, N. H., ZULKIPLI, I. N., MOHD YASIN, H., JA'AFAR, F., AHMAD, N., WAN AHMAD, W. A. N. & AHMAD, S. R. 2021. Systematic review of medicinal plants used for treatment of diabetes in human clinical trials: An ASEAN perspective. *Evidence-Based Complementary and Alternative Medicine,* 2021.

SALTIEL, A. R. 2021. Insulin signaling in health and disease. *The Journal of clinical investigation,* 131.

SASSE, D., SPORNITZ, U. M. & MALY, I. P. 1992. Liver architecture. *Enzyme,* 46**,** 8-8.

SCHULZE, R. J., SCHOTT, M. B., CASEY, C. A., TUMA, P. L. & MCNIVEN, M. A. 2019. The cell biology of the hepatocyte: A membrane trafficking machine. *Journal of Cell Biology,* 218**,** 2096-2112.

SCOTT, G., SPRINGFIELD, E. P. & COLDREY, N. 2004. A Pharmacognostical Study of 26 South African Plant Species Used as Traditional Medicines. *Pharmaceutical Biology,* 42**,** 186-213.

SEMENYA, S., POTGIETER, M. & ERASMUS, L. 2012a. Ethnobotanical survey of medicinal plants used by Bapedi healers to treat diabetes mellitus in the Limpopo Province, South Africa. *Journal of Ethnopharmacology,* 141**,** 440-445.

SEMENYA, S., POTGIETER, M. & ERASMUS, L. J. J. O. E. 2012b. Ethnobotanical survey of medicinal plants used by Bapedi healers to treat diabetes mellitus in the Limpopo Province, South Africa. 141**,** 440-445.

SEN, S., CHAKRABORTY, R., SRIDHAR, C., REDDY, Y. & DE, B. 2010. Free radicals, antioxidants, diseases and phytomedicines: current status and future prospect. *International journal of pharmaceutical sciences review and research,* 3**,** 91-100.

SHANKAR, K. & MEHENDALE, H. M. 2014. Oxidative stress. *Encyclopedia of Toxicology***,** pp. 735–737.

SHARMA, D. R., SUNKARIA, A., WANI, W. Y., SHARMA, R. K., VERMA, D., PRIYANKA, K., BAL, A. & GILL, K. D. 2015. Quercetin protects against aluminium induced oxidative stress and promotes mitochondrial biogenesis via activation of the PGC-1α signaling pathway. *Neurotoxicology,* 51**,** 116-137.

SHOKRZADEH, M., ABDI, H., ASADOLLAH-POUR, A. & SHAKI, F. 2016. Nanoceria attenuated high glucose-induced oxidative damage in HepG2 cells. *Cell Journal (Yakhteh),* 18**,** 97.

SIBULESKY, L. 2013. Normal liver anatomy. *Clin Liver Dis (Hoboken),* 2**,** S1-S3.

SIES, H. & JONES, D. P. 2020. Reactive oxygen species (ROS) as pleiotropic physiological signalling agents. *Nature reviews Molecular cell biology,* 21**,** 363-383.

SINGH, B., KUMAR, A., SINGH, H., KAUR, S., ARORA, S. & SINGH, B. 2022. Protective effect of vanillic acid against diabetes and diabetic nephropathy by attenuating oxidative stress and upregulation of NF-κB, TNF-α and COX-2 proteins in rats. *Phytotherapy Research,* 36**,** 1338-1352.

SLIWINSKA, A., KASZNICKI, J., KOSMALSKI, M., MIKOŁAJCZYK, M., ROGALSKA, A., PRZYBYLOWSKA, K., MAJSTEREK, I. & DRZEWOSKI, J. 2017. Tumour protein 53 is linked with type 2 diabetes mellitus. *The Indian journal of medical research,* 146**,** 237.

SOH, D., BAKANG, B. T., TCHOUBOUN, E. N., NGANSO, Y. O. D., DEFOKOU, U. D., SIDJUI, L. S., AHMED, A., TEPONNO, R. B., LATEEF, M. & ALI, M. S. 2020. New cucurbitane type triterpenes from Momordica foetida Schumach.(Cucurbitaceae). *Phytochemistry Letters,* 38**,** 90-95.

SOKOLOVSKA, J., DEKANTE, A., BAUMANE, L., PAHIRKO, L., VALEINIS, J., DISLERE, K., ROVITE, V., PIRAGS, V. & SJAKSTE, N. 2020. Nitric oxide metabolism is impaired by type 1 diabetes and diabetic nephropathy. *Biomedical Reports,* 12**,** 251-258.

STOCKERT, J. C., HOROBIN, R. W., COLOMBO, L. L. & BLAZQUEZ-CASTRO, A. 2018. Tetrazolium salts and formazan products in Cell Biology: Viability assessment, fluorescence imaging, and labeling perspectives. *Acta histochemica,* 120**,** 159-167.

SUBRAMANIYAN, S. D. & NATARAJAN, K. A. 2017. Citral, a monoterpene protect against high glucose induced oxidative injury in HepG2 cell in vitro-an experimental study. *Journal of clinical and diagnostic research: JCDR,* 11**,** BC10.

SUN, H., SAEEDI, P., KARURANGA, S., PINKEPANK, M., OGURTSOVA, K., DUNCAN, B. B., STEIN, C., BASIT, A., CHAN, J. C. & MBANYA, J. C. 2022. IDF Diabetes Atlas: Global, regional and country-level diabetes prevalence estimates for 2021 and projections for 2045. *Diabetes research and clinical practice,* 183**,** 109119.

SZEWCZUK, M., BOGUSZEWSKA, K., KAŹMIERCZAK-BARAŃSKA, J. & KARWOWSKI, B. T. 2020. The role of AMPK in metabolism and its influence on DNA damage repair. *Molecular Biology Reports,* 47**,** 9075-9086.

TABIBIAN, J. H. A. L., N.F. 2014. Liver and Bile. *Reference Module in Biomedical Sciences.* Elsevier.

TANG, Y., CHOI, E. J., HAN, W. C., OH, M., KIM, J., HWANG, J. Y., PARK, P. J., MOON, S. H., KIM, Y. S. & KIM, E. K. 2017. Moringa oleifera from Cambodia Ameliorates Oxidative Stress, Hyperglycemia, and Kidney Dysfunction in Type 2 Diabetic Mice. *J Med Food,* 20**,** 502-510.

TANGVARASITTICHAI, S. 2015a. Oxidative stress, insulin resistance, dyslipidemia and type 2 diabetes mellitus. *World journal of diabetes,* 6**,** 456.

TANGVARASITTICHAI, S. J. W. J. O. D. 2015b. Oxidative stress, insulin resistance, dyslipidemia and type 2 diabetes mellitus. 6**,** 456.

TANIGUCHI, C. M., EMANUELLI, B. & KAHN, C. R. 2006. Critical nodes in signalling pathways: insights into insulin action. *Nature reviews Molecular cell biology,* 7**,** 85-96.

TAO, L., FAN, X., SUN, J. & ZHANG, Z. 2021. Metformin prevented high glucose-induced endothelial reactive oxygen species via OGG1 in an AMPKα-Lin-28 dependent pathway. *Life Sciences,* 268**,** 119015.

TEO, Z. L., THAM, Y.-C., YU, M., CHEE, M. L., RIM, T. H., CHEUNG, N., BIKBOV, M. M., WANG, Y. X., TANG, Y. & LU, Y. 2021. Global prevalence of diabetic retinopathy and projection of burden through 2045: systematic review and meta-analysis. *Ophthalmology,* 128**,** 1580-1591.

THOMPSON, P. S. & CORTEZ, D. 2020. New insights into abasic site repair and tolerance. *DNA repair,* 90**,** 102866.

TIWARI, B. K., PANDEY, K. B., ABIDI, A. & RIZVI, S. I. 2013. Markers of oxidative stress during diabetes mellitus. *Journal of biomarkers,* 2013.

TOUBOUL, T., HANNAN, N. & VALLIER, L. 2012. Directed Differentiation of Human Pluripotent Stem Cells into Fetal-Like Hepatocytes. *Human Stem Cell Manual.* Elsevier.

TURACLI, I. D., CANDAR, T., YUKSEL, E. B., KALAY, S., OGUZ, A. K. & DEMIRTAS, S. 2018. Potential effects of metformin in DNA BER system based on oxidative status in type 2 diabetes. *Biochimie,* 154**,** 62-68.

UMPIERREZ, G. E. 2020. Hyperglycemic crises: diabetic ketoacidosis and hyperglycemic hyperosmolar state. *Diabetes Complications, Comorbidities and Related Disorders*, 595-614.

UNUOFIN, J. O. & LEBELO, S. L. 2020. Antioxidant effects and mechanisms of medicinal plants and their bioactive compounds for the prevention and treatment of type 2 diabetes: an updated review. *Oxidative medicine and cellular longevity,* 2020.

VAN DE VENTER, M., ROUX, S., BUNGU, L. C., LOUW, J., CROUCH, N. R., GRACE, O. M., MAHARAJ, V., PILLAY, P., SEWNARIAN, P. & BHAGWANDIN, N. 2008. Antidiabetic screening and scoring of 11 plants traditionally used in South Africa. *Journal of ethnopharmacology,* 119**,** 81-86.

VAN MEERLOO, J., KASPERS, G. J. & CLOOS, J. 2011. Cell sensitivity assays: the MTT assay. *Cancer cell culture.* Springer.

VAN SCHAFTINGEN, E. & GERIN, I. 2002. The glucose-6-phosphatase system. *Biochemical Journal,* 362**,** 513-532.

VELLA, A., FREEMAN, J. L., DUNN, I., KELLER, K., BUSE, J. B. & VALCARCE, C. 2019. Targeting hepatic glucokinase to treat diabetes with TTP399, a hepatoselective glucokinase activator. *Science translational medicine,* 11.

VENKATESH, S., REDDY, B. M., REDDY, G. D., MULLANGI, R. & LAKSHMAN, M. 2010. Antihyperglycemic and hypolipidemic effects of Helicteres isora roots in alloxan-induced diabetic rats: a possible mechanism of action. *Journal of natural medicines,* 64**,** 295-304.

VIAL, G., DETAILLE, D. & GUIGAS, B. 2019. Role of mitochondria in the mechanism (s) of action of metformin. *Frontiers in endocrinology,* 10**,** 294.

WAAKO, P., GUMEDE, B., SMITH, P. & FOLB, P. 2005. The in vitro and in vivo antimalarial activity of Cardiospermum halicacabum L. and Momordica foetida Schumch. Et Thonn. *Journal of Ethnopharmacology,* 99**,** 137-143.

WANG, J. & GUO, H. M. 2019. Astragaloside IV ameliorates high glucose-induced HK-2 cell apoptosis and oxidative stress by regulating the Nrf2/ARE signaling pathway. *Experimental and therapeutic medicine,* 17**,** 4409-4416.

WANG, J., WU, T., FANG, L., LIU, C., LIU, X., LI, H., SHI, J., LI, M. & MIN, W. 2020. Anti-diabetic effect by walnut (Juglans mandshurica Maxim.)-derived peptide LPLLR through inhibiting α-glucosidase and α-amylase, and alleviating insulin resistance of hepatic HepG2 cells. *Journal of Functional Foods,* 69**,** 103944.

WANG, Q. & ZOU, M.-H. 2018. Measurement of reactive oxygen species (ROS) and mitochondrial ROS in AMPK knockout mice blood vessels. *AMPK.* Springer.

WANG, W.-X., LUO, S.-B., JIANG, P., XIA, M.-M., HEI, A.-L., MAO, Y.-H., LI, C.-B., HU, G.-X. & CAI, J.-P. 2017. Increased oxidative damage of RNA in early-stage nephropathy in db/db mice. *Oxidative medicine and cellular longevity,* 2017.

WASHABAU, R. J. & DAY, M. J. 2012. *Canine and feline gastroenterology*, Elsevier Health Sciences.

WESELER, A. R. & BAST, A. 2010. Oxidative stress and vascular function: implications for pharmacologic treatments. *Current hypertension reports,* 12**,** 154-161.

WHITE, M. F. & KAHN, C. R. 2021. Insulin action at a molecular level–100 years of progress. *Molecular Metabolism,* 52**,** 101304.

WILKE, T., PICKER, N., MUELLER, S., GEIER, S., FOERSCH, J., ABERLE, J., MARTIN, S., RIEDL, M., GABLER, M. J. D., METABOLIC SYNDROME, TARGETS, O. & THERAPY 2019. Real-world insulin therapy in German type 2 diabetes mellitus patients: patient characteristics, treatment patterns, and insulin dosage. 12**,** 1225.

WILLIAMS, R., KARURANGA, S., MALANDA, B., SAEEDI, P., BASIT, A., BESANÇON, S., BOMMER, C., ESTEGHAMATI, A., OGURTSOVA, K. & ZHANG, P. 2020. Global and regional estimates and projections of diabetes-related health expenditure: Results from the International Diabetes Federation Diabetes Atlas. *Diabetes research and clinical practice,* 162**,** 108072.

WORLDWIDE.PROMEGA.COM. 2022. *Mitochondrial ToxGlo™ Assay* [Online]. Available: https://worldwide.promega.com/products/cell-health-assays/oxidative-stress-assays/mitochondrial-toxicity-assay/?catNum=G8000 [Accessed March 2022].

YAN, J., WANG, C., JIN, Y., MENG, Q., LIU, Q., LIU, Z., LIU, K. & SUN, H. 2018. Catalpol ameliorates hepatic insulin resistance in type 2 diabetes through acting on AMPK/NOX4/PI3K/AKT pathway. *Pharmacological Research,* 130**,** 466-480.

YANG, Z., HUANG, W., ZHANG, J., XIE, M. & WANG, X. 2019. Baicalein improves glucose metabolism in insulin resistant HepG2 cells. *European journal of pharmacology,* 854**,** 187-193.

YARAHMADI, A., SARABI, M. M., SAYAHI, A. & ZAL, F. 2021. Protective effects of quercetin against hyperglycemia-induced oxidative stress in hepatic HepG2 cell line. *Avicenna Journal of Phytomedicine,* 11**,** 269.

YARIBEYGI, H., SATHYAPALAN, T., ATKIN, S. L. & SAHEBKAR, A. 2020a. Molecular mechanisms linking oxidative stress and diabetes mellitus. *Oxidative medicine and cellular longevity,* 2020.

YARIBEYGI, H., SATHYAPALAN, T., ATKIN, S. L., SAHEBKAR, A. J. O. M. & LONGEVITY, C. 2020b. Molecular mechanisms linking oxidative stress and diabetes mellitus. 2020.

YUAN, T., YANG, T., CHEN, H., FU, D., HU, Y., WANG, J., YUAN, Q., YU, H., XU, W. & XIE, X. 2019. New insights into oxidative stress and inflammation during diabetes mellitus-accelerated atherosclerosis. *Redox biology,* 20**,** 247-260.

YUNG, J. H. M. & GIACCA, A. 2020. Role of c-Jun N-terminal kinase (JNK) in obesity and type 2 diabetes. *Cells,* 9**,** 706.

ZHANG, W.-Q., ZHAO, T.-T., GUI, D.-K., GAO, C.-L., GU, J.-L., GAN, W.-J., HUANG, W., XU, Y., ZHOU, H. & CHEN, W.-N. 2019. Sodium butyrate improves liver glycogen metabolism in type 2 diabetes mellitus. *Journal of agricultural and food chemistry,* 67**,** 7694-7705.

ZHAO, Z. 2019. Iron and oxidizing species in oxidative stress and Alzheimer's

disease. *aging medicine,* 2.

ZHENG, D. W., XU, L., LI, C. X., DONG, X., PAN, P., ZHANG, Q. L., LI, B., ZENG, X. & ZHANG, X. Z. 2018. Photo-Powered Artificial Organelles for ATP Generation and Life-Sustainment. *Advanced Materials,* 30**,** 1805038.

ZHOU, B., ZHANG, Y., LI, S., WU, L., FEJES-TOTH, G., NARAY-FEJES-TOTH, A. & SOUKAS, A. A. 2021. Serum-and glucocorticoid-induced kinase drives hepatic insulin resistance by directly inhibiting AMP-activated protein kinase. *Cell reports,* 37**,** 109785.

ZHU, J., YU, C., ZHOU, H., WEI, X. & WANG, Y. 2021. Comparative evaluation for phytochemical composition and regulation of blood glucose, hepatic oxidative stress and insulin resistance in mice and HepG2 models of four typical Chinese dark teas. *Journal of the Science of Food and Agriculture,* 101**,** 6563-6577.

ZOBOLO, A. & MKABELA, Q. 2006. Traditional knowledge transfer of activities practised by Zulu women to manage medicinal and food plant gardens. *African Journal of Range and Forage Science,* 23**,** 77-80.

ZOROVA, L. D., POPKOV, V. A., PLOTNIKOV, E. Y., SILACHEV, D. N., PEVZNER, I. B., JANKAUSKAS, S. S., BABENKO, V. A., ZOROV, S. D., BALAKIREVA, A. V. & JUHASZOVA, M. 2018. Mitochondrial membrane potential. *Analytical biochemistry,* 552**,** 50-59.

APPENDIX

Appendix 1: Preparation of media, buffers, and antibodies

High glucose media

Media was made by dissolving 225mg of D (+) glucose in 50ml of CCM media (EMEM containing 10% FBS and 1% gentamicin) for 15 minutes under ultraviolet light.

Metformin

Metformin treatment was prepared by dissolving 5mg in 1ml of PBS. Stock was made up fresh on the day.

Cell storage

To cryopreserve HepG2 cells, 1.8ml of CCM and 200µl DMSO are pipetted into a 2ml cryo-vile and then stored at -80°C.

Running buffer (10X)

In 180ml of dH2O, tris (6,06g), glycine (28.8g), and SDS (2g) were weighed and dissolved. The solution was then thoroughly mixed with a magnetic stirrer until it was completely dissolved. A volume of 20ml was added thereafter to top up the volume to 200ml. The buffer was stored at 4°C.

Transfer buffer

Tris (0.76g), glycine (3.6g) were weighed and dissolved in 200ml of dH2O. A volume of 50ml of methanol was then added. The pH was adjusted to 8.3 and the volume was topped up to 600ml with dH_2O.

TTBS wash buffer

In 800ml dH_2O, 8g of NaCl, 0.2g of KCl, 3g of Tris were weighed and dissolved. After that, the pH was adjusted to 7.5. Distilled water was added to bring the total to 1000ml. Tween 20 was added in a volume of 500µl, and the buffer was stored at 4°C.

Antibody

To prepare primary (1˚) and (2˚) secondary antibody dilution: 5µl of 1˚ was a diluted in 5000µl BSA (5%) and 2µl of 2˚ was diluted in 5000µl BSA (5%).

Appendix 2: Sodium nitrate standard curve

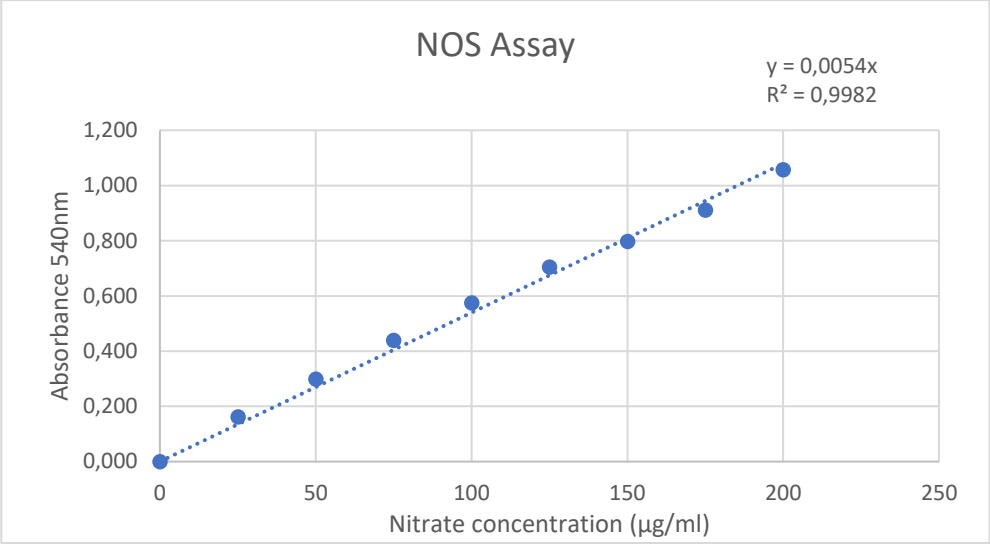

Figure 1: Nitrate standard curve generated to evaluate NOS activity

Appendix 3: Protein standardisation

Table 1: BSA analysis used for protein quantification curve construction

Standards (mg/mL)	Abs1(595nm)	Abs2(595nm)	Average(595nm)	Avg-blnk(595nm)
0	0,102	0,091	0,097	0
0,2	0,248	0,246	0,247	0,151
0,4	0,356	0,361	0,359	0,262
0,6	0,476	0,482	0,479	0,383
0,8	0,606	0,590	0,598	0,502
1	0,680	0,660	0,670	0,574

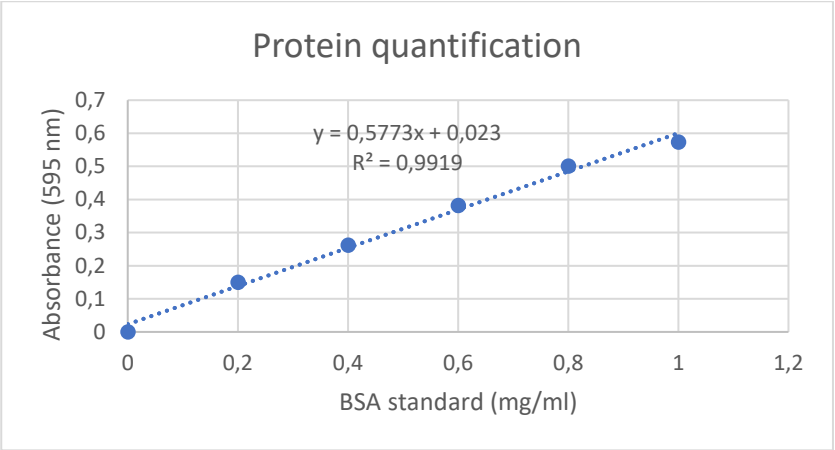

Figure 2: Protein quantification using bovine serum albumin as standards.

Table 2: Total protein concentration of samples determined using a standard curve generated from bovine serum albumin analysis

Samples	Average Absorbance	Protein (mg/ml)	C2 (mg/ml)	V1 (µl)	V2 (µl)
Normal control	2,05	3,51	1.84	0	200
High glucose	2,04	3,49	1.84	0	200
Metformin	2,45	4,21	1.84	34,23	165,75
MF1	2,20	3,78	1.84	15,33	184,68
MF2	2,15	3,68	1.84	10,77	189,23
MF3	2,16	3,71	1.84	11,96	188,04

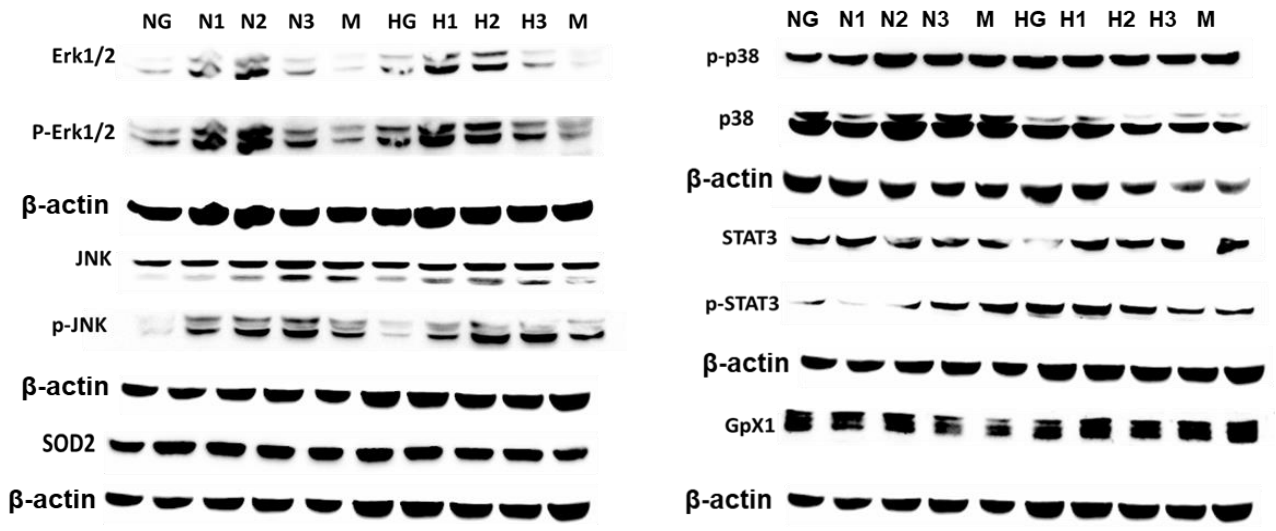

Figure 3: Western blots of normoglycemia and hyperglycemia proteins and β-Actin. NG represents normoglycemia and HG represents hyperglycemia. H1&N1- *M. foetida* 125mg/ml, H2&N2- *M. foetida* 500mg/ml, H3&N3-*M. foetida* 1000mg/ml.

Appendix 4: qPCR

Table 3: Standardization of mRNA concentrations obtained from Nanodrop

Samples	[RNA] ng/ml	C2 ng/ml	V1 µl	V2 µl	RNA purity[A260/A280]
Normal control	952	800	8,4	10	2.16
High glucose control	836	800	9,57	10	2.17
Metformin	970	800	8,25	10	2.18
MF1	1353	800	5,91	10	2.13
MF2	1663	800	4,81	10	2.22
MF3	1384	800	5,78	10	2.18

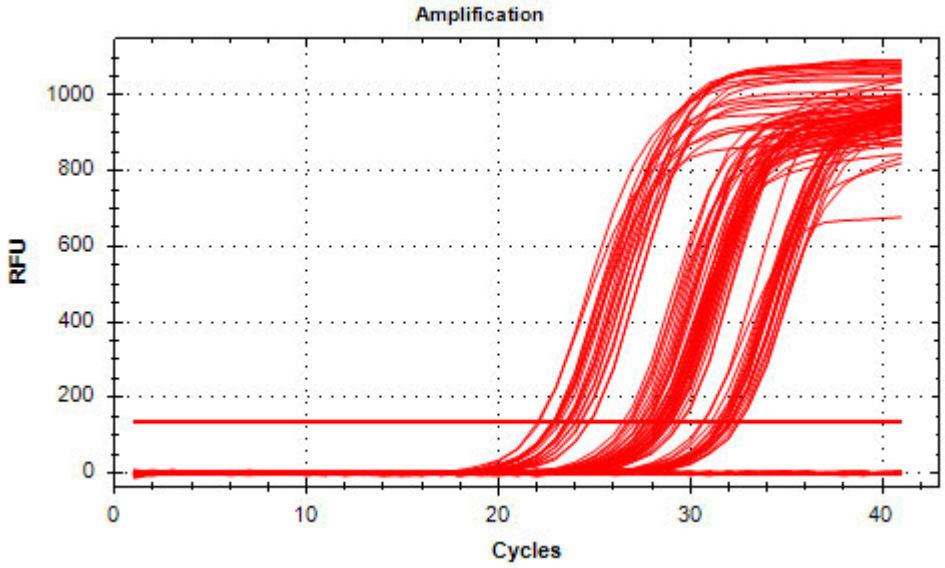

Figure 3: Real time PCR amplification curve showing mRNA expression of *CAT*, *p53*, *OGG1* on HepG2 cells with or without *M. foetida* treatment generated at each reaction cycle using NAPDH as a standard

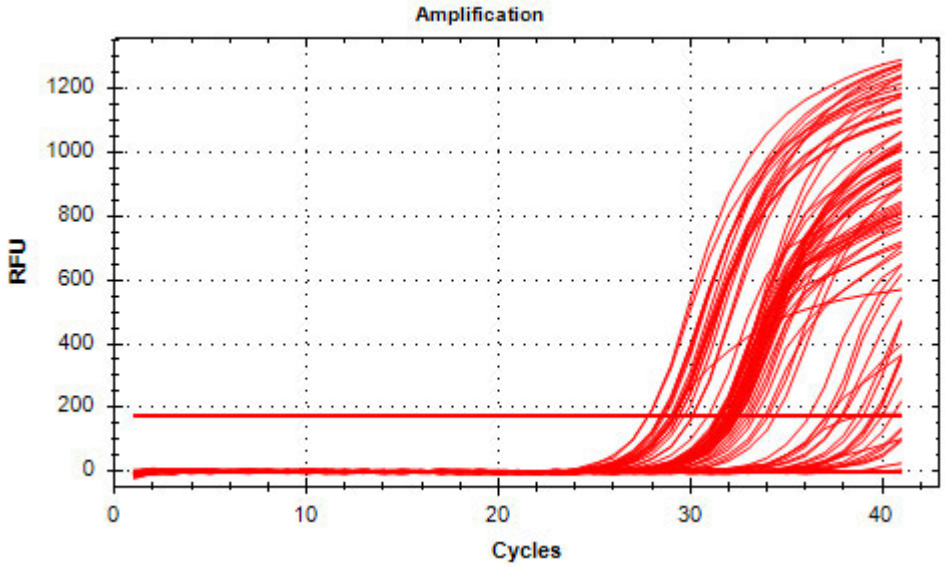

Figure 4: Real time PCR amplification curve showing mRNA expression of *NRF2*, *NFKB*, *PI3K* on HepG2 cells with or without *M. foetida* treatment generated at each reaction cycle using NAPDH as a standard

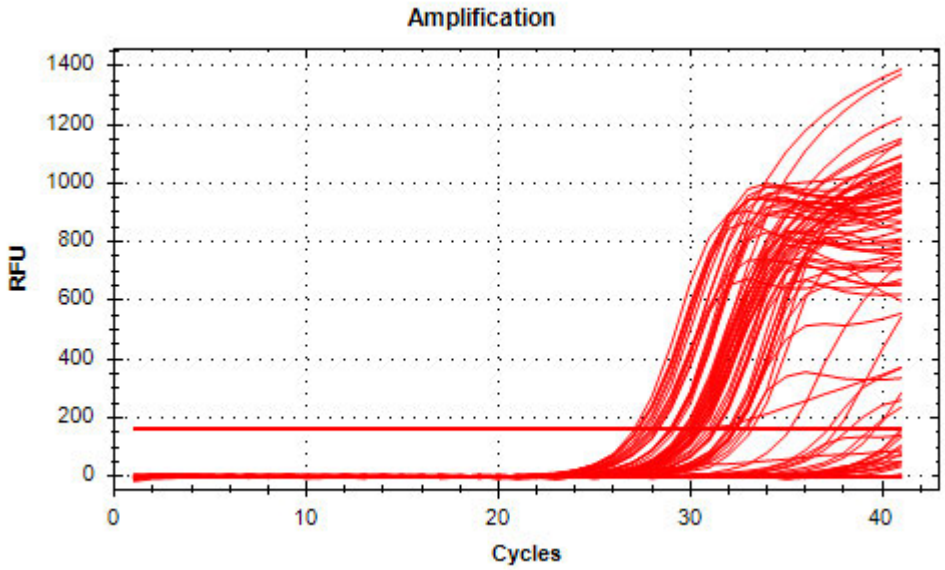

Figure 5: Real time PCR amplification curve showing mRNA expression of *IRS, GLUT2, glucokinase* on HepG2 cells with or without *M. foetida* treatment generated at each reaction cycle using NAPDH as a standard.

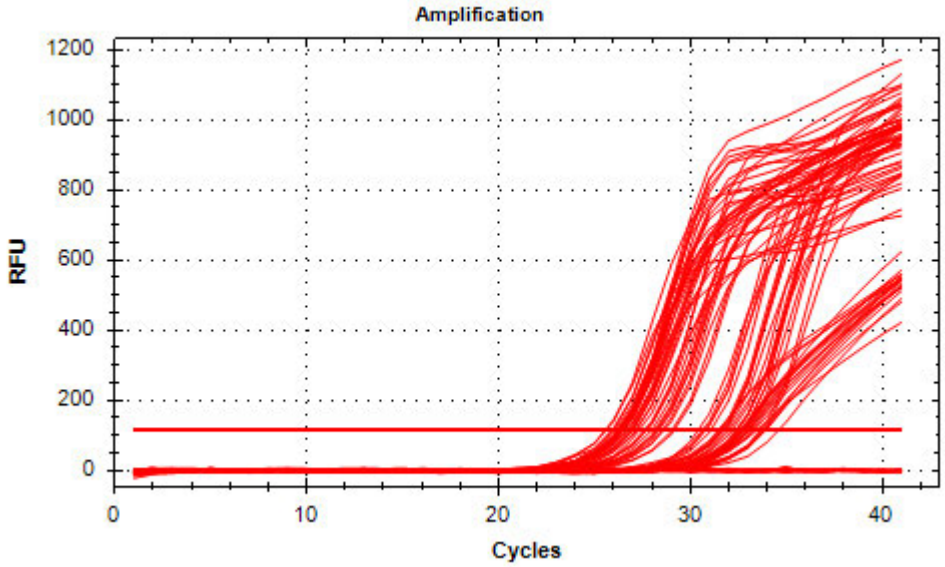

Figure 6: Real time PCR amplification curve showing mRNA expression of *glycogen synthase* and *AMPKα2* on HepG2 cells with or without *M. foetida* treatment generated at each reaction cycle using NAPDH as a standard.

turnitin

Digital Receipt

This receipt acknowledges that Turnitin received your paper. Below you will find the receipt information regarding your submission.

The first page of your submissions is displayed below.

Submission author:	Fulufhelo Netshitangani
Assignment title:	Thesis
Submission title:	Masters Thesis
File name:	Fulufhelo_Netshitangani_Masters_Thesis.docx
File size:	6M
Page count:	107
Word count:	33,188
Character count:	190,397
Submission date:	11-Jun-2022 10:03PM (UTC+0200)
Submission ID:	1854950578

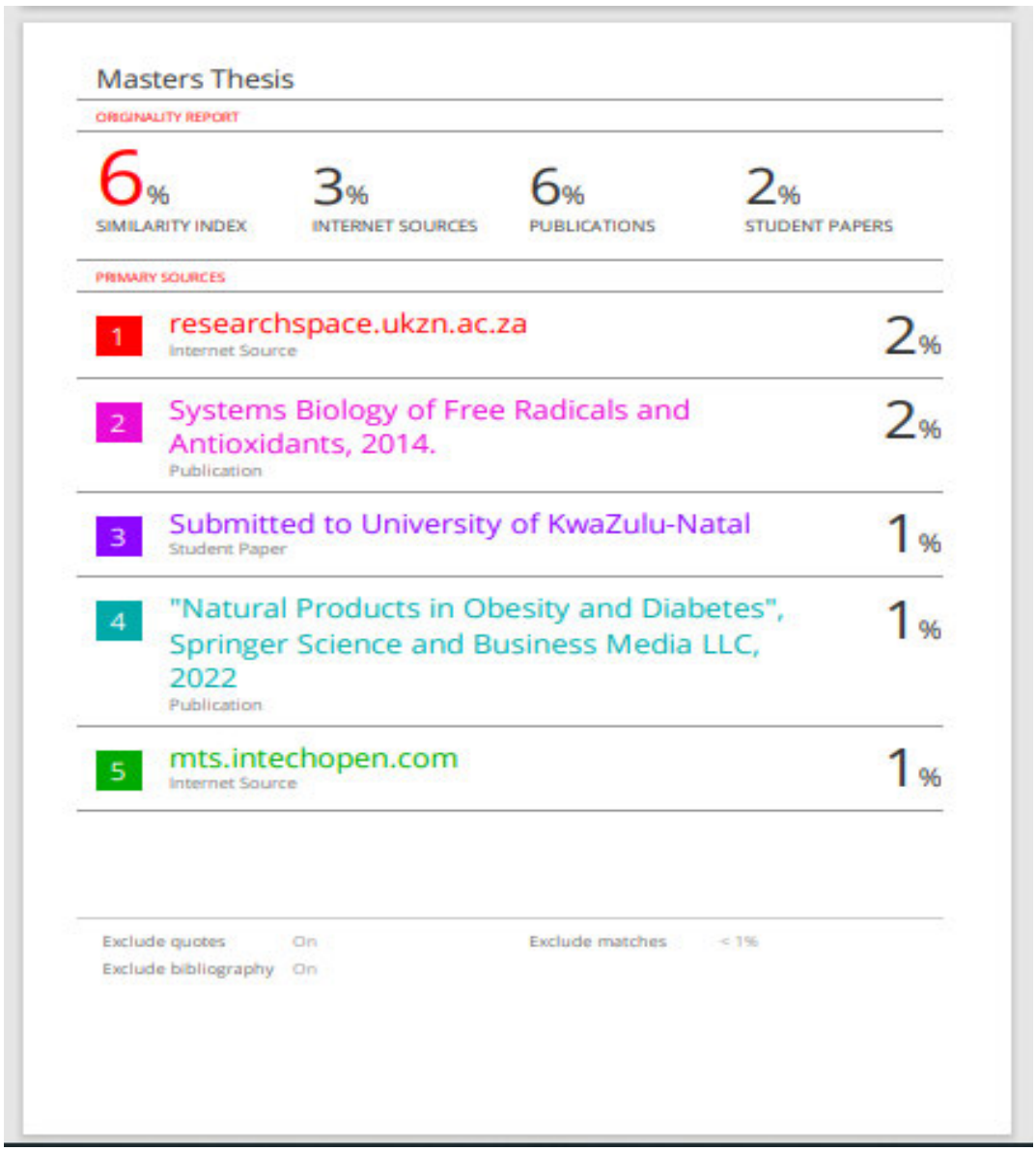

Masters Thesis

ORIGINALITY REPORT

6%	3%	6%	2%
SIMILARITY INDEX	INTERNET SOURCES	PUBLICATIONS	STUDENT PAPERS

PRIMARY SOURCES

1	researchspace.ukzn.ac.za Internet Source	2%
2	Systems Biology of Free Radicals and Antioxidants, 2014. Publication	2%
3	Submitted to University of KwaZulu-Natal Student Paper	1%
4	"Natural Products in Obesity and Diabetes", Springer Science and Business Media LLC, 2022 Publication	1%
5	mts.intechopen.com Internet Source	1%

Exclude quotes On
Exclude bibliography On
Exclude matches < 1%